

Role of Tumor necrosis factor receptor 1 in a mouse model of chronic liver inflammation

Dissertation

Zur Erlangung der Würde des Doktors der Naturwissenschaften
des Fachbereichs Biologie, der Fakultät für Mathematik, Informatik und
Naturwissenschaften,
der Universität Hamburg

vorgelegt von
Laura Katharina Berkhout
aus Oldenburg
Hamburg 2019

Tag der Disputation: 21.02.2020

Vorsitzender der Prüfungskommission

Prof. Dr. Stefan Hoth

Universität Hamburg

Institut für Pflanzenwissenschaften und Mikrobiologie

Gutachter der Dissertation:

Prof. Dr. Gisa Tiegs

Universitätsklinikum Hamburg-Eppendorf

Institut für Experimentelle Immunologie und Hepatologie

PD Dr. Hartwig Lüthen

Universität Hamburg

Institut für Pflanzenwissenschaften und Mikrobiologie

Index

Eidesstattliche Versicherung.....	III
List of publications.....	IV
Articles published in peer reviewed journals.....	IV
Abstracts of congress presentations	IV
Further congress presentations.....	V
Declaration of own contribution to presented published work.....	VI
Abbreviations.....	VI
List of Tables	X
List of Figures.....	XI
1 Introduction.....	1
1.1 The liver	1
1.2 Chronic liver disease	2
1.2.1 The role of cytokines in chronic liver inflammation.....	4
1.2.2 Immune cells shape the progression of chronic liver disease	7
1.3 Bile.....	9
1.3.1 The multi-drug resistance p-glycoprotein 2 knockout mice	10
1.4 Aim of the study	12
2 Materials and Methods.....	13
2.1 Technical equipment.....	13
2.2 Consumables	14
2.3 Reagents and Kits	15
2.4 Buffers and Solutions.....	16
2.5 Antibodies	17
2.6 Oligonucleotide sequences	18

2.7	Software and databases	19
2.8	Mice.....	19
2.9	Sampling of biological material.....	20
2.10	Assessment of liver enzyme activity	20
2.11	Isolation of hepatic non-parenchymal cells	20
2.12	Ex vivo restimulation of hepatic NPCs	21
2.13	Flow cytometry	21
2.13.1	Staining and analysis of hepatic NPCs	21
2.13.2	Gating strategy.....	21
2.14	Fluorescence activated cell sort.....	24
2.15	Hydroxyproline Assay	24
2.16	Hematoxylin & Eosin staining	25
2.17	Sirius Red staining	25
2.18	Beadbased multiplex analysis of cytokine concentrations	25
2.19	Quantitative real-time reverse-transcriptase polymerase chain reaction.....	26
2.20	Protein isolation from mouse liver and western blot analysis.....	27
2.21	Statistical Analysis	27
3	Results	28
3.1	Tissue injury in livers of Tnfr1 ^{-/-} /Mdr2 ^{-/-} mice	28
3.2	Cell death in livers of Tnfr1 ^{-/-} /Mdr2 ^{-/-} mice.....	29
3.3	Fibrosis in livers of Tnfr1 ^{-/-} /Mdr2 ^{-/-} mice.....	31
3.4	Proliferation in livers of Tnfr1 ^{-/-} /Mdr2 ^{-/-} mice.....	33
3.1	Cytokine production in livers of Tnfr1 ^{-/-} /Mdr2 ^{-/-} mice	35
3.1.1	Hepatic cytokine expression.....	36
3.2	Immune cell composition in livers of Tnfr1 ^{-/-} /Mdr2 ^{-/-} mice	38

3.2.1	T helper cell subsets	39
3.2.2	Correlation between IL-17A production of hepatic non-parenchymal cells and extent of tissue injury in Tnfr1 ^{-/-} /Mdr2 ^{-/-} mice	39
3.2.3	Hepatic chemokine expression profile of Tnfr1 ^{-/-} /Mdr2 ^{-/-} mice	40
3.2.4	Myeloid cell subsets in livers of Tnfr1 ^{-/-} /Mdr2 ^{-/-} mice	41
3.3	Role of RIPK3 in livers of Tnfr1 ^{-/-} /Mdr2 ^{-/-} mice	43
3.4	Immune cell accumulation in livers of Tnfr1 ^{-/-} /Mdr2 ^{-/-} mice over time	45
4	Discussion	47
4.1	Ablation of TNFR1 does not protect from tissue injury and fibrosis	48
4.2	Ablation of TNFR1 does not compromise regenerative proliferation	49
4.3	Ablation of TNFR1 alters the cytokine milieu in the chronically inflamed liver	51
4.4	Ablation of TNFR1 leads to an increased presence of T _H 17 cells and neutrophils in the chronically inflamed liver	52
4.5	RIPK3 performs a necroptosis independent role in livers of Tnfr1 ^{-/-} /Mdr2 ^{-/-} mice	54
4.6	Outlook	56
5	Abstract	58
5.1	Graphical abstract	59
6	Zusammenfassung	60
7	References	i
8	Danksagung	viii
9	Confirmation of linguistic accuracy by a native speaker	x

Eidesstattliche Versicherung

Hiermit erkläre ich an Eides statt, dass ich die vorliegende Dissertation selbst verfasst und keine anderen als die angegebenen Quellen und Hilfsmittel benutzt habe.

A handwritten signature in blue ink, appearing to read 'Boellert', is written above a horizontal line.

Hamburg, 30.10.2019

List of publications

Articles published in peer reviewed journals

Barikbin R*, **Berkhout L***, Bolik J, Schmidt-Arras D, Ernst T, Ittrich H, Adam G, Parplys A, Casar C, Krech T, Karimi K, Sass G, Tiegs G. Early heme oxygenase 1 induction delays tumour initiation and enhances DNA damage repair in liver macrophages of *Mdr2*^{-/-} mice. *Sci Rep*. 2018;8(1):16238. Published 2018 Nov. 2.¹ (* authors contributed equally)

Berkhout L, Barikbin R, Schiller B, Ravichandran G, Krech T, Neumann K, Sass G, Tiegs G. Deletion of tumour necrosis factor α receptor 1 elicits an increased TH17 immune response in the chronically inflamed liver. *Sci Rep*. 2019. Published 2019 Mar. 12.²

Ravichandran G*, Neumann K*, **Berkhout L**, Weidemann S, Langeneckert AE, Schwinge D, Poch T, Huber S, Schiller B, Hess LU, Ziegler AE, Oldhafer KJ, Barikbin R, Schramm C, Altfeld M, Tiegs G. Interferon- γ -dependent immune responses contribute to the pathogenesis of sclerosing cholangitis in mice. *J Hepatol*. 2019, Published online 2019 June 4.³ (* authors contributed equally)

Abstracts of congress presentations

L Berkhout, B Schiller, G Ravichandran, T Krech, G Sass, G Tiegs, R Barikbin. Deletion of tumor necrosis factor alpha receptor 1 leads to an increased Th17 cell response in the chronically inflamed liver. *J Hepatol* 2018; 68:458.

L Berkhout, B Schiller, G Ravichandran, T Krech, G Sass, G Tiegs, R Barikbin. Deletion of tumor necrosis factor α receptor 1 leads to increased tissue damage and fibrosis in the chronically inflamed liver. *Z Gastroenterol* 2018; 56(01): E2-E89.

B Schiller, C Wegscheid, **L Berkhout**, A Zarzycka, U Steinhoff, N Fischer, G Tiegs. The role of microbiota in concanavalin A-mediated liver injury. *Z Gastroenterol* 2018; 56(01): E2-E89

Berkhout LK, Krech T, Tiegs G, Barikbin R. Inflammation and Fibrosis in the livers of TNFR1/MDR2ko mice. *J Hepatol* 2016; 64(2):S568.

Berkhout LK, Krech T, Tiegs G, Barikbin R. Inflammation and Fibrosis in the livers of TNFR1/MDR2ko mice. *Z Gastroenterol* 2016; 54(12): 1343-1404.

Schiller B, Wegscheid C, **Berkhout L**, Zarzycka AE, Steinhoff U, Fischer N, et al. Gut Microbiota as a Target in T cell-mediated hepatic Injury. *Z Gastroenterol* 2016; 54(12): 1343-1404.

Schiller B, Wegscheid C, **Berkhout L**, Zarzycka AE, Steinhoff U, Fischer N, et al. The Gut Microbiota as a Target in T cell-mediated hepatic Injury. *Hepatology*. 2016;64:361a-a.

Further congress presentations

L Berkhout, B Schiller, G Ravichandran, T Krech, G Sass, G Tiegs, R Barikbin. Deletion of tumor necrosis factor α receptor 1 leads to increased tissue damage and fibrosis in the chronically inflamed liver. 47th Annual Conference of the German Society of Immunology, 2017, Erlangen, Germany.

B Schiller, C Wegscheid, **L Berkhout**, A Zarzycka, U Steinhoff, N Fischer, G Tiegs. Role of the microbiome in CD4⁺ T cell mediated liver injury. 47th Annual Conference of the German Society of Immunology, 2017, Erlangen, Germany.

Berkhout LK, Krech T, Tiegs G, Barikbin R. Inflammation and Fibrosis in the livers of TNFR1/MDR2ko mice. 46th Annual Conference of the Society of Immunology, Hamburg.

Declaration of own contribution to presented published work

Parts of the presented data in this thesis have previously been published in SCIENTIFIC REPORTS as "Deletion of tumour necrosis factor α receptor 1 elicits an increased TH17 immune response in the chronically inflamed liver" by **Laura Berkhout**, Roja Barikbin, Birgit Schiller, Gevitha Ravichandran, Till Krech, Kathrin Neumann, Gabriele Sass und **Gisa Tiegs**. The publication is the result of a collaborative effort to which I substantially contributed to the planning and performing of the experiments, analysis of data and writing of the manuscript. The following delineates my contributions and those of my colleagues.

Gisa Tiegs, Gabriele Sass, and Roja Barikbin planned this study and obtained funding. Till Krech performed and analyzed the hematoxylin and eosin staining. I planned and performed the experiments. In complex and time-consuming experiments, I was supported by Birgit Schiller, Gevitha Ravichandran, and Katrin Neumann. I analyzed and interpreted the data under the supervision of Roja Barikbin and Gisa Tiegs. I drafted the manuscript under the supervision of Gisa Tiegs. All authors critically revised the manuscript.

HH, 22.06.2020

Date and place



Prof. Dr. Gisa Tiegs

Abbreviations

ABCB	ATP binding cassette subfamily B
AFP	α -feto protein
ALD	alcoholic liver disease
ALP	alkaline phosphatase
ALT	alanine aminotransferase
AP	activator protein
APC	antigen presenting cells
BA	bile acid
BSEP	bile salt export pump
Casp	caspase
CCL/R	C-C motif chemokine ligand /receptor
CCl ₄	carbon tetrachloride
Ccn	cyclin
CD	cluster of differentiation
CDK	cyclin dependent kinase
ciAP	cellular inhibitors of apoptosis
CLD	chronic liver disease
CXCL/R	C-X-C motif chemokine ligand / receptor
DAMP	danger associated molecular pattern
DC	dendritic cell
ECM	extracellular matrix
ELISA	enzyme-linked immunosorbent assay
FADD	Fas-associated protein with death domain
FasL	Fas ligand
FSC	forward angle scattered scattered light
H&E	hematoxylin and eosin
HBSS	Hank's buffered salt solution
HCC	hepatocellular carcinoma
HSC	hepatic stellate cells

Hyp	hydroxyproline
I/R	ischemia/reperfusion
IBD	inflammatory bowel disease
IFN	interferone
IL	interleukin
IV	intravenous
KC	Kupffer cell
LPS	lipopolysaccharide
LSEC	liver sinusoidal endothelial cells
MAPK	mitogen-activated protein kinase
MDR	multi drug resistance protein
MHC	major histocompatibility complex
MLKL	mixed lineage kinase domain-like
MMP	matrix metalloproteinases
NAFLD	non-alcoholic fatty liver disease
NF κ B	nuclear factor 'kappa-light-chain-enhancer' of activated B-cells
NPC	non-parenchymal cells
OPN	osteopontin
PAMP	pathogen associated molecular pattern
PBS	phosphate buffered saline
PC	phosphatidylcholine
PCNA	proliferating cell nuclear antigen
PMA	phorbol-12-myristate-13-acetate
PSC	primary sclerosing cholangitis
qRT-PCR	quantitative real-time reverse transcriptase polymerase chain reaction
RIPK	receptor interacting protein Serine/Threonine kinase
ROR γ t	RAR-related orphan receptor γ t
ROS	reactive oxygen species
sma	smooth muscle actin
Spp	secreted phospho protein

SSC	side angle scattered light
STAT3	signal transducer and activator of transcription 3
TCR	T cell receptor
TGF	transforming growth factor
TIMP	tissue inhibitor of MMPs
TLR	Toll-like receptor
Tnfaip	tumor necrosis factor α induced protein
TNFR	tumor necrosis factor receptor
TRADD	TNFR1 associated death domain protein
TRAF	TNF α receptor-associated factor
WB	western blot

List of Tables

Table 1: List of technical equipment.....	13
Table 2: List of consumables.....	14
Table 3: List of reagents and kits.....	15
Table 4: List of buffers and solutions.....	16
Table 5: Antibodies for flow cytometry	17
Table 6: Antibodies for western blot	18
Table 7: List of oligonucleotide sequences used in RT-qPCR.....	18
Table 8: Software and databases.....	19

List of Figures

Figure 1: Liver anatomy.....	1
Figure 2: Progression of chronic liver disease.....	3
Figure 3: Simplified overview of signaling pathways induced by TNFR1.....	5
Figure 4: Enterohepatic circulation.....	9
Figure 5: Role of MDR2 in bile excretion.....	11
Figure 6: Gating strategy for flow cytometric analysis of T cell subsets.....	22
Figure 7: Gating strategy for flow cytometric analysis of myeloid cell subsets..	23
Figure 8: Gating strategy for fluorescent activated cell sorting of monocytes according to CX3CR1 expression.	24
Figure 9: The absence of TNFR1 increases tissue injury in the <i>Mdr2</i> ^{-/-} mouse model.	28
Figure 10: Markers for cholestasis in <i>Tnfr1</i> ^{-/-} / <i>Mdr2</i> ^{-/-} mice.	29
Figure 11: Mediators of cell death.	30
Figure 12: The absence of TNFR1 increases hepatic extracellular matrix deposition in response to chronic tissue injury.....	31
Figure 13: The expression of <i>markers of fibrosis and fibrotic tissue remodeling is upregulated in Tnfr1</i> ^{-/-} / <i>Mdr2</i> ^{-/-} mice.	33
Figure 14: Mediators of proliferation are up-regulated in livers of <i>Tnfr1</i> ^{-/-} / <i>Mdr2</i> ^{-/-} mice.	34
Figure 15: Hepatic expression of tumor marker in livers of <i>Tnfr1</i> ^{-/-} / <i>Mdr2</i> ^{-/-} mice.....	35
Figure 16: Absence of TNFR1 influences plasma cytokine concentrations.....	36
Figure 17: Hepatic gene expression associated with T _H 17 differentiation.....	37
Figure 18: Hepatic T cell subsets of <i>Mdr2</i> ^{-/-} and <i>Tnfr1</i> ^{-/-} / <i>Mdr2</i> ^{-/-} mice.....	38
Figure 19: Cytokine concentrations in supernatants of <i>ex vivo</i> restimulated hepatic NPCs..	40
Figure 20: Hepatic gene expression of chemokines and chemokine receptors in <i>Mdr2</i> ^{-/-} and <i>Tnfr1</i> ^{-/-} / <i>Mdr2</i> ^{-/-} mice.	41
Figure 21: Frequencies of myeloid subsets in the livers of <i>Mdr2</i> ^{-/-} and <i>Tnfr1</i> ^{-/-} / <i>Mdr2</i> ^{-/-} mice.	42
Figure 22: Correlation between hepatic <i>Ripk3</i> and <i>Cx3cr1</i> expression in livers of <i>Tnfr1</i> ^{-/-} / <i>Mdr2</i> ^{-/-} mice.	43

Figure 23: <i>Ripk3</i> gene expression is up-regulated in CD11b ⁺ CX3CR1 ⁺ cells derived from livers of <i>Tnfr1</i> ^{-/-} / <i>Mdr2</i> ^{-/-} mice.....	44
Figure 24: CX3CR1 ⁺ monocytes and TH17 cells accumulate in livers of <i>Tnfr1</i> ^{-/-} / <i>Mdr2</i> ^{-/-} mice with disease progression.....	45
Figure 25: Graphical abstract	59

1 Introduction

1.1 The liver

The liver is located in the upper abdominal cavity and receives a dual blood supply of 80 % venous blood rich in nutrients, microbial compounds, and low in oxygen from the portal vein and 20 % of oxygen-rich blood supplied by the hepatic artery. The liver parenchyma is organized in functional units called liver lobules (Figure 1). The central vein, a terminal branch of the hepatic vein, is positioned at the center of the liver lobule.⁴

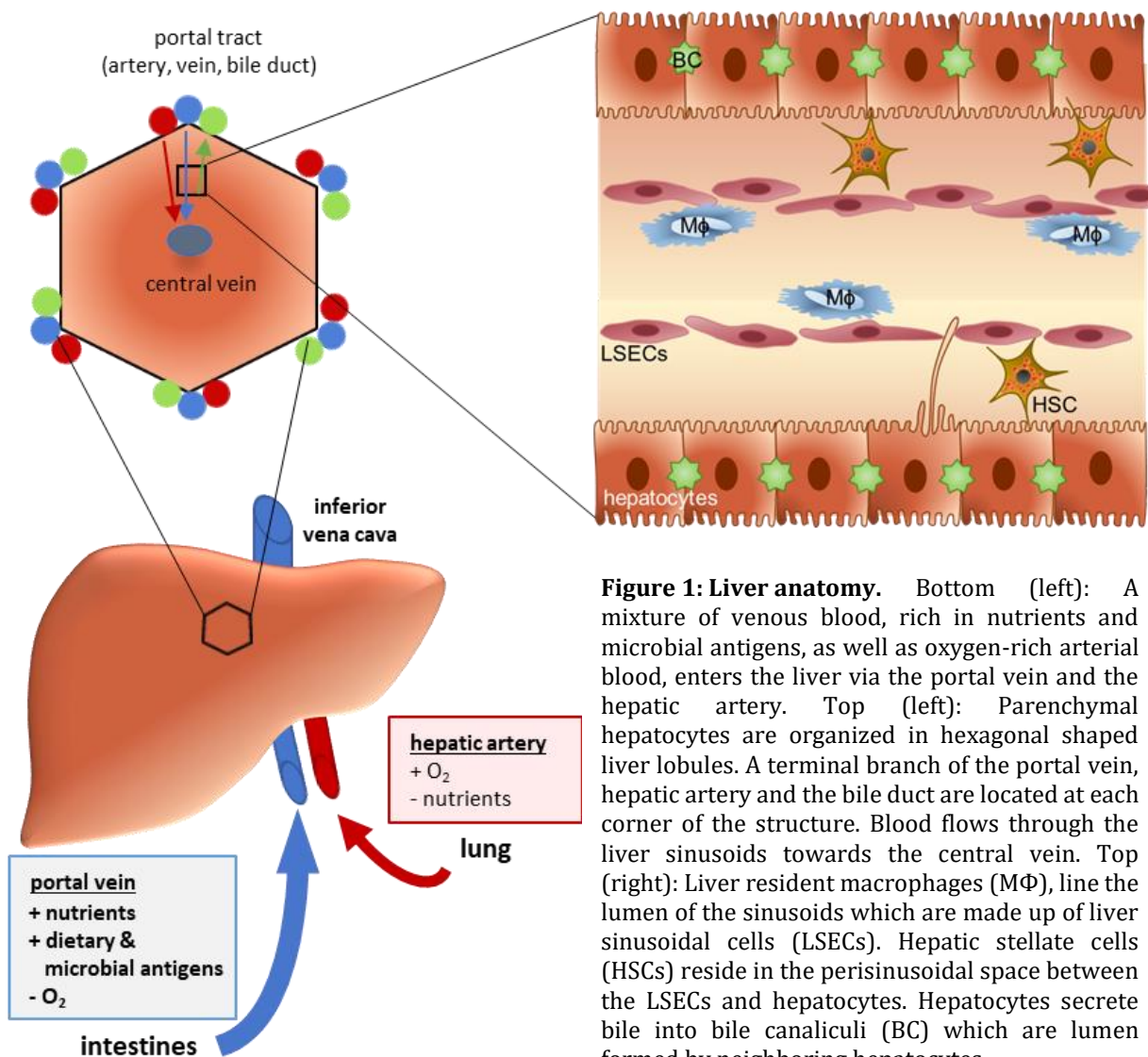


Figure 1: Liver anatomy. Bottom (left): A mixture of venous blood, rich in nutrients and microbial antigens, as well as oxygen-rich arterial blood, enters the liver via the portal vein and the hepatic artery. Top (left): Parenchymal hepatocytes are organized in hexagonal shaped liver lobules. A terminal branch of the portal vein, hepatic artery and the bile duct are located at each corner of the structure. Blood flows through the liver sinusoids towards the central vein. Top (right): Liver resident macrophages (Mφ), line the lumen of the sinusoids which are made up of liver sinusoidal cells (LSECs). Hepatic stellate cells (HSCs) reside in the perisinusoidal space between the LSECs and hepatocytes. Hepatocytes secrete bile into bile canaliculi (BC) which are lumen formed by neighboring hepatocytes.

Hepatocytes, the main parenchymal cells of the liver, are organized in plates around the central vein radiating outward in an increasingly anastomosing fashion toward the portal tracts which are located at each corner of the hexagonal structure. The portal tracts, often referred to as the portal triads, are comprised of one branch of each the portal vein, hepatic artery, and bile duct. Between the plates of hepatocytes run the sinusoids. These are small vessels made up of fenestrated liver sinusoidal endothelial cells (LSECs) that allow for direct exchange of macromolecules between the circulation and hepatocytes. The luminal side of the sinusoids is lined with liver resident macrophages, also called Kupffer cells (KCs). The perisinusoidal space separates sinusoids from the liver parenchyma. Within this space reside the hepatic stellate cells (HSC), which store large amounts of vitamin A within cytoplasmic lipid droplets in a quiescent state but transdifferentiate into pro-fibrotic myofibroblasts upon liver injury. In between the hepatocytes run the bile canaliculi, which are tubular structures formed by apical microvilli of neighboring hepatocytes.⁴⁻⁶

The liver performs a series of metabolic functions, which include the production, storage, and donation of carbohydrates, lipids, and proteins. It produces and excretes bile and is further responsible for detoxification of potentially harmful dietary products, toxins, microbial compounds, and metabolites. The liver serves as the body's main store of iron, it controls the blood sugar level, oncotic pressure, and performs organ-specific as well as systemic immune surveillance and modulation. Due to this diverse functional repertoire and its central position in the systemic circulation, the liver plays a critical role in the maintenance of overall health.⁴

1.2 Chronic liver disease

Chronic liver disease (CLD) is a major global health burden and the cause of over a million deaths each year making up 2 % of all deaths worldwide.⁷ CLD is loosely defined as a progressive parenchymal injury of the liver resulting in fibrosis and cirrhosis.⁸ This broad definition includes a wide spectrum of pathologies including viral infections, substance abuse, metabolic disorders, and autoimmune liver disease. Despite these greatly varying etiologies with unique mechanisms of injury, CLD progresses through distinct stages with a high degree of coherency, independent of the underlying pathology. Initial tissue injury in form of intense cellular stress and cell death leads to the activation of liver resident immune

cells and further the recruitment of circulating immune cells into the liver. The ensuing inflammatory response is aimed at the rapid eradication of potential harm e.g. infected, damaged or malignant cells. Removal of the source of injury would then induce the resolution of inflammation, promotion of regeneration, and the restoration of homeostasis. However, when the source of initial injury cannot be removed, sustained inflammation leads to continued cell death and the successive displacement of functional liver parenchyma by non-functional scar tissue, in a process called fibrosis (Figure 2).⁹

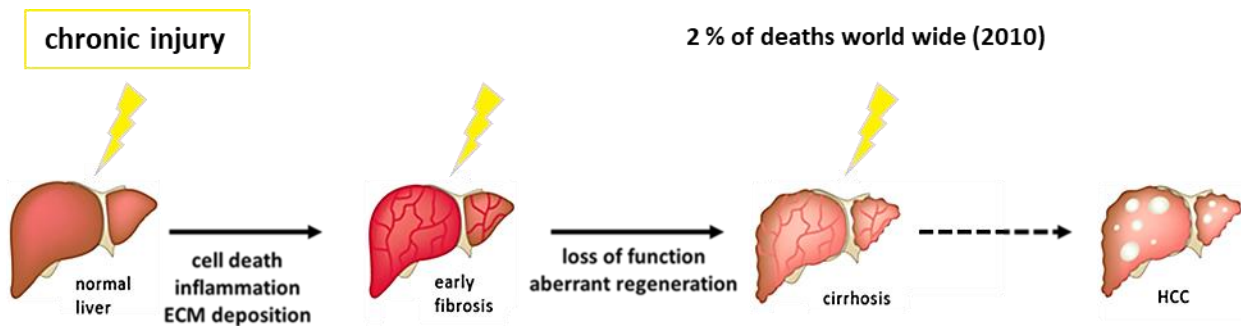


Figure 2: Progression of chronic liver disease. Tissue injury in form of cell death initiates an inflammatory response that intensifies cellular decay and activates pro-fibrotic cell types to produce an ECM scaffold to maintain the structural integrity of the liver (fibrosis). Over time, increasing displacement of liver tissue with non-functional scar tissue leads to liver failure (cirrhosis). Furthermore, chronic inflammation in combination with sustained proliferation increases the risk of malignant transformation and subsequent tumor development. Adapted from Pellicoro *et al.*, 2014.⁹

HSCs are termed master regulators of fibrosis. Activated HSCs transdifferentiate into myofibroblasts and become the major source of extracellular matrix components (ECM) including collagens, but also enzymes involved in ECM remodeling such as matrix metalloproteinases (MMPs) and their tissue inhibitors (TIMPs).⁹ To maintain liver function, hepatocytes continuously proliferate to replace tissue lost to inflammation. Over time sustained liver injury accompanied by progressive fibrotic tissue remodeling eventually leads to irreversible liver cirrhosis and subsequent liver failure. Furthermore, sustained regenerative proliferation in an inflammatory environment increases the risk of proliferation-induced mutagenesis and consequently malignant transformation and tumor development. In accordance with that, approximately 80 % of all cases of hepatocellular carcinoma (HCC), the fourth most common cause of cancer-related deaths, arise in chronically inflamed and cirrhotic livers (Figure 2).^{10,11}

1.2.1 The role of cytokines in chronic liver inflammation

Chronic inflammation is a complex multilayered process that is shaped by a multitude of pleiotropic influences. Important mediators of inflammation are cytokines. These small signaling molecules with pro- as well as anti-inflammatory properties, regulate the activation state, differentiation and subset-specific recruitment of immune cells.^{12,13} Furthermore, they facilitate a variety of cellular responses in parenchymal cells including the induction of cell death, the release of inflammatory mediators and proliferation. Due to their pleiotropic functions, cytokines play an essential role in the onset as well as the maintenance of inflammation. The composition of the cytokine milieu is, therefore, a key factor in determining the type, magnitude, duration and ultimately the outcome of the inflammatory response.¹⁴

2.2.1.1 Tumor necrosis factor α receptor 1 signaling and chronic inflammation

TNF α is a well-described pro-inflammatory cytokine that is closely associated with many types of inflammatory diseases including acute as well as chronic liver inflammation. Increased TNF α -mediated signaling has been shown to amplify cell death, promote the release of pro-inflammatory cytokines, and facilitates the activation of immune cells as well as pro-fibrotic HSCs upon liver injury.^{15,16} Despite these pathological functions, TNF α is also essential for the induction of pro-survival signaling, regenerative proliferation in parenchymal cells and adequate immune responses to protect against infection.^{17,18}

TNF α has two known receptors, TNF α receptor (TNFR) 1 and 2. Despite the considerable overlap in their downstream signaling cascades, many of the pathological functions of TNF α have been ascribed to TNFR1 rather than TNFR2. This is in part due to differences in their expression patterns, their affinity to soluble TNF α and the ability to directly induce cell death, which is exclusive to TNFR1. TNFR1 is ubiquitously expressed in all cell types and shows a high affinity for both the membrane-bound and soluble form of TNF α . In contrast, TNFR2 is primarily expressed in bone marrow-derived cells and has a much higher affinity to the membrane-bound form.¹⁹

Figure 3 depicts a simplified overview of the signaling cascade initiated by TNFR1 and its potential functional consequences.

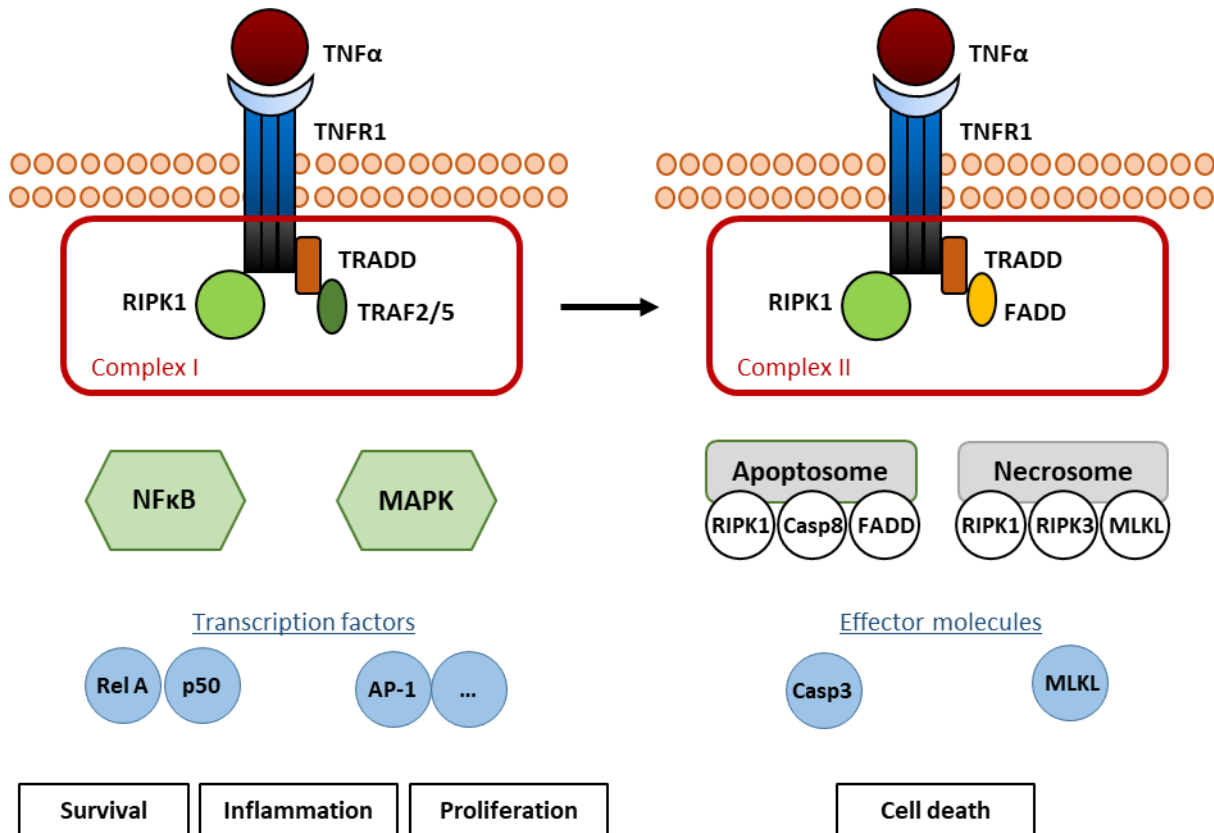


Figure 3: Simplified overview of signaling pathways induced by TNFR1. Binding of TNF α to TNFR1 leads to the formation of receptor complex 1 through the recruitment of receptor-interacting kinase (RIPK) 1, TNFR1 associated death domain protein (TRADD) and TNF α receptor-associated factors 2 and 5 (TRAF2/5). Downstream signaling of complex I induces the Nuclear Factor κ of activated B cells (NF κ B) and the mitogen-activated protein kinase (MAPK) pathway via the activation of several transcription factors including the heterodimer RelA/p50 and activator protein 1 (AP-1)). These transcription factors induce the expression of multiple genes involved in cell survival, inflammation, differentiation, and proliferation. If complex I is not stabilized, cell death pathways for either apoptosis or necroptosis are induced. Apoptosis is mediated by the effector Caspase 3 (Casp3) which is activated in response to the formation of the apoptosome consisting of RIPK1, Caspase 8 (Casp8) and Fas associated protein with death domain (FADD). Necroptosis is mediated by necrosome consisting of RIPK1, RIPK3 and mixed lineage kinase like (MLKL) leading to the activation of MLKL and subsequent pore formation in the cell membrane.

The binding of TNF α to TNFR1 leads to the trimerization of the receptor chains. This conformational change allows the recruitment of receptor-interacting kinase (RIPK) 1, TNFR1 associated death domain protein (TRADD) and TNF α receptor-associated factors 2 and 5 (TRAF2/5). These and other accessory proteins form the proximal receptor complex I. Anti-apoptotic mediators such as cellular inhibitors of apoptosis 1 and 2 (cIAP1/2; not shown) stabilize this complex and initiate the recruitment of further active components. Sequential phosphorylation and ubiquitination events lead to the initiation of the nuclear factor κ of activated B cells (NF κ B) and the mitogen-activated protein kinase (MAPK)

pathway. Both pathways involve the activation of transcription factors and their subsequent translocation into the nucleus. Target genes of the NF κ B heterodimer, consisting of p50 and RelA, include a variety of genes including those of pro-inflammatory cytokines such as IL-6, IL-1 β , and TNF α , growth factors, as well as pro-survival mediators that inhibit the induction of cell death upon TNFR1 activation. Beyond perpetuating inflammation, cytokines like IL-6 initiate additional responses in target cells including proliferation.²⁰ Similarly, activation of the MAPK pathway is transduced by the release of an array of transcription factors including activator protein 1 (AP-1) that induce the expression of a wide array of mediators of inflammation, differentiation, and proliferation.²¹

TNFR1 also contains an intracellular death domain that can induce cell death in form of apoptosis and necroptosis.²² However, cell death only occurs when increased TNF α levels coincide with additional stress signals that in combination inhibit or override the strong pro-survival signals induced via NF κ B activation. In that case, complex I is destabilized, which leads to the internalization of the receptor complex and the recruitment of Fas-associated protein with death domain (FADD) to TRADD. This serves as the base for the formation of complex II, which in the presence of Caspase (Casp) 8 leads to the formation of the apoptosome. Core components of the apoptosome are either TRADD, FADD, and Casp8 (complex IIa; not shown) or alternatively RIPK1, FADD, and Casp8 (complex II2b). Activation of Casp8 initiates the downstream activation of effector Casp3, which ultimately induces the sequential fragmentation of cellular structures including DNA and the packaging of cellular components into small vesicles that are taken up by neighboring phagocytes.²³

Necroptotic cell death downstream of TNFR1 activation is mediated by the necrosome, which consists of RIPK1, RIPK3, and mixed lineage kinase like (MLKL). Upon autophosphorylation of RIPK3 by the RIPK1/RIPK3 complex, RIPK3 in turn activates MLKL via phosphorylation. Active MLKL forms a pore complex in the cell membrane leading to necroptosis by disrupting membrane integrity.

Regulated cell death is an essential function for the maintenance of tissue homeostasis and the survival of multicellular organisms.²³ On the other hand, cell death in response to injury leads to the release of intracellular components into extracellular space. These components are recognized by immune cells as damage associated molecular patterns (DAMPs), which

lead to their activation. Consequently, increased cellular demise drives inflammatory responses and subsequent tissue destruction, which makes it a central feature in chronic inflammatory diseases including CLD.

1.2.2 Immune cells shape the progression of chronic liver disease

Immune cells are both the main source and target of cytokines. The liver is populated with a unique composition of immune cells that protect the body from potentially harmful substances such as toxins or pathogens escaping from the intestinal tract into the venous circulation. During homeostasis, liver resident immune cells remain in a hyporesponsive state as they are continuously exposed to foreign dietary products and microbial compounds derived from commensal intestinal bacteria. However, an increased concentration of pathogen associated molecular patterns (PAMPs) or DAMPs released from dying cells, leads to the initiation of pro-inflammatory signaling cascades in hepatic antigen-presenting cells (APCs). These signaling cascades induce the upregulation of major histocompatibility complex (MHC) I and II, co-stimulatory molecules, and the release of pro-inflammatory cytokines. In response, massive amounts of infiltrating immune cells such as T cells, neutrophils, and monocytes enter the liver to amplify immune responses.²⁴

2.2.2.1 T helper cells

Among the infiltrating T cells are large numbers of naïve CD4⁺ T helper (T_H) cells which differentiate into specific subsets upon activation by liver resident APCs. Several distinct lineages of T_H cells have been identified including T_H1, T_H2, and T_H17 cells. Naïve CD4⁺ T cells commit to their lineage in response to the local cytokine milieu. For each T_H cell subset, a specific cytokine profile has been identified which leads to the induction of a master transcription factor that initiates a complex transcriptional network that orchestrates the differentiation into mature T effector cells or regulatory T cells. Differentiation of T_H1 cells is induced in response to IL-12, which activates the transcription factor Tbet that facilitates the maturation of IFN γ producing T_H1 cells. Naïve CD4⁺ T cells differentiate into T_H2 cells in response to IL-4, which activates the transcription factor GATA3 and leads to the production of IL-4, IL-13, and IL-5. The more recently identified T_H17 cells develop in the presence of IL-1 β , IL-6, and TGF β , but need IL-23 for the induction of pathogenicity. The master

transcription factor for T_H17 cell differentiation is the RAR-related orphan receptor γ t (ROR γ t). Activated T_H17 cells produce large amounts of IL-17, IL-21, and IL-22.²⁵ T_H cells exert several inflammatory and immune-modulatory functions during CLD, which include recruitment and activation of other immune cells and shaping of the cytokine composition.²⁶

2.2.2.2 Neutrophils

Neutrophils are important cellular components of the innate immune response to tissue injury of an infectious or sterile nature. Tissue injury leads to the release of cytokines with chemotactic properties called chemokines. Neutrophils are recruited to the site of injury by several chemokines including CC chemokine ligand (CCL) 2 and CXC chemokine ligand 1 (CXCL1). The upregulation of adhesion molecules on endothelial cells facilitates the arrest of circulating neutrophils and transmigration through the vascular bed into the tissue. Neutrophils are activated by pro-inflammatory cytokines including TNF α , IL-1 β , and IL-17, as well as components of the complement system. During inflammation, the main function of neutrophils is the removal of dead or dying cells as well as cellular debris, which would then induce the resolution of inflammation by removing the pro-inflammatory stimuli. However, prolonged activation of neutrophils leads to the release of major pro-inflammatory mediators including reactive oxygen species (ROS), tissue degrading elastase, as well as Fas ligand (FasL). Interactions between FasL and its receptor Fas promote apoptosis in target cells in a similar fashion as observed for activation of TNFR1 by TNF α .²⁷

2.2.2.3 Monocytes

Different monocytic subtypes continuously circulate within the bloodstream and are recruited to the site of injury via chemokines. Within the diverse repertoire of monocytes, specific subtypes are distinguished by their expression of distinct chemokine receptors, which include C-C chemokine receptor type 2 (CCR2) and CX3C chemokine receptor 1 (CX3CR1)²⁸. Infiltrating monocytes differentiate into monocyte-derived macrophages or DCs with either pro-inflammatory or restorative functions depending on the microenvironment. Inflammatory monocytic subsets produce large amounts of pro-inflammatory and pro-fibrotic cytokines, growth factors and ROS, while restorative subsets produce anti-

inflammatory mediators and promote healing by removing dying cells, cellular debris or infectious particles through phagocytosis.²⁹

1.3 Bile

The liver produces approximately 0.75 L of bile per day, which makes it the largest gland in the human body. Bile is an aqueous secretion with a water content of approximately 95 %. Solid components include primary bile acids (BAs), phospholipids, cholesterol, conjugated bilirubin, hormones, cytokines, and antibodies. Bile functions as the main excretory route for cholesterol and other lipophilic substances, such as environmental toxins, xenobiotics, and drugs. Bile is produced in the liver and delivered to the intestine via the common bile duct. In the intestine, BAs are essential for the emulsification of dietary fats and fat-soluble vitamins, which facilitates their uptake by the intestinal epithelium (Figure 4).^{30,31}

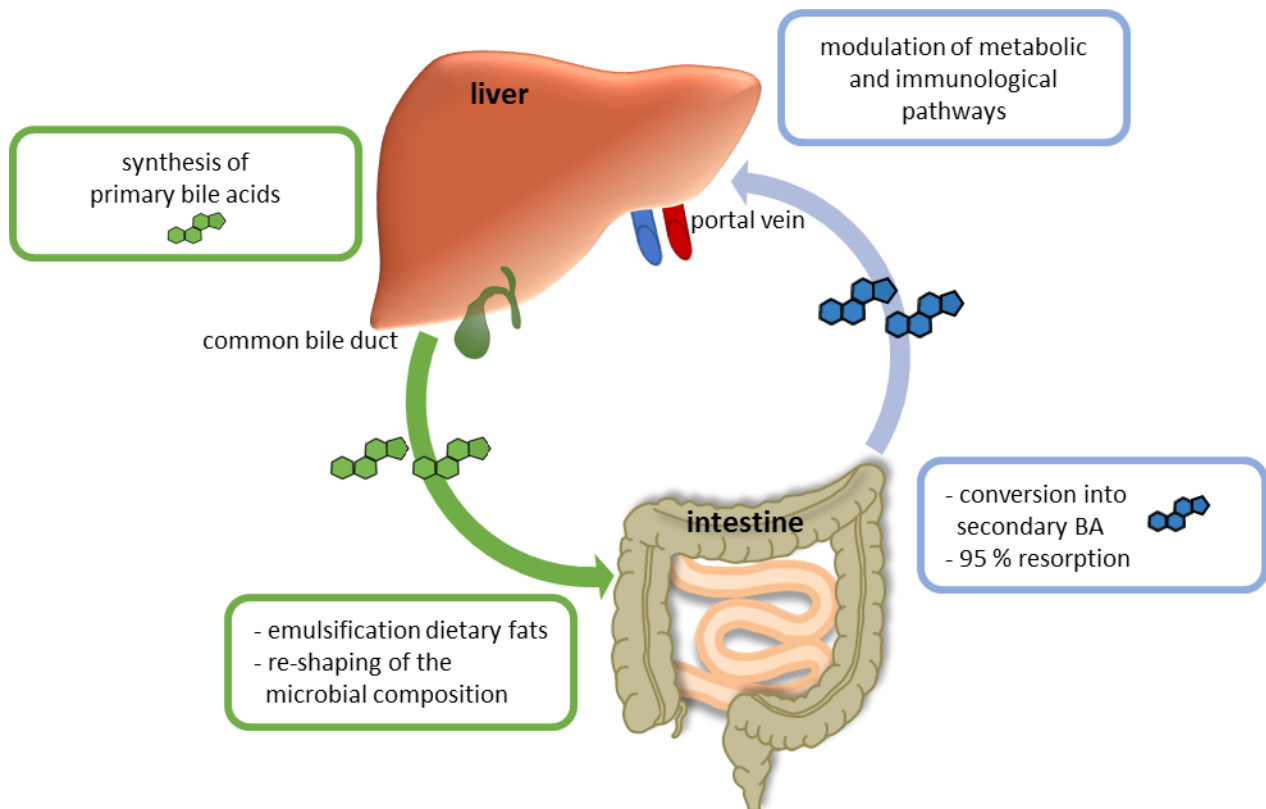


Figure 4: Enterohepatic circulation. The liver produces bile acids (BAs) and other biliary components that are delivered to the intestine via the common bile duct. BAs are converted into secondary BAs by the gut microbiota, which are re-adsorbed and transported to the liver via the portal vein. In the liver secondary BAs facilitate signaling pathways involved in the modulation of both metabolism and hepatic inflammation.

The liver-derived BA pool and other biliary components shape the microbial composition of the intestinal microbiota and immune cell composition. In turn, primary BAs are converted into secondary BAs by the intestinal microbiota which are reabsorbed and transported back to the liver via the portal vein. In the liver, secondary BAs act as signaling molecules that modulate a series of metabolic and inflammatory pathways. This bidirectional communication between the liver and the intestine via bioactive biliary components is called the enterohepatic circulation (Figure 4).³¹

Disturbances in bile synthesis, composition and/or flow are associated with severe consequences for the liver including cholestasis as well as liver inflammation, but are also often reflected in malabsorption, dysbiosis and inflammatory responses in the intestine.^{30,31} Primary sclerosing cholangitis (PSC) is a prominent example of a chronic biliary disease that is tightly associated with pathologies of the intestine. While the underlying cause of PSC remains unknown, 80 % of PSC patients suffer from comorbid inflammatory bowel disease (IBD), which is assumed to promote disease progression in the liver.³² To date there are no curative treatment options, which necessitates a liver transplantation for most PSC patients.³³ A well-established mouse model for the study of PSC is the MDR2 knockout mouse model as it closely resembles liver histopathology and disease progression observed in PSC patients.³⁴

1.3.1 The multi-drug resistance p-glycoprotein 2 knockout mice

The murine multi-drug resistance p-glycoprotein 2 (MDR2) and its human homolog MDR3 are transmembrane transporters belonging to the ATP binding cassette subfamily B (ABCB) and play an essential role during bile formation. The MDR2 protein facilitates the transport of phosphatidylcholine (PC) from the inner leaflet of the hepatocyte membrane to the luminal side of the bile canaliculi. Primary BAs enter the canaliculi via the bile salt export pump (Bsep) and extract PC from the luminal side of the hepatocyte membrane and incorporate it into their micelle structure forming mixed micelles. PC drastically reduces the detergent properties of BA micelles, while simultaneously increasing the capacity to incorporate cholesterol.³⁵ Cholesterol is transported into the canaliculi by sterolin, a heterodimer formed

by ABC subfamily G 5 and G 8. In the canaliculi cholesterol is solubilized for transport by mixed micelles of BAs and PC (Figure 5; left).³⁶

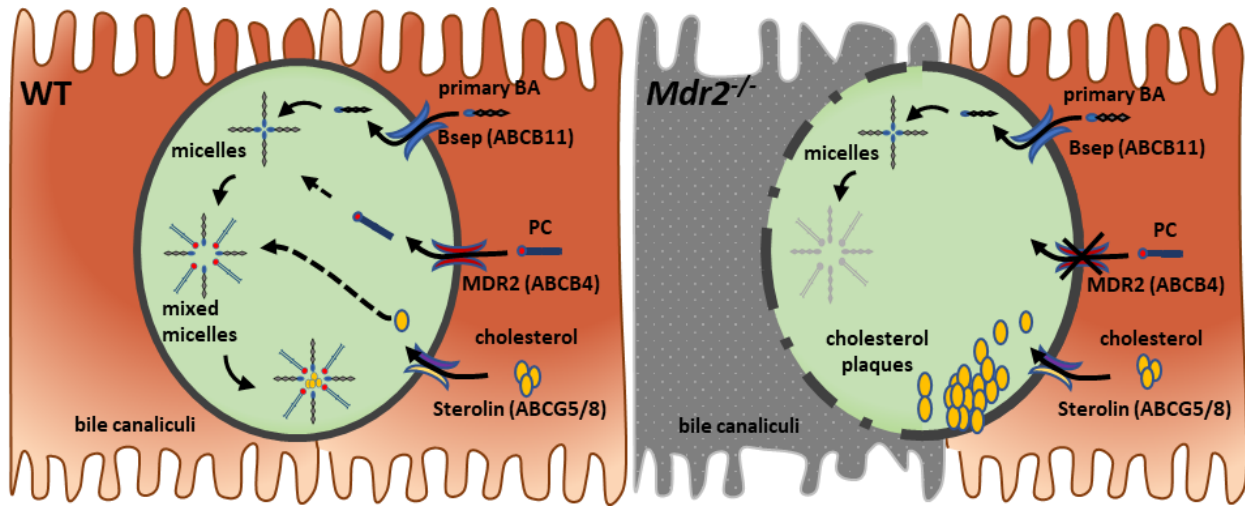


Figure 5: Role of multi-drug resistance p-glycoprotein 2 (MDR2) in bile excretion. Primary bile acids (BAs) are transported across the hepatocytes membrane by the bile export pump (Bsep). In the bile canaliculi BAs form micelles with high detergent activity. In the healthy liver (left) MDR2 transports phosphatidylcholine (PC) from the inner to the outer leaflet of hepatocyte membranes. PC is incorporated into BA micelles, which leads to reduced detergent properties of BAs and increased cholesterol solubility. In the absence of MDR2 (right), hydrophobic BAs damage surrounding hepatocytes causing long-term tissue injury. Furthermore, cholesterol is insufficiently solubilized which leads to plaque formation and regurgitation of toxic bile.

Genetic ablation of *Mdr2* in mice (*Mdr2*^{-/-}) leads to the complete absence of PC in bile, resulting in an accumulation of cytotoxic BAs with high detergent activity. In addition, cholesterol evacuation is severely impaired in *Mdr2*^{-/-} mice, which leads to plaque formation causing cholestatic accumulation of toxic bile (Figure 5; right).³⁷ Persistent exposure to cytotoxic BAs causes cellular stress responses and eventual cell death of hepatocytes and bile duct epithelial cells, resulting in leakage of toxic bile into the parenchyma. Livers of *Mdr2*^{-/-} mice show chronic inflammation, bile duct proliferation and portal fibrotic tissue remodeling, similar to livers of PSC patients.³⁴ In addition to the investigation of inflammatory and fibrotic responses, *Mdr2*^{-/-} mice have been used to investigate the underlying mechanisms of inflammation associated tumor development as they reliably develop HCC within 12 months of age.³⁸

1.4 Aim of the study

Due to the high incidence and mortality rate of CLD, extensive research is currently aimed at improving treatment options. The primary therapeutic objective is the eradication of the source of initial injury. However, in many cases this remains unfeasible as the underlying cause is a genetic predisposition, of multiple origin, or even unknown as is the case for PSC. Accordingly, other avenues of research focus on disrupting pathological processes induced by persistent liver injury. These include pro-inflammatory, pro-fibrotic, and pro-tumorigenic signaling events. TNFR1 is known to promote cell death and drive inflammatory disease progression through multiple pro-inflammatory and pro-fibrotic pathways mediated by NF κ B and MAPK activation. Hence, TNFR1 has been postulated as a potential drug target in CLD. However, the essential involvement in supporting cell survival and regenerative proliferation may ultimately prove TNFR1 as an unsuitable target for therapeutic intervention. This work is aimed to elucidate the role of TNFR1 mediated signaling during chronic cholestatic liver disease, and the consequences of its absence. For that purpose, TNFR1 knockout mice (*Tnfr1*^{-/-}) were bred with *Mdr2*^{-/-} mice creating a double knockout mouse model. It was analyzed how the constitutive knockout of *Tnfr1* in a mouse model of chronic liver inflammation would shape cytokine and chemokine production, immune cell recruitment and ultimately influence disease progression.

2 Materials and Methods

2.1 Technical equipment

Table 1: List of technical equipment

Equipment	Supplier
BD FACSAria™ II	Becton Dickinson, Franklin Lakes, NJ
BD FACSCanto™ III	Becton Dickinson, Franklin Lakes, NJ
BD LSRFortessa™	Becton Dickinson, Franklin Lakes, NJ
C1000 Thermal Cycler	BioRad, München
Centrifuge 5417	Eppendorf, Hamburg
Centrifuge 5810 R	Eppendorf, Hamburg
CK40 microscope	Olympus, Hamburg
Cobas Integra 400	Roche, Basel
constant displacement pump	Medorex e.K., Nörten-Hardenberg
Eppendorf Research® Plus Pipettes	Eppendorf, Hamburg
HandyStep® electronic	BRAND GmbH, Wertheim
KL2 shaker	Edmund Bühler, Hercules, CA
Mini Trans-Blot® Cell	Bio-Rad, Hercules, CA
MSC Advantag, Clean Bench	Thermo Fisher Scientific, Waltham, MA
My Cycler™ thermal cycler	BioRad, München
NanoDrop ND-1000	PEQLAB, Erlangen
PowerPac™ HC High-Current Power Supply	Bio-Rad, Hercules, CA
Roller mixer SRT9	Cole-Parmer, Vernon Hills, IL
TE124S scale	Sartorius, Göttingen
Tecan infinite M200	Tecan, Crailsheim
TissueLyser II	Qiagen, Hilden
VersaDoc™ 4000 MP Imaging System	Bio-Rad, Hercules, CA
vortexer	Heidolph, Schwabach
XCell SureLock™ Electrophoresis System	Thermo Fisher Scientific, Waltham, MA

2.2 Consumables

Table 2: List of consumables

Consumables	Supplier
Abgene PCR tubes	Abgene, ThermoFisher, Hamburg
cell strainer (100 μm)	Corning Inc., Corning, NY
96-well cell culture plates, round bottom	Sarstedt, Nümbrecht
Parafilm M	American National Can, Chatsworth, CA
hollow needles/ canulaes	B.Braun, Melsungen AG, Melsungen
PCR tubes	Kisker Biotech GmbH, Steinfurt
pipette tips (10 μL , 200 μL , 1000 μL)	Sarstedt, Nümbrecht
pipette tips, sterile and RNase free (10 μL , 200 μL , 1000 μL)	Sarstedt, Nümbrecht
pipettes (2 mL, 5 mL, 10 mL, 25 mL)	Sarstedt, Nümbrecht
positive displacement tips (500 μL , 2.5 mL, 5 mL 12.5 mL)	BRAND GmbH, Wertheim
reaction tubes (15 mL, 50 mL)	Sarstedt, Nümbrecht
reaction tubes, sterile and RNase free (1.5 mL, 2 mL)	Sarstedt, Nümbrecht
sealing tape, optically clear	Sarstedt, Nümbrecht
syringe	B.Braun, Melsungen AG, Melsungen
syringe filter 0.22 μm	TPP, Trasadingen
tubes for flow cytometer	Sarstedt, Nümbrecht

2.3 Reagents and Kits

Table 3: List of reagents and kits

Reagents and Kits	Supplier
2-Mercaptoethanol	Thermo Fisher Scientific, Waltham, MA
acetic acid	Roth, Karlsruhe
ALT reagents	Roche, Basel
ALP reagents	Roche, Basel
dNTPs (10mM)	Invitrogen; Thermo Fisher Scientific, Waltham, MA
Entellan mounting medium	Merck, Darmstadt
ethanol (100 %)	Roth, Karlsruhe
heparin-sodium-25000-ratiopharm ®	ratiopharm, Ulm
hydrochloric acid	Roth, Karlsruhe
ketamine	Albrecht GmbH, Aulendorf
LEGENDplex™ Mouse Th Cytokine Panel	Biolegend, San Diego, CA
Maxima™ SYBR Green/ROX qPCR Master Mix (2X)	Fermentas, Thermo Fisher Scientific, Waltham, MA
nuclease-free water	Invitrogen, Thermo Fisher Scientific, Waltham, MA
NucleoSpin RNA II Kit	Machery & Nagel, Düren
NuPage™ LDS sample buffer	Life Technologies, San Francisco, CA
PCR Buffer (10x)	Invitrogen, Darmstadt
penicillin / streptomycin (100U/ml)	Gibco®, Invitrogen, Darmstadt
percoll	GE Healthcare, Glattbrugg/Zürich
PhosSTOP™	Roche, Basel
picric acid	Morphisto, Frankfurt a. M.
Precision Plus Protein™ WesternC™ Standards	Bio-Rad, Hercules, CA
rDNase	Machery & Nagel, Düren
RNeasy® Micro Kit	Machery & Nagel, Düren
Rompun 2 %	Bayer, Leverkusen
RPMI medium	Gibco®, Invitrogen, Darmstadt
Tris/HLC	Roth, Karlsruhe
TrueStain fcX™, Clone: 93	Biolegend, San Diego, CA
trypan blue	Sigma-Aldrich, Taufkirchen

Reagents and Kits	Supplier
tween 20	Roth, Karlsruhe
Verso cDNA Kit	Abgene, Thermo Scientific, Hamburg
xylo	Thermo Fisher Scientific, Waltham, MA

2.4 Buffers and Solutions

Table 4: List of buffers and solutions

Buffer / Solution	Compounds
10x Phosphate Buffered Saline (PBS) [1 L]	137.9 mM NaCl 6.5 mM Na ₂ HPO ₄ x 2 H ₂ O 1.5 mM KH ₂ PO ₄ 2.7 mM KCl ad to 1 L H ₂ O, pH 7.4
10x Tris-buffered saline (TBS) [1 L]	1.5 M NaCl 1 M Tris-Base, Ad to 1 L H ₂ O, pH 7.4
4 % Paraformaldehyde [200 mL]	8 g Paraformaldehyde 20 mL PBS (10x) 10 mM NaOH ad 200 mL H ₂ O, pH 7,4
5 % Milk solution	TBS-T 5 % dry milk powder
Acetate citrate buffer [1 L]	0.88 M Sodium Acetate Tri-hydrate 0.24 M Citric Acid 0.2 M Acetic Acid 0.85 M NaOH ad to 1 L H ₂ O; pH 6.5
Ammoniumchloride (NH ₄ CL) [1 L]	19 mM Tris-HCL 140 mM NH ₄ CL ad to 1 L H ₂ O, pH 7.2
Chloramine-T solution [10 ml]	127 mg Chloramine-T 2 ml n-Propanol [50 % v/v] ad to 10 mL Acetate citrate buffer
ECL solution	1.25 mM Luminol/TrisHCl 15 mM Para-hydroxy-Coumarinacid/DMSO 30 %H ₂ O ₂
Ehrlich's reagent [10 ml]	6.6 mL n-Propanol 3.3 mL Perchloric acid 1.5 g Dimethylaminobenz-aldehyde
Fluorescence activated cell sorting buffer [1 L]	980 mL 1x PBS 2 mL NaN ₃ [0,02 % w/v] 20 mL FCS

Buffer / Solution	Compounds
Hank's Balanced Salt Solution (HBSS) [1 L]	403 mg KCL 53 mg Na ₂ HPO ₄ 54 mg KH ₂ PO ₄ 353 mg NaHCO ₃ 191 mg KCl 102 mg MgCl ₂ 148 mg MgSO ₄ 8 g NaCl 1,11 g D-Glucose Add 1 L H ₂ O, pH 7.4
Ketamine-Xylazine-Heparin	8 % Rompun (2 %) 12% Ketamine (100 mg/mL) 20 % Heparin 5000 (IU/mL) 60 % isotonic NaCl
TBS-T	1 x TBS 0.1 % Tween-20

2.5 Antibodies

Table 5: Antibodies for flow cytometry

	Target	Fluorophore	Clone	Distributed by
T cells	TCR (β chain)	Pe-Cy7	H57-597	BioLegend, San Diego, CA
	CD4	FITC	RM4-5	BioLegend, San Diego, CA
	IL-17	Alexa Fluor 700	TC11-18H10.1	BioLegend, San Diego, CA
Monocytes	CD45	BV570	30-F11	BioLegend, San Diego, CA
	CD11b	Alexa Fluor 700	M1/70	BioLegend, San Diego, CA
	F4/80	APC	REA126	Miltenyi, Bergisch Gladbach
	Ly6G	Pe-Cy7	1A8	BioLegend, San Diego, CA
	CX3CR1	BV785	SA011F11	BioLegend, San Diego, CA
	Fluorescence-activated cell sorting			
	CD11b	PerCp-Cy5.5	M1/70	BioLegend, San Diego, CA
	CX3CR1	BV785	SA011F11	BioLegend, San Diego, CA

TCR: T cell receptor; CD: Cluster of differentiation; IL: Interleukin; APC: Allophycocyanin; BV: Brilliant Violet; FITC: Fluorescein isothiocyanate.

Table 6: Antibodies for western blot

Target	Host	Clone	Conjugate	Distributed by
primary antibody				
Caspase 3	rabbit	IG10	none	Cell Signalling, Danvers, MA
P-RIPK3	goat	EPR9516(N)-25	none	Abcam, Cambridge, UK
P-MLKL	goat	EPR9515(2)	none	BD Pharmigen, San Jose, CA
GAPDH	goat	polyclonal	none	Santa Cruz, Dallas, TX
secondary antibody				
anti-rabbit IgG	goat	polyclonal	HRP	Jackson Immunoresearch, West Grove, PA
anti-mouse IgG	horse	polyclonal	HRP	Cell Signalling, Danvers, MA
anti-goat IgG	rabbit	polyclonal	HRP	Jackson Immunoresearch, West Grove, PA

HRP: horseradish peroxidase

2.6 Oligonucleotide sequences

Table 7: List of oligonucleotide sequences used in RT-qPCR

Target	Forward Primer	Reverse Primer	Reference
<i>Acta2</i>	GCATCCACGAAACCACCTAT	AGGTAGACAGCGAAGCCAAG	X13297
<i>Afp</i>	AGCAAAGCTGCGCTCTCTAC	GAGTTCACAGGGCTTGCTTC	NM007423
<i>Atp5b</i>	ATTGCCATCTTGGGTATGGA	AATGGGTCCCACCATGTAGA	NM_016774
<i>Ccl2</i>	TCCCAATGAGTAGGCTGGAG	GCTGAAGACCTTAGGGCAGA	NM_011333.3
<i>Ccna2</i>	GTGGTGATTCAAACTGCCA	AGAGTGTGAAGATGCCCTGG	NM_009828.2
<i>Ccr6</i>	GTTGAACATGGCCATCACAG	CGTCAGTGTCTGGAGCGTA	NM001190333
<i>Cdk1</i>	GGCGACTCAGAGATTGACCA	TTGCCAGAGATTTCGTTTGGC	NM_007659.3
<i>Col1a1</i>	GAGCGGAGAGTACTGGATCG	TACTCGAACGGGAATCCATC	NM007742
<i>Col3a1</i>	GTCCACGAGGTGACAAAGGT	GATGCCCACTTGTTCCATCT	NM009930
<i>Cxcl1</i>	GCTGGGATTCACCTCAAGAA	TGGGGACACCTTTTAGCATC	NM_008176.3
<i>Cxcr6</i>	TAGTGGCTGTGTTCCCTGCTG	GGCAGCCGATATCCTTCATA	NM030712
<i>Il17a</i>	TCCAGAAGGCCCTCAGACTA	AGCATCTTCTCGACCCTGAA	U043088
<i>Il1b</i>	TCATGGGATGATGATGATAAC	CCCATACTTTAGGAAGACACG	NM_008361.4
<i>Il23</i>	GA CTCAGCCAACTCCTCCAG	GGCACTAAGGGCTCAGTCAG	NM031252
<i>Mmp2</i>	CAGCAAGTAGATGCTGCC	CAGCAGCCCAGCCAGTC	NM008610
<i>Mmp9</i>	CATTCGCGTGGATAAGGAGT	ACCTGGTTCACCTCATGGTC	NM_013599
<i>Pcna</i>	CCACATTGGAGATGCTGTTG	CAGTGGAGTGGCTTTTGTGA	X53068
<i>Ripk1</i>	CCCCGATTTGAAGAGGCTTG	CTTCGTTTCCAGCTCCTTCG	X80937
<i>Ripk3</i>	GTACTTGGACCCAGAGCTGT	CTGTACACACTGTTTCCCG	AF178953
<i>Rorc</i>	GAGCCAAGTTCTCAGTCATGAG	GGCCAAACTTGACAGCATCT	AAD46913
<i>Spp1</i>	CTCTGATCAGGACAACAAC	CCTCAGAAGATGAACTCTC	AF515708
<i>Tgfb1</i>	GAAGTGGATCCACGAGCC	CTGCACTTGCAGGAGCGC	M13177
<i>Timp1</i>	CATCAATGCCTGCAGCTTC	CAAGCAAAGTGACGGCTC	NM011593
<i>Timp2</i>	CTCTGTGACTTCATTTGTC	CACGCGCAAGAACCATCAC	NM011594
<i>Tnfaip3</i>	CCAGGTTCCAGAACAATGTC	CTC CAT ACAGAGTTCTC AC	U19463

2.7 Software and databases

Table 8: Software and databases

Software	Distributor
MS Office 2010	Microsoft GmbH
Windows 10	Microsoft GmbH
GraphPad Prism 7	GraphPad Software
TBASE	Abase
BD FACS Diva™	BD Biosciences
Flowjo	BD Biosciences
Mendeley	Elsevier
Keyence BZ-II Analyzer	Keyence

2.8 Mice

For the analysis of the phenotypic characteristics of the *Tnfr1 Mdr2* double knockout mice (*Tnfr1*^{-/-}/*Mdr2*^{-/-}) a C57BL/6 background was chosen. The *Mdr2* knockout (*Mdr2*^{-/-}; C57BL/6.129P2-Abcb4tm1Bor) mice were kindly provided by Daniel Goldenberg (Jerusalem, Israel) and the *Tnfr1* knockout (*Tnfr1*^{-/-}; C57BL/6-Tnfrsf1atm1Imx/J) mice were kindly provided by Volker Vielhauer (Munich, Germany). The double knockout was generated by crossbreeding of homozygous specimen of the single knockouts. All mice were bred in the Manfred Eigen Campus of the University Medical Center Hamburg Eppendorf (UKE) under specific pathogen free conditions. Mice were transferred to the barrier 1 of the animal husbandry of the UKE two weeks before mice were sacrificed and organs were harvested for analysis. Mice were housed in individual ventilated cages under controlled conditions (22 °C, 55 % humidity, and 12-hour day-night rhythm) and fed a standard laboratory chow (LasVendi, Altromin). All mice received human care according to the guidelines of the National Institutes of Health as well as to the legal requirements in Germany.

Unless specified otherwise, the following analyses were performed using female mice of the respective genotypes at 12 weeks of age. Female *Mdr2*^{-/-} mice have proven to present with an increased pathological phenotype, allowing for a more detailed analysis of the underlying processes³⁹. The age of 12 weeks was chosen, in order to be able to see both the inflammatory processes which are strongest at early time points and fibrotic remodeling which is only seen in older mice⁴⁰.

2.9 Sampling of biological material

The mice were anesthetized by an intravenous injection of (100 µL/10 g mouse) a ketamine [120 mg/ kg] xylazine [16 mg/ kg] heparine [8333 I.E./ kg] solution and sacrificed by cervical dislocation. Cardiac blood was retrieved via syringe (0.40 x 12 mm needle) and centrifuged for 5 min (2×10^4 xg; 4 °C). Plasma was retrieved and stored at -20 °C prior to the analysis of liver enzyme activity and cytokine concentrations. The liver was removed and dissected according to further use. Liver tissue samples for RNA and protein isolation as well as for quantification of hepatic hydroxyproline content were shock frozen in liquid nitrogen. The quadrate lobe was placed in 4 % para-formaldehyde (PFA) and later embedded in paraffin for histological analysis. The remaining liver mass was placed in Hank's balanced salt solution (HBSS) and used for flow cytometric analysis of the immune cell compartment.

2.10 Assessment of liver enzyme activity

Liver damage was assessed by measuring plasma enzyme activity of alanine aminotransferase (ALT) and alkaline phosphatase (ALP) with a Cobas Integra 400. Prior to analysis plasma samples were diluted 1:5 with ddH₂O.

2.11 Isolation of hepatic non-parenchymal cells

The liver was passed through a cell strainer (100 µm; Corning, CA) and collected in HBSS. After centrifugation (5 min; 500 xg; RT), the pellet was resuspended in a 36 % Percoll solution containing heparin (100 U/ L) and centrifuged (20 min, 800 xg, brake: 7; RT). The top layer containing cellular debris was removed and the supernatant discarded. Erythrocytes were removed by resuspension and incubation (10 min) in ammonium chloride (140 mM) containing Tris/HCl (19 mM). After centrifugation (5 min; 500 xg; 4 °C), the non-parenchymal cells (NPCs) were resuspended in RPMI Medium containing 10 % fetal calf serum, and 1 % penicillin-streptomycin, and counted using a Neubauer chamber.

2.12 *Ex vivo* restimulation of hepatic NPCs

NPC were restimulated *ex vivo* in order to analyze cytokine production either in the culture supernatant or intracellularly. For that purpose, a total of 5×10^5 NPCs per liver were transferred into a 96-well round bottom culture dish (1×10^5 cells/ well) and were incubated in RPMI medium containing FCS (10 %), Pen-Strep (1 %), phorbol 12-myristate 13-acetate (PMA, 50 ng/ mL), and ionomycin (1 μ g/mL) for 4 h at 37 °C. The supernatant was collected after centrifugation (300 xg, 10 min, RT) and stored at -20 °C until further analysis. For the analysis of T_H17 cells via flow cytometry cytokine secretion needed to be inhibited. For that purpose, Brefeldin A (50 ng/ mL) and Monensin (1 μ g/ mL) were added to the medium to allow for intracellular cytokine accumulation.

2.13 Flow cytometry

2.13.1 Staining and analysis of hepatic NPCs

T cell and myeloid cell subsets in the liver were analyzed via flow cytometry according to a standard protocol. In brief, 1×10^6 NPCs, either freshly isolated or restimulated *ex vivo* as described above (section 2.12), were pre-treated with an anti-CD16/32 antibody (clone: 93) in order to block unspecific antibody binding to F_c-receptors. After cells were washed (PBS, 500 xg, 4 °C), they were stained with the respective antibody cocktail, which included a viability dye (Fixable Viability Dye eFluor™ 506. Details about the antibodies used in the respective cocktails are summarized in Table 5. For the analysis of monocytes, cells were then washed a final time (PBS, 500 xg, 4 °C) and analyzed with a LSR Fortessa™ flow cytometer. Cells stained with the antibody cocktail for the analysis of T cell subsets, were permeabilized using the BD Cytofix/Cytoperm™ Kit according to manufacturer's instructions. The cells were then incubated with the anti-IL-17A antibody, washed twice, and also analyzed with a LSR Fortessa™ flow cytometer.

2.13.2 Gating strategy

The collected flow cytometric data was analyzed using Flowjo software. The gating strategy applied to identify T cell subsets is outlined in Figure 6. Initially leukocytes were identified

within the cellular debris according to their size (area of forward scatter: FSC-A) and granularity (area of sideward scatter: SSC-A). In order to exclude cell aggregates, cells were plotted according to their height (FSC-H) vs. size (FSC-A) and single cells were gated as a diagonal line. Next, cells that did not take up the viability dye were gated as living cells. T cells were identified by their expression of the common β chain of the T cell receptor (TCR β). Within these cells CD4⁺ T cells and further the IL-17A expressing TH17 cells were identified.

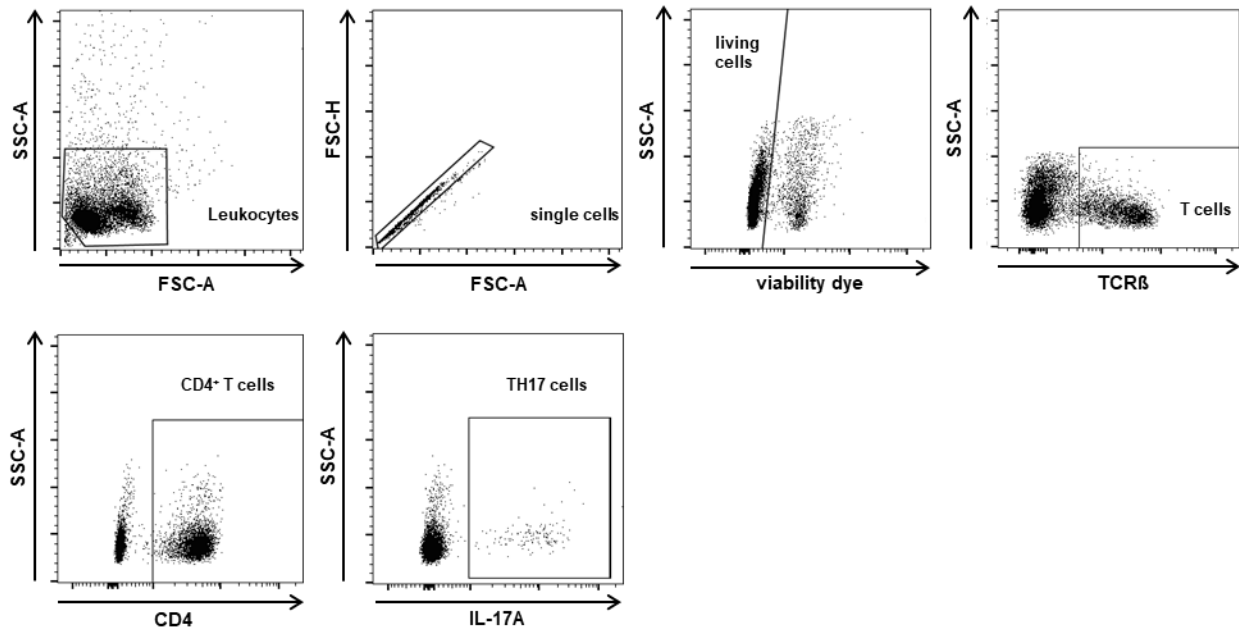


Figure 6: Gating strategy for flow cytometric analysis of T cell subsets. Representative dot blots of the gating strategy applied to identify TCR β ⁺ T cells, CD4⁺ T cells and IL-17A producing TH17 cells in livers of *Mdr2*^{-/-} and *Tnfr1*^{-/-}/*Mdr2*^{-/-} mice.

For the analysis of the myeloid cell subsets, depicted in Figure 7A, initial gating also included gates for the exclusion of debris, single and living cells. However, the first gate also included cells higher in SSC-A and FSC-A to allow for bigger cells and those of higher granularity. Living cells were then plotted CD11b vs Ly6G which allowed the identification of CD11b⁺Ly6G⁺ neutrophils. In addition, living cells were gated on the single CD11b⁺ population. Within these cells F4/80⁺ macrophages were identified. The gating strategy applied to analyze the CX3CR1 expression of CD11b⁺ cells is displayed in Figure 7A. In addition to the gating strategy described above, cells were also gated for CD45⁺, which is an additional marker to identify total leukocytes. Otherwise, the gating strategy included gates for the exclusion of debris, single cells, and living cells and CD11b⁺ cells.

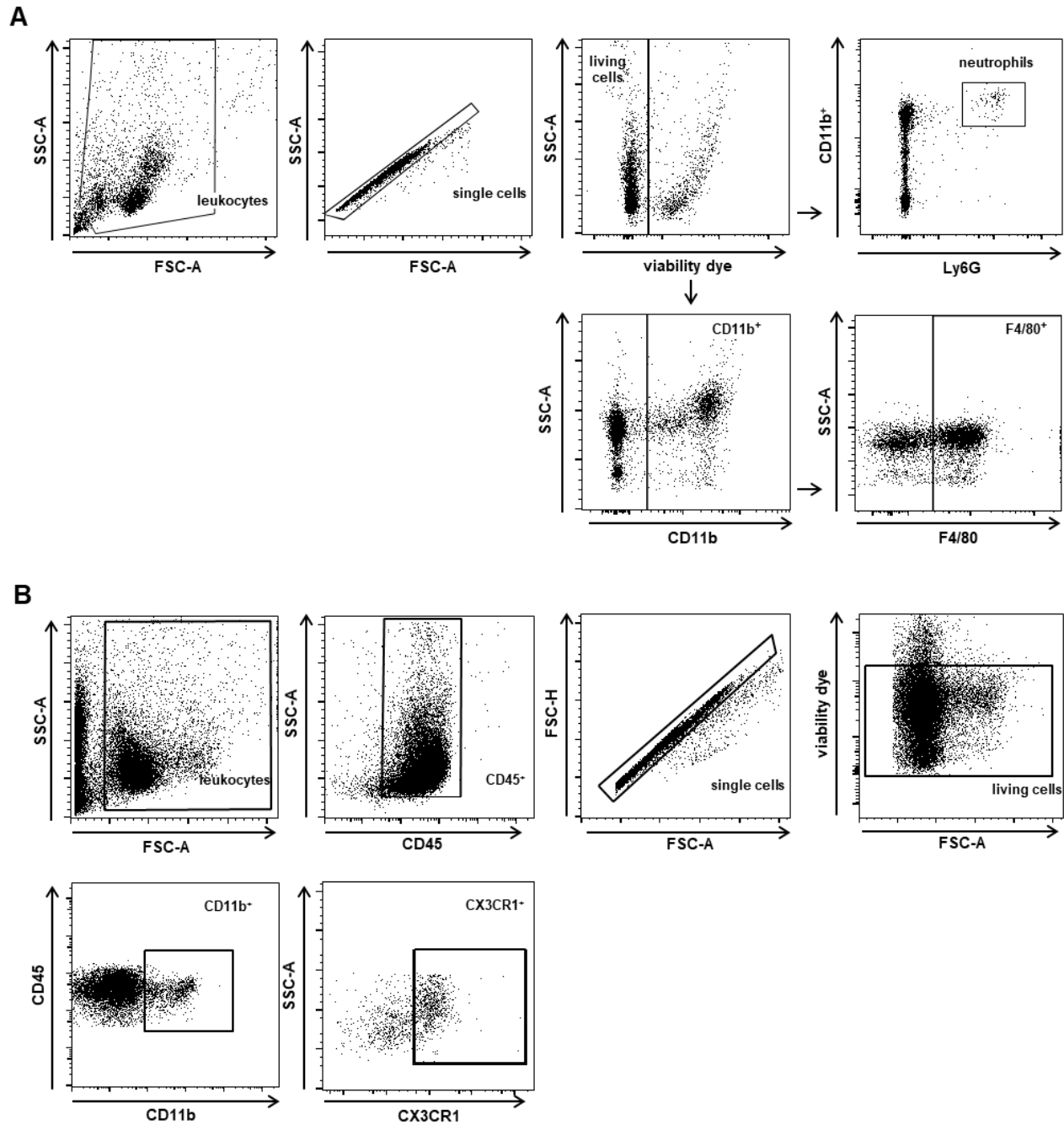


Figure 7: Gating strategy for flow cytometric analysis of myeloid cell subsets. (A) Representative dot blots of the gating strategy applied to identify CD11b⁺ monocytes, CD11b⁺F4/80⁺ macrophages, and CD11b⁺Ly6G⁺ neutrophils in livers of *Mdr2*^{-/-} and *Tnfr1*^{-/-}/*Mdr2*^{-/-} mice. (B) Representative dot blots of the gating strategy applied to identify CX3CR1⁺ as well as CX3CR1⁻ monocytes in livers of *Mdr2*^{-/-} and *Tnfr1*^{-/-}/*Mdr2*^{-/-} mice.

2.14 Fluorescence activated cell sort

Isolated hepatic NPCs were stained with an antibody cocktail containing a viability dye, anti-CD11b and anti-CX3CR1 antibodies as described in section 2.13. CD11b⁺CX3CR1⁺ as well as CD11b⁺CX3CR1⁻ were sorted with a BDFACSaria™ III. The gating strategy to identify CD11b⁺CX3CR1⁻ as well as CD11b⁺CX3CR1⁺ cells (CD11b vs CX3CR1) included gates for the exclusion of debris (SSC-A vs FSC-A), single cells (FSC-H vs FSC-A), and living cells (SSC-A vs viability dye) (Figure 8). Sorted cells were collected in RPMI Medium containing FCS (10 %) and Pen-Strep (2 %). Afterwards cells were washed in PBS and RNA was isolated and transcribed into cDNA as described in section 2.19.

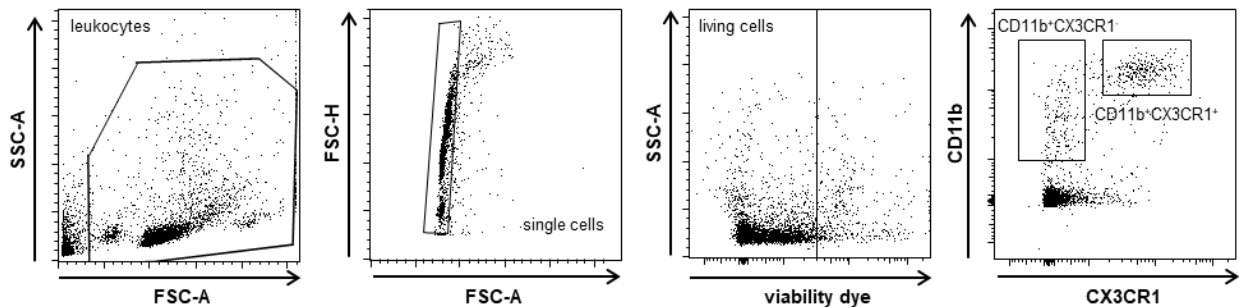


Figure 8: Gating strategy for fluorescent activated cell sorting of monocytes according to CX3CR1 expression. Representative dot plots of the gating strategy applied to sort CX3CR1⁺ as well as CX3CR1⁻ monocytes cells in livers of *Mdr2*^{-/-} and *Tnfr1*^{-/-}/*Mdr2*^{-/-} mice.

2.15 Hydroxyproline Assay

The analysis of the hepatic hydroxyproline (Hyp) content was performed as described previously⁴¹. In brief, 100 mg of snap frozen liver tissue was homogenized in ddH₂O (900 μ L, 4 °C) with a tissue lyser (2 min, 30 HZ). Protein was precipitated by adding trichloric acid (125 μ L, 50 % v/v) and samples were placed on ice (20 min). The precipitate was centrifuged (4x10³ xg, 20 min) and resuspended in ethanol (100 %, 0 °C, 3 x). After final centrifugation, the supernatant was discarded and precipitate was completely dried. The dried sample was resuspended in HCL (800 μ L, 6 M) and heated to a 110 °C for 18 h. After cooling to RT, samples were centrifuged (18x10³ xg, 10 min) and filtered through a 0.22 μ m sterile filter. The Hyp standards were prepared as a series of dilution of the Hyp working solution (0.5 μ g/ mL) with HCL (6 M), ranging from 0 to 0.5 μ g/ mL. 40 μ L per sample or standard

were mixed with 10 μL of NaOH (10 M) and 450 μL of Chloramine-T solution. After 30 min (RT), 500 μL of Ehrlich's reagent was added and the samples were heated to 65 $^{\circ}\text{C}$ for 20 min. 200 μL per sample were transferred in triplicates to a 96-well round bottom plate, the standards were prepared in doublets. The plate was then analyzed by a TECAN Infinite® M200 at 540 nm excitation/ absorbance.

2.16 Hematoxylin & Eosin staining

Basic histomorphological features were identified in hematoxylin and eosin (H&E) stained tissue sections. For that purpose, tissue sections of 3 μm thickness were cut from paraffin embedded liver tissue and stored at RT until use. H&E staining was performed in cooperation with the department of pathology (UKE) using standard procedure. Images of stained sections were taken with a Keyence BZ-9000 microscope (Keyence, Neu-Isenburg).

2.17 Sirius Red staining

In order to visualize fibrotic remodeling of the liver, Sirius Red staining of hepatic collagen was performed. For that purpose, tissue sections of 5 μm thickness, were deparaffinised by sequential submersion in xylol (2 x 5 min), a series of ethanol in descending concentrations (5 min each; 100 %, 96 %, 80 %, 70 %, 50 %) and finally ddH₂O (5 min). Slides were incubated in 0.1 % Sirius red in saturated picric acid (90 min) and then placed in acidified water (0.01 N HCL) for 15 s. Prior to mounting with Entellan mounting medium, slides were dehydrated in a series of ethanol washes with ascending concentrations (50 % for 30 s, 70 % for 1 min, 100 % for 4 min) and xylol (2 x 5 min). Images of Sirius Red stained sections were taken with a Keyence BZ-9000 microscope. Quantification of Sirius Red positive areas was done with the Keyence BZ-II Analyzer software.

2.18 Beadbased multiplex analysis of cytokine concentrations

Cytokine concentrations of TNF α , IFN γ , IL-4, IL-6, and IL-22 were determined via Legendplex™ Mouse Th Cytokine Panel, a bead based multiplex analysis assay. This approach is very similar to the better known enzyme-linked immunosorbent assay (ELISA), with the distinction that the capture antibody is attached to beads and multiple analytes are analyzed

simultaneously via flow cytometry. The assay was performed according to manufacturer's instructions. In brief, 6.25 μ L of cell culture supernatants, plasma samples (diluted 1:2 with assay buffer) and standard samples (0 to 1×10^4 pg/ mL, serial diluted in assay buffer) were incubated with capture antibody coated beads in assay buffer (12.5 μ L) on a shaker approximately 14 h (4 °C). The next day, the secondary biotinylated antibody was added (6.25 μ L). The plate was sealed from light and placed on a shaker (2 h). Subsequently the fluorescent dye PE conjugated streptavidin was added (6.25 μ L; 0.5 h, sealed from light). After washing (washing buffer, 1×10^3 xg; 5 min), the supernatant was discarded and samples were resuspended in washing buffer (200 μ L), transferred into round bottom tubes and analyzed with a Canto II. The obtained data was analyzed using Legendplex software.

2.19 Quantitative real-time reverse-transcriptase polymerase chain reaction

Quantitative real-time reverse-transcriptase polymerase chain reaction (qRT-PCR) was performed in order to analyze the expression of genes known to be involved in inflammation, fibrosis, immune cell recruitment and cell death. For isolation of total RNA from liver tissue the NucleoSpin® RNA II Isolation Kit was used according to manufacturer's instruction. RNA from sorted hepatic NPCs was isolated with a RNeasy® Micro Kit again according to manufacturer's instruction. RNA concentration was determined photometrically using a NanoDrop ND-1000. A total of 1 μ g of RNA was transcribed into complementary DNA (cDNA) using the Verso cDNA Synthesis kit according to manufacturer's instructions and a MyCycler™ thermal cycler. This Verso cDNA Synthesis kit uses anchored oligo dT primers to specifically transcribe mRNA. Oligonucleotides for qRT-PCR analysis were designed using Primer3 software and obtained from Metabion International AG. Details about the oligonucleotides are summarized in Table 7. qRT-PCR analysis was performed using Maxima™ SYBR Green qPCR Master Mix and a C1000 Thermal Cycler + CFX 96 Real-Time System. For the analysis of genes encoding for cytokines and transcription factors 1 μ L of undiluted cDNA was used in a total reaction volume of 10 μ L. For the analysis of all other target genes 1 μ L of diluted RNA (1:10 in Rnase free water) was used. PCR product specificity was confirmed by analysis of the melting curve and via agarose gel electrophoresis.

2.20 Protein isolation from mouse liver and western blot analysis

In order to visualize the amount and activation status of different mediators of cell death in the liver, western blot analysis was performed. Snap frozen liver tissue section were lysed in a lysis buffer containing a protease inhibitor cocktail (1:100) and if applicable a phosphatase inhibitor (1:10). Mechanical disruption was achieved with a tissue lyser (2 min, 30 Hz). Samples were then placed on ice for 30 min and vortexed every 10 min. For the removal of the remaining cellular debris, the lysates were centrifuged ($4 \times 10^3 \times g$, 5 min, 4 °C) and the supernatants were stored at -80 °C until further use. Protein concentrations were determined via Bradford assay. A total of 50 µg of protein were added to sample buffer and incubated for 5 min at 95 °C. Samples were loaded next to a molecular marker onto a gradient gel (4-12 % Bis-Tris Protein Gel). Gels were run (100 V) for approximately 1 h. Proteins were blotted on a nitrocellulose membrane using the wet blot method (300 mA, 70 min). Membranes were washed (TBST) and blocked in TBST containing 5 % milk powder. The membranes were placed in 50 mL tubes and incubated with the primary antibody overnight (4 °C, rolling). Details about the antibodies used are summarized in Table 6. The next day membranes were washed (3 x 10 min) with TBST. Afterwards the membranes were incubated in the respective secondary antibody for 1 h (RT) on a shaker. Western blots were developed in enhanced chemiluminescence solution, images of the blots were taken with a VersaDoc™, 4000 MP imaging system.

2.21 Statistical Analysis

Statistical analyses were performed using graph pad prism 7. All of the data is presented as mean ± SEM. Group comparisons were performed using one-way ANOVA ($P = 0.05$) with a Tukey's post-hoc test. Comparison between 2 groups were performed using non-parametric Mann-Whitney test. Spearman nonparametric correlation test was used to determine correlation between two parameters. The ROUT method was used to identify outliers. Different levels of significance were indicated by an increasing number of asterisks. * $P < 0.05$, ** $P > 0.01$, *** $P < 0.001$, **** $P < 0.0001$. Asterisks above columns represent the significance of the difference between the respective genotype and the WT. Asterisks on bars represent the significance of the difference between certain genotypes.

3 Results

3.1 Tissue injury in livers of *Tnfr1*^{-/-}/*Mdr2*^{-/-} mice

To get a general overview, how the absence of TNFR1 in the *Mdr2*^{-/-} mouse model influences disease severity, H&E stained tissue sections of *Tnfr1*^{-/-}/*Mdr2*^{-/-} mice were analyzed and compared to those of *Mdr2*^{-/-}, *Tnfr1*^{-/-}, and WT mice (Figure 9A). The representative tissue sections of WT and *Tnfr1*^{-/-} display the portal fields of healthy liver parenchyma, with hepatocytes anastomosing towards the portal tracts. The clearly visible sinusoids separate the sheets of hepatocytes. In case of the *Mdr2*^{-/-} and *Tnfr1*^{-/-}/*Mdr2*^{-/-} clear signs of cholestasis, inflammation and tissue degeneration can be observed. Both tissue sections display increased immune cell infiltration, pronounced bile duct proliferation and distortion of tissue organization. Enzymatic activity of plasma alanine aminotransferase (ALT) and alkaline phosphatase (ALP) were measured, as they are reliable markers for hepatic tissue injury (Figure 9B-C)⁴².

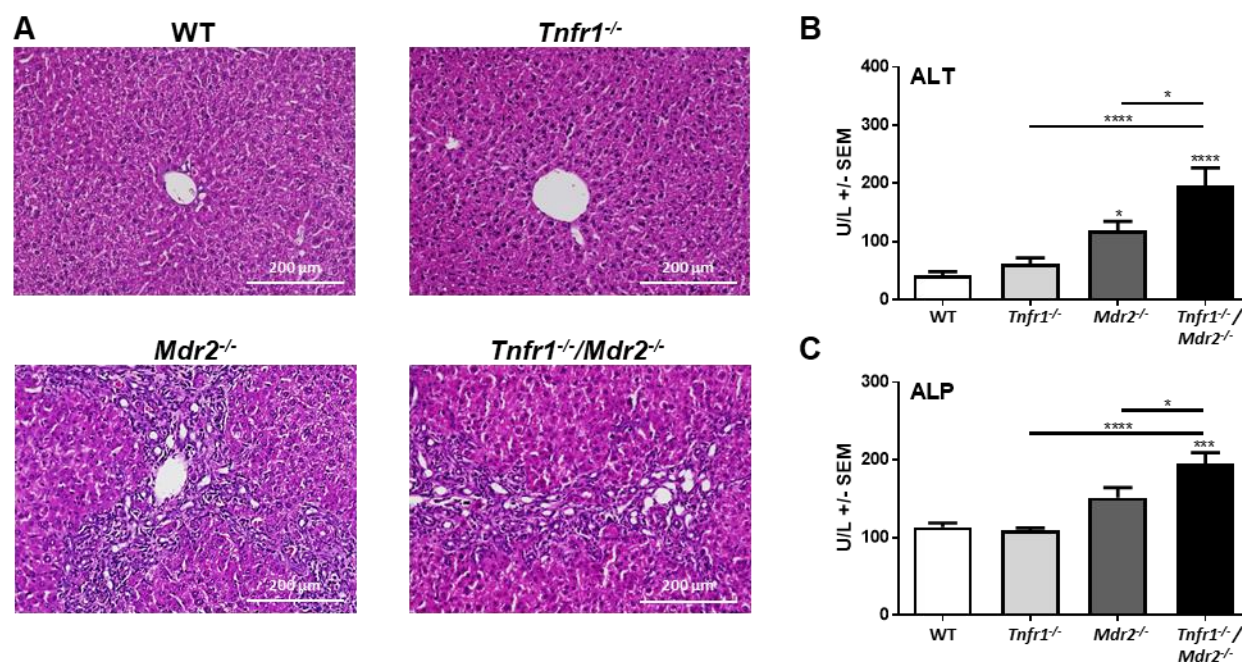


Figure 9: The absence of TNFR1 increases tissue injury in the *Mdr2*^{-/-} mouse model. (A) Representative images (10 x) of hematoxylin and eosin stained tissue sections of WT, *Tnfr1*^{-/-}, *Mdr2*^{-/-}, and *Tnfr1*^{-/-}/*Mdr2*^{-/-} mice. (B) ALT and (C) ALP levels of WT (n ≥ 6), *Tnfr1*^{-/-} (n ≥ 8), *Mdr2*^{-/-} (n ≥ 11), and *Tnfr1*^{-/-}/*Mdr2*^{-/-} (n ≥ 10) mice determined in plasma with a cobas integra. *P ≤ 0.05, ***P ≤ 0.001, ****P ≤ 0.0001.

Both markers for liver injury were at physiological levels (ALT: 20-88 U/L; ALP: 58-96)⁴³ in WT as well as *Tnfr1*^{-/-} mice. While plasma levels of ALP were slightly increased in *Mdr2*^{-/-} mice, levels of ALT were significantly increased compared to WT mice. *Tnfr1*^{-/-}/*Mdr2*^{-/-} mice displayed significantly increased plasma levels of ALT and ALP compared to WT mice as well as *Mdr2*^{-/-} mice.

The absence of PC in bile of *Mdr2*^{-/-} mice decreases the solubility of cholesterol, often resulting in the formation of cholesterol plaques and an obstructed bile flow. Impaired bile flow, also called cholestasis, is marked by an insufficient clearing of biliary components such as bilirubin from the blood stream and a diminished cholesterol pool.⁴⁴

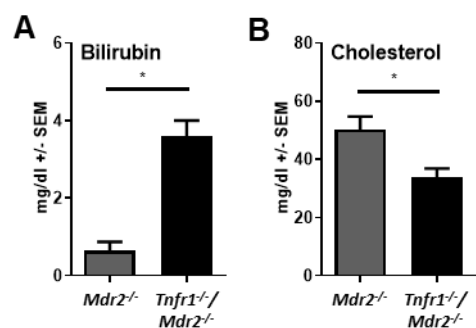


Figure 10: Markers for cholestasis in *Tnfr1*^{-/-}/*Mdr2*^{-/-} mice. (A) Plasma concentrations of bilirubin and (B) cholesterol in *Mdr2*^{-/-} (n = 4) and *Tnfr1*^{-/-}/*Mdr2*^{-/-} (n = 5) mice determined in plasma with a cobas integra. *P ≤ 0.05.

Figure 10 shows that *Tnfr1*^{-/-}/*Mdr2*^{-/-} mice showed more severe signs of cholestasis compared to *Mdr2*^{-/-} mice. Plasma levels of bilirubin were significantly increased in *Tnfr1*^{-/-}/*Mdr2*^{-/-} mice, while the plasma levels of cholesterol were significantly decreased.

Overall the data presented in Figure 9-10 indicate that the absence of TNFR1 does not protect from but rather aggravates tissue injury and cholestasis in the *Mdr2*^{-/-} mouse model.

3.2 Cell death in livers of *Tnfr1*^{-/-}/*Mdr2*^{-/-} mice

Cell death is a central feature of the onset as well as the progression of CLD. Through its intracellular death domain TNFR1 can directly induce apoptotic as well as RIPK3 mediated necroptosis.⁴⁵ In order to analyze how the absence of TNFR1 influences the occurrence of cell death during chronic liver injury, western blot (WB) analysis of central mediators of either apoptosis or necroptosis was performed (Figure 11).

The effector caspase of apoptosis Casp3 is activated through cleavage of the 32 kDa precursor into the active 12 and 17 kDa subunits.⁴⁶ Figure 11A displays the WB analysis of the cleaved 17 kDa Casp3 subunit in liver lysates of WT, *Tnfr1*^{-/-}, *Mdr2*^{-/-}, and *Tnfr1*^{-/-}/*Mdr2*^{-/-} mice. In liver samples of the three WT mice, two showed a distinct band of stained Casp3, while in the group of *Tnfr1*^{-/-} mice, two showed a band of a slightly increased intensity. Both *Mdr2*^{-/-} and *Tnfr1*^{-/-}/*Mdr2*^{-/-} mice showed similarly increased bands of the 17 kDa Casp3 subunit, with the exception of one mouse within the *Mdr2*^{-/-} group which displayed a band with higher intensity than all other animals. The observed increase of cleaved Casp3 in animals lacking the MDR2 protein is in line with continuous cellular demise.

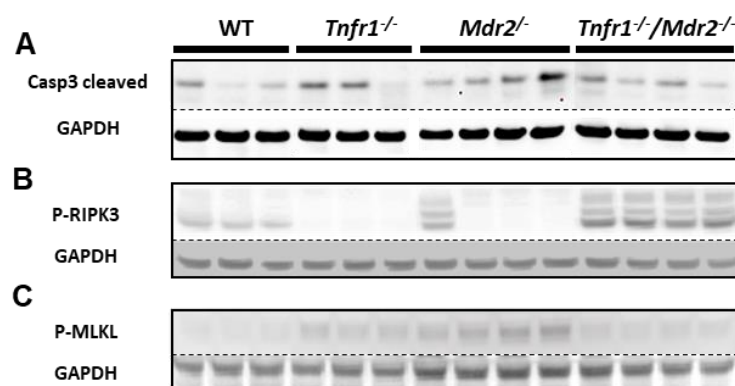


Figure 11: Mediators of cell death. Western blot analysis of mediators of cell death (A) Cleaved Casp3, (B) P-RIPK3 and (C) P-MLKL in liver lysates of WT ($n \geq 3$), *Tnfr1*^{-/-} ($n \geq 3$), *Mdr2*^{-/-} ($n \geq 4$), and *Tnfr1*^{-/-}/*Mdr2*^{-/-} ($n \geq 4$) mice. All analysis included staining for the housekeeping protein GAPDH as loading control displayed underneath the respective bands.

Induction of necroptosis is mediated by the necrosome, a cytosolic protein complex which includes RIPK1, RIPK3 and MLKL.⁴⁷ Figure 11B-C displays the WB analysis of the active i.e. phosphorylated forms of RIPK3 (P-RIPK3; 53 kDa) and MLKL (P-MLKL; 54 kDa) in liver lysates of WT, *Tnfr1*^{-/-}, *Mdr2*^{-/-}, and *Tnfr1*^{-/-}/*Mdr2*^{-/-} mice. Samples of WT animals showed a weak band of P-RIPK3, while P-RIPK3 appears to be virtually absent in the *Tnfr1*^{-/-} animals. Interestingly, in liver lysates of the four *Mdr2*^{-/-} mice only one had a weak band of the expected size. In contrast, all samples derived from livers of *Tnfr1*^{-/-}/*Mdr2*^{-/-} mice displayed bands of increased intensity, indicating that high levels of activated P-RIPK3 were present in the livers of *Tnfr1*^{-/-}/*Mdr2*^{-/-} mice. However, the opposite effect was observed for P-MLKL (Figure 11C). In liver lysates of WT animals, P-MLKL was undetectable, while in samples of *Tnfr1*^{-/-} animals only very weak bands could be observed. Interestingly, in liver lysates of *Mdr2*^{-/-} mice bands of slightly increased intensity could be seen, whereas for the *Tnfr1*^{-/-}/*Mdr2*^{-/-} mice only very weak and indistinct bands of P-MLKL could be detected. Since

MLKL is indispensable for necroptotic cell death, these findings suggest that necroptosis most likely does not play a major role neither in the *Mdr2*^{-/-} nor *Tnfr1*^{-/-}/*Mdr2*^{-/-} phenotype.⁴⁸ However, a necroptosis-independent role of RIPK3 in the livers of *Tnfr1*^{-/-}/*Mdr2*^{-/-} mice must be considered.

Overall, the data presented in Figure 11 shows that the absence of TNFR1 influences the expression and activation of several key mediators of cell death in the chronically injured liver.

3.3 Fibrosis in livers of *Tnfr1*^{-/-}/*Mdr2*^{-/-} mice

Chronic liver injury inevitably induces fibrotic responses, which leads to the accumulation of fibrous scar tissue.⁹ To determine whether the absence of TNFR1 influenced fibrotic tissue remodeling the extent of hepatic ECM deposition of all genotypes were compared. For that purpose, the hepatic collagen deposition was visualized via Sirius Red staining in liver tissue sections (Figure 12A).

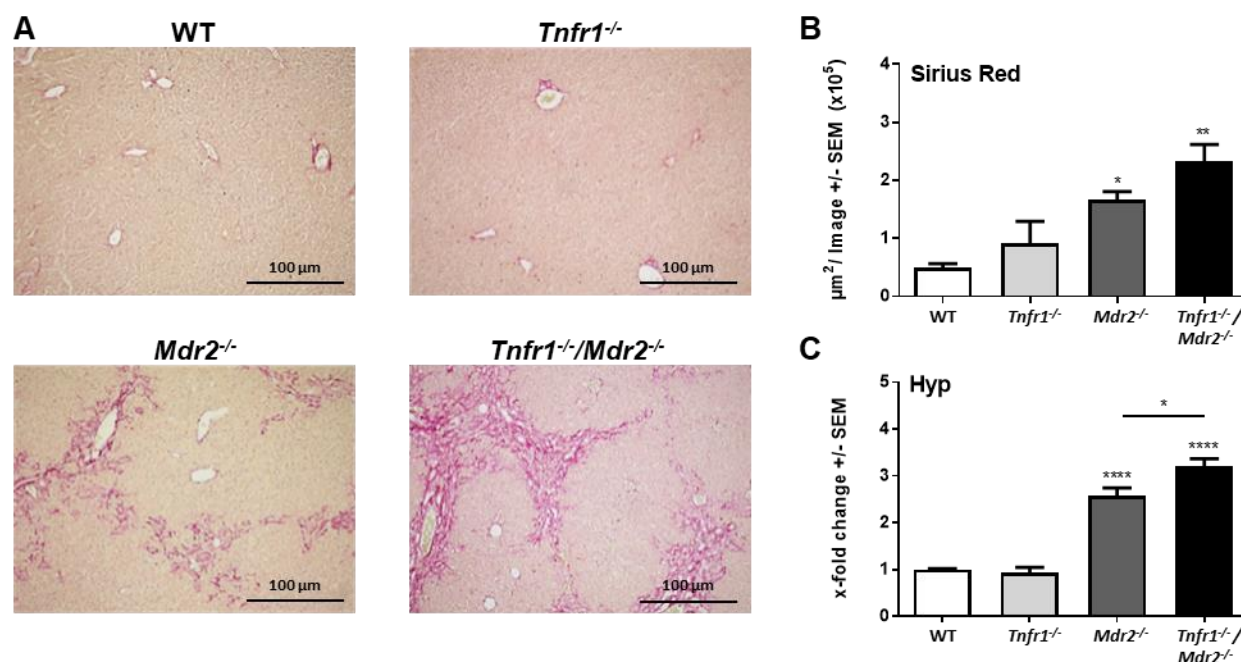


Figure 12: The absence of TNFR1 increases hepatic extracellular matrix deposition in response to chronic tissue injury. (A) Representative images (10x) of Sirius Red stained tissue sections of WT, *Tnfr1*^{-/-}, *Mdr2*^{-/-}, and *Tnfr1*^{-/-}/*Mdr2*^{-/-} mice. (B) Quantification of Sirius Red staining in tissue sections of WT (n ≥ 4), *Tnfr1*^{-/-} (n ≥ 6), *Mdr2*^{-/-} (n ≥ 9), and *Tnfr1*^{-/-}/*Mdr2*^{-/-} (n ≥ 9) mice. (C) Relative hepatic hydroxyproline content of mice described in (B). *P ≤ 0.05, **P ≤ 0.01, ****P ≤ 0.0001.

The representative sections of the WT and *Tnfr1*^{-/-} mice show the presence of minimal amounts of hepatic collagen, which is restricted to the basement membrane of the vasculature. The tissue section of the *Mdr2*^{-/-} mouse displays distinct features of fibrosis, such as collagen enrichment around the portal areas with fibrous extension and some portal to portal bridging.

Figure 12B displays the average coverage of Sirius Red stained areas per section, which shows that the livers of *Mdr2*^{-/-} as well as *Tnfr1*^{-/-}/*Mdr2*^{-/-} mice contained significantly more collagen than WT mice. An alternative method of quantifying the amount of hepatic connective tissue is measuring the amount of hydroxyproline (Hyp) in the liver. Hyp is a modified amino acid which is exclusively found in collagen and elastin helices, both of which are integral parts of fibrous connective tissue.⁴⁹ The relative hepatic Hyp content depicted in Figure 12C shows that while WT and *Tnfr1*^{-/-} mice had comparable amounts of hepatic Hyp, *Mdr2*^{-/-} and *Tnfr1*^{-/-}/*Mdr2*^{-/-} mice showed significantly increased Hyp levels compared to WT mice. Moreover, the relative amount of Hyp in the livers of *Tnfr1*^{-/-}/*Mdr2*^{-/-} mice was significantly higher compared to *Mdr2*^{-/-} mice, which indicates a more pronounced fibrotic response.

Fibrosis is most dominantly mediated by hepatic stellate cells (HSCs), which upon activation transform into collagen producing myofibroblasts.⁵⁰ A reliable marker of HSC activation is the upregulation of α -smooth muscle actin (α -sma).⁵¹ Activated HSCs orchestrate tissue remodeling not only by the secretion of collagen and elastin, but also by the release of matrix metallo proteinases (MMPs), such as MMP2 and 9 as well as their respective tissue inhibitors (TIMPs) including TIMP1.⁵² The gene expression profile depicted in Figure 13A shows that the gene expression level of *Acta2* (α -sma), *Col1a1* (Collagen I), and *Col3a1* (Collagen III), were slightly upregulated in *Mdr2*^{-/-} animals. However, only the expression of Collagen I was significantly increased compared to WT mice. In case of *Tnfr1*^{-/-}/*Mdr2*^{-/-} mice the expression of the HSC activation marker α -sma as well as Collagen I and Collagen III were all significantly upregulated compared to WT mice. Furthermore, the relative hepatic expression of α -sma and collagen III in *Tnfr1*^{-/-}/*Mdr2*^{-/-} mice was significantly increased in comparison to *Mdr2*^{-/-} mice, which is in line with the observed increased amount of hepatic Hyp described above.

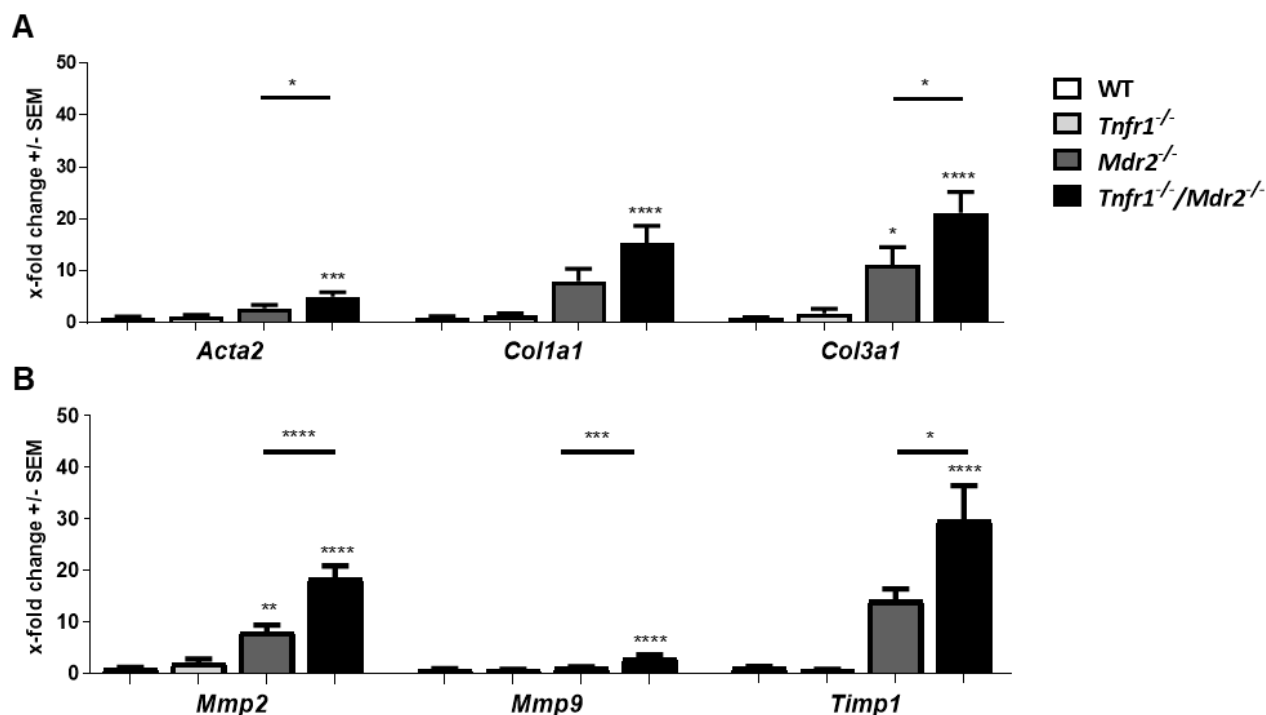


Figure 13: The expression of markers of fibrosis and fibrotic tissue remodeling is upregulated in *Tnfr1*^{-/-}/*Mdr2*^{-/-} mice. (A) Relative hepatic expression of *Acta2* (α -sma), *Col1a1* (collagen I), and *Col3a1* (collagen III) of WT ($n \geq 9$), *Tnfr1*^{-/-} ($n \geq 6$), *Mdr2*^{-/-} ($n \geq 9$) and *Tnfr1*^{-/-}/*Mdr2*^{-/-} ($n \geq 10$) mice normalized to WT mice. (B) Relative hepatic expression of *Mmp2*, *Mmp9* and *Timp1* of mice described in A normalized to WT mice. * $P \leq 0.05$, ** $P \leq 0.01$, *** $P \leq 0.001$, **** $P \leq 0.0001$.

A similar effect is observed in the hepatic expression profile of matrix remodeling enzymes displayed in Figure 13B. While *Mdr2*^{-/-} mice showed a significant increase of *Mmp2* expression compared to WT mice, *Mmp9* and *Timp1* expression was only slightly and not significantly elevated. The *Tnfr1*^{-/-}/*Mdr2*^{-/-} mice, on the other hand, the expression of *Mmp2*, *Mmp9* and *Timp1* were all highly upregulated in *Tnfr1*^{-/-}/*Mdr2*^{-/-} mice which was significant when compared to WT as well as to *Mdr2*^{-/-} mice. Overall, the data in Figure 12Figure 13 indicates a stronger fibrotic response in the absence of TNFR1 signaling within the *Mdr2*^{-/-} mouse model.

3.4 Proliferation in livers of *Tnfr1*^{-/-}/*Mdr2*^{-/-} mice

Chronic liver injury independent of the cause always initiates a wound healing response.⁵³ TNFR1 has been shown to be essential for successful initiation of liver regeneration, via the

NFκB, IL-6, STAT3 axis.⁵⁴ In order to investigate whether compensatory proliferation is compromised in *Tnfr1*^{-/-}/*Mdr2*^{-/-} mice, gene expression analysis of several proliferation markers such as proliferating cell nuclear antigen (*Pcna*), Cyclin A2 (*Ccna2*) and Cyclin dependent kinase 1 (*Cdk1*) was performed. Figure 14 shows no differences in *Pcna* gene expression compared to the WT and only a slight increase of *Ccna2* and *Cdk1* expression in livers of *Mdr2*^{-/-} mice, which was only significant in case of *Ccna2*. In contrast, all of these markers were significantly up-regulated in livers of *Tnfr1*^{-/-}/*Mdr2*^{-/-} mice in comparison to livers of WT mice, which implicates active proliferation.

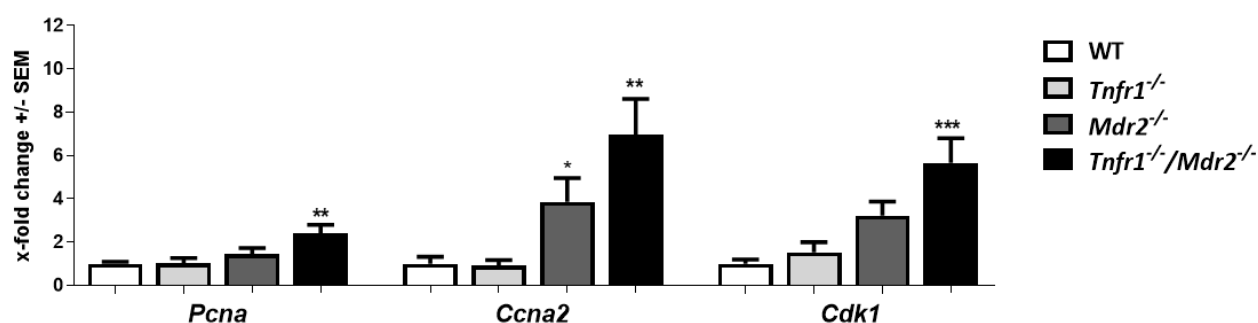


Figure 14: Mediators of proliferation are upregulated in livers of *Tnfr1*^{-/-}/*Mdr2*^{-/-} mice. Hepatic gene expression analysis of proliferation marker *Pcna*, *Ccna2*, and *Cdk1* in WT (n ≥ 10), *Tnfr1*^{-/-} (n = 9), *Mdr2*^{-/-} (n ≥ 9), and *Tnfr1*^{-/-}/*Mdr2*^{-/-} (n ≥ 10) determined by RT-qPCR. **P ≤ 0.01, ***P ≤ 0.001.

While compensatory proliferation is a necessity to replace tissue lost to injury, prolonged proliferation in an inflammatory environment, increase the risk of malignant transformation⁵⁵. In order to investigate whether the absence of TNFR1 may promote tumor development, expression analysis of several genes previously described to be upregulated in HCC were performed. These genes included tumor necrosis factor α induced protein (*Tnfaip*, A20), secreted phospho protein 1 (*Spp1*, OPN) and α-feto protein (*Afp*).⁵⁶⁻⁵⁸ Figure 15 shows that all of the above mentioned markers are upregulated in *Tnfr1*^{-/-}/*Mdr2*^{-/-} mice when compared to the expression in livers of WT mice. In contrast *Mdr2*^{-/-} mice on the other hand, showed significantly up-regulated expression of *Spp1* when compared to WT mice. The slightly elevated expression levels of *Tnfaip3* and *Afp* were not significantly higher than those of WT mice. The gene expression of *Tnfaip3*, *Spp1*, and *Afp* in livers of *Tnfr1*^{-/-} mice was equivalent to that of WT mice. The expression profiles described above indicate active proliferation with signs of possible dedifferentiation in *Tnfr1*^{-/-}/*Mdr2*^{-/-} mice.

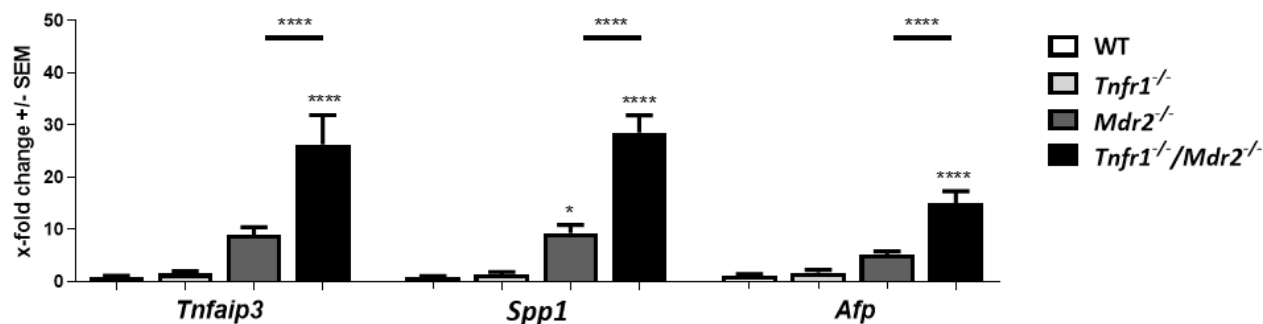


Figure 15: Hepatic expression of tumor marker in livers of *Tnfr1*^{-/-}/*Mdr2*^{-/-} mice. Hepatic gene expression analysis of *Tnfaip3*, *Spp1*, and *Afp* in WT (n ≥ 10), *Tnfr1*^{-/-} (n = 9), *Mdr2*^{-/-} (n ≥ 9), and *Tnfr1*^{-/-}/*Mdr2*^{-/-} (n ≥ 10) determined by RT-qPCR. *P ≤ 0.05, ***P ≤ 0.001, ****P ≤ 0.0001.

3.1 Cytokine production in livers of *Tnfr1*^{-/-}/*Mdr2*^{-/-} mice

Cytokines are key signaling molecules for the dynamic reshaping of the immune response tailored to the specific insult inflicted upon the host organism.⁵⁹ The cytokine composition is indicative of the presence of specific immune cells and their activation state. Plasma cytokine profile

Figure 16 gives an overview of plasma concentrations of cytokines often involved in chronic inflammatory diseases. TNF α is produced in large amounts by macrophages, LSECs and several other activated immune cells.⁶⁰

Figure 16A shows that WT, *Tnfr1*^{-/-}, and *Mdr2*^{-/-} mice had similar plasma levels of TNF α . Only *Tnfr1*^{-/-}/*Mdr2*^{-/-} mice show significantly increased levels TNF α compared to WT and *Mdr2*^{-/-} mice. IL-2 serves as a marker for overall T helper cell activation, as its production is upregulated by naïve CD4⁺ T cell subtypes upon activation, although to varying degrees.⁶¹ The plasma levels of IL-2 did not differ significantly between WT, *Tnfr1*^{-/-}, *Mdr2*^{-/-} and *Tnfr1*^{-/-}/*Mdr2*^{-/-} mice (Figure 16B). The same is seen for the signature cytokines of both major T cell subsets TH1 (IFN γ , Figure 16C) and TH2 cells (IL-4, Figure 16D). IL-6 is a central mediator of acute and chronic inflammation and tissue regeneration upon liver injury.^{60,62} *Tnfr1*^{-/-}, *Mdr2*^{-/-} as well as *Tnfr1*^{-/-}/*Mdr2*^{-/-} mice show no significant differences in plasma levels of IL-6 compared to WT mice, nor were significant differences between any these groups observed (Figure 16E). Figure 16F shows plasma levels of IL-22, a cytokine produced

by T_H17 and T_H22 . IL-22 promotes pro- as well as anti-inflammatory processes depending on the microenvironment and is known to induce tissue regeneration⁶³.

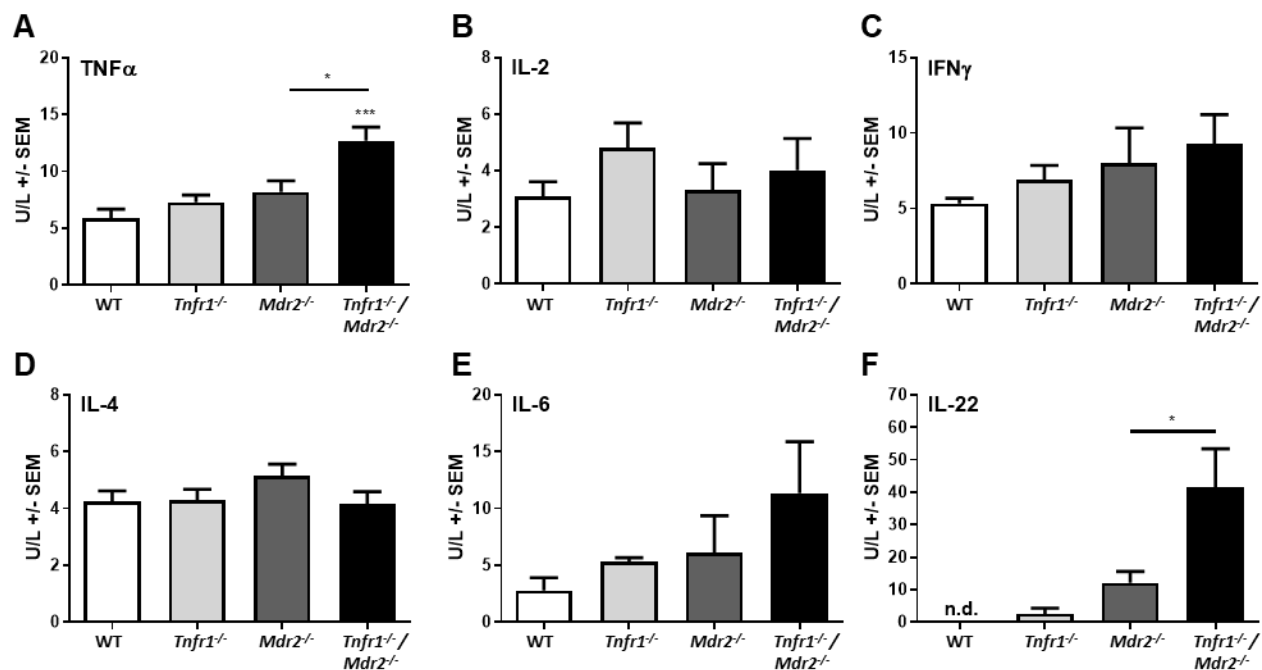


Figure 16: Absence of TNFR1 influences plasma cytokine concentrations. (A) Plasma concentration of TNF α , (B) IL-2, (C) IFN γ , (D) IL-4, (E) IL-6, and (F) IL-22 in WT (n \geq 5), *Tnfr1*^{-/-} (n \geq 6), *Mdr2*^{-/-} (n \geq 5) and *Tnfr1*^{-/-}/*Mdr2*^{-/-} (n \geq 5) mice determined with bead-based multiplex analysis. *P \leq 0.05, ***P \leq 0.001.

In plasma samples of WT animals IL-22 was not detectable, while low levels could be measured in plasma of *Tnfr1*^{-/-} mice, indicating that the absence of TNFR1 under physiological conditions was sufficient to increase IL-22 plasma levels. *Mdr2*^{-/-} mice display slightly increased levels of IL-22, which were still significantly lower than those of *Tnfr1*^{-/-}/*Mdr2*^{-/-} mice. This is further evidence that the absence of TNFR1 influences IL-22 turn-over. Overall the data depicted in Figure 16 showed no dramatic differences in the plasma cytokine profile of WT, *Tnfr1*^{-/-}, *Mdr2*^{-/-}, and *Tnfr1*^{-/-}/*Mdr2*^{-/-} mice, in which only TNF α and IL-22 showed significant differences.

3.1.1 Hepatic cytokine expression

In order to gain a more defined overview of the cytokine profile in the liver of *Tnfr1*^{-/-}/*Mdr2*^{-/-} mice, qRT-PCR analysis of prominent inflammatory cytokines were

performed. Initial analyses confirmed the above described effect that the hepatic expression of cytokines associated with either T_H1 or T_H2 were not strongly influenced by the absence of TNFR1 (data not shown).

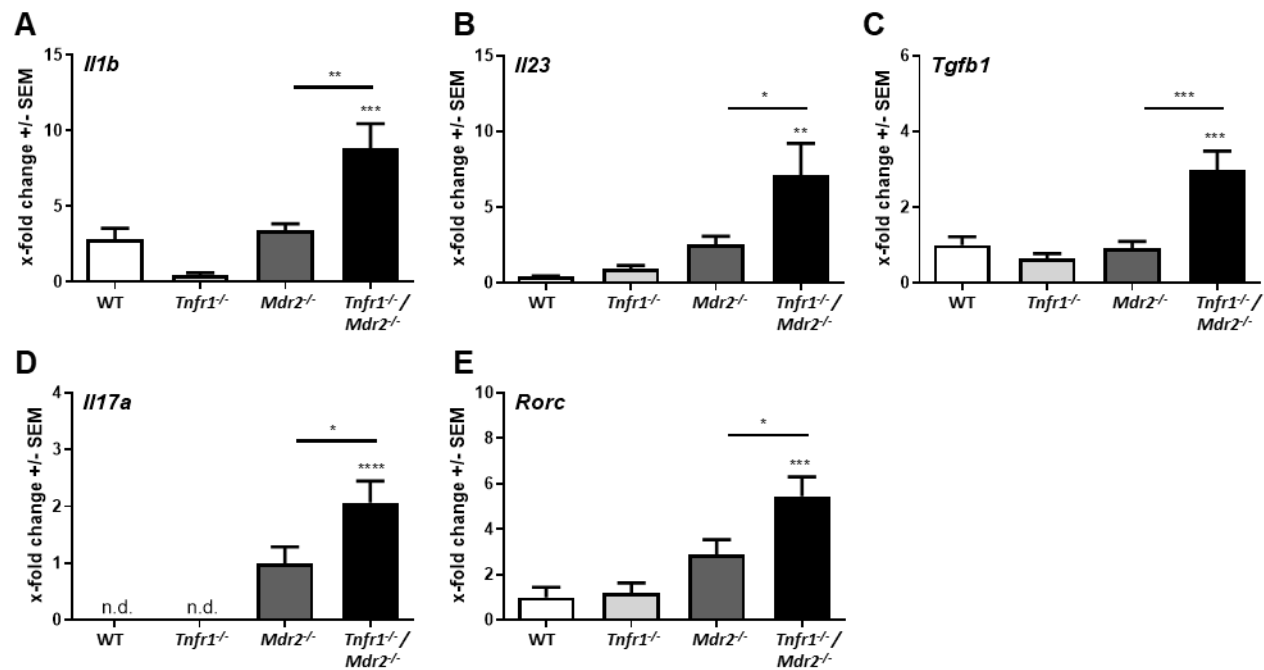


Figure 17: Hepatic gene expression associated with T_H17 differentiation. Relative hepatic expression levels of (A) *Il1b*, *Il23*, *Tgfb1*, *Il-17A* and, *Rorc* of WT (n ≥ 7), *Tnfr1*^{-/-} (n ≥ 7), *Mdr2*^{-/-} (n ≥ 5), and *Tnfr1*^{-/-}/*Mdr2*^{-/-} (n ≥ 6) mice determined by RT-qPCR. *P ≤ 0.05, **P ≤ 0.01, ***P ≤ 0.001, ****P ≤ 0.0001.

However, more detailed analyses identified several genes of cytokines to be differentially expressed in the livers of *Mdr2*^{-/-} and *Tnfr1*^{-/-}/*Mdr2*^{-/-} mice. These genes included *Il1b* (IL-1β), *Il23* (IL-23), *Tgfb1* (TGFβ) (Figure 17A-C), which were significantly upregulated only in *Tnfr1*^{-/-}/*Mdr2*^{-/-} but not *Mdr2*^{-/-} mice. The expression of the T_H17 signature cytokine IL-17A was not detectable under physiological conditions as was seen in WT and *Tnfr1*^{-/-} mice. Both *Mdr2*^{-/-} and *Tnfr1*^{-/-}/*Mdr2*^{-/-} mice showed detectable levels of IL-17 expression, however, the expression was significantly increased in *Tnfr1*^{-/-}/*Mdr2*^{-/-} mice (Figure 17D). The gene of the master transcription factor of T_H17 cell differentiation RORγt (*Rorc*) was expressed in mice of all genotypes, but again *Tnfr1*^{-/-}/*Mdr2*^{-/-} mice showed a significantly increased expression in comparison to WT and *Mdr2*^{-/-} mice. Overall, the displayed cytokine and *Rorc* expression indicates an increased presence of T_H17 cells in livers of *Tnfr1*^{-/-}/*Mdr2*^{-/-} mice compared to *Mdr2*^{-/-} mice (Figure 17E).

3.2 Immune cell composition in livers of *Tnfr1*^{-/-}/*Mdr2*^{-/-} mice

Both progression and resolution of inflammation is mediated by immune cells, whose recruitment and activation is mediated by the present chemokine and cytokine milieu.⁶⁴ In consideration of the skewed expression profile of cytokines in livers of *Tnfr1*^{-/-}/*Mdr2*^{-/-} mice, it is very likely that the absence of TNFR1 affects the immune cell composition of the chronically inflamed liver. In order to elucidate whether the aggravated phenotype of *Tnfr1*^{-/-}/*Mdr2*^{-/-} mice may be the result of an altered immune cell composition, flow cytometric analyses of major T cell and myeloid cell populations were performed.

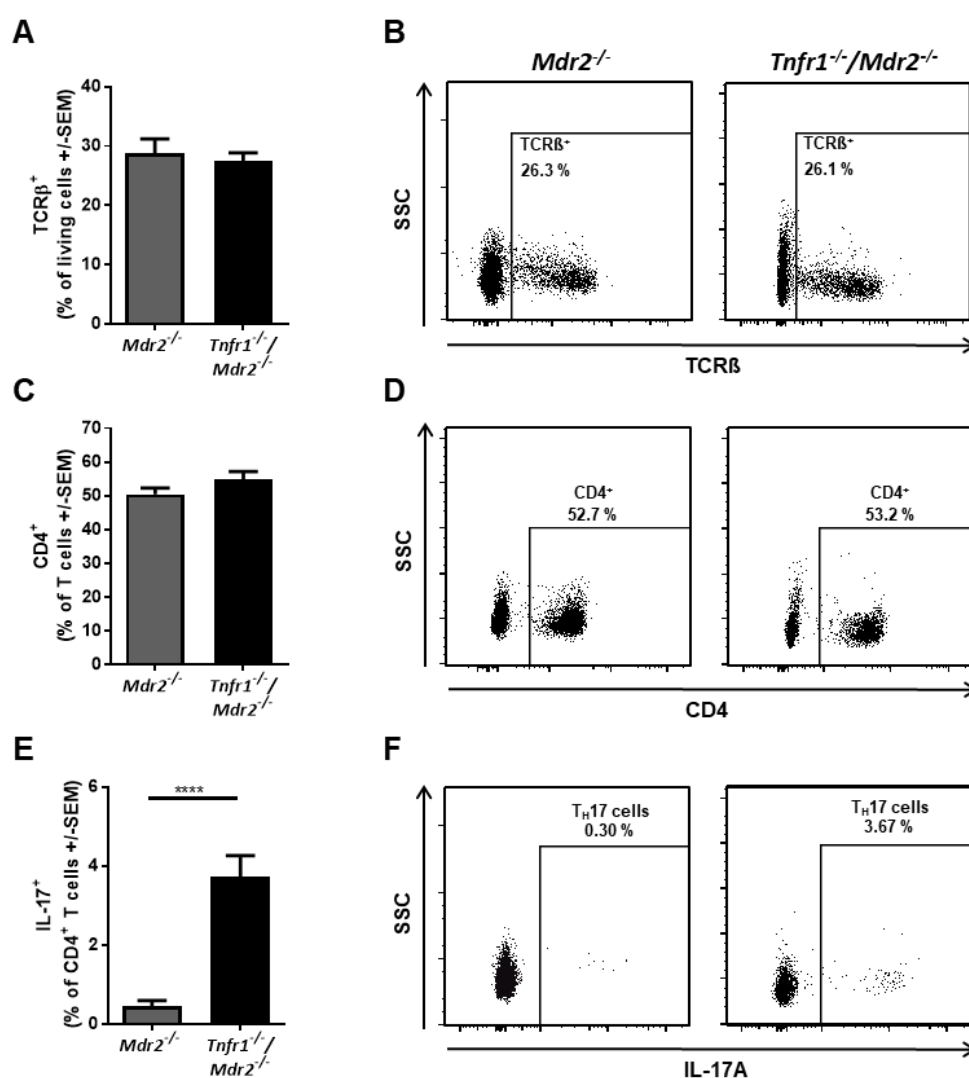


Figure 18: Hepatic T cell subsets of *Mdr2*^{-/-} and *Tnfr1*^{-/-}/*Mdr2*^{-/-} mice. (A) Frequencies (left) and representative dot plots (right) of TCRβ⁺ T cells, (B) CD4⁺ T cells, and TCRβ⁺CD4⁺IL17⁺ TH17 in livers of *Mdr2*^{-/-} (n ≥ 6), and *Tnfr1*^{-/-}/*Mdr2*^{-/-} (n ≥ 5) mice determined by flow cytometry. ****P ≤ 0.0001.

3.2.1 T helper cell subsets

The increased gene expression of several cytokines and the transcription factor *Rorc* in livers of *Tnfr1^{-/-}/Mdr2^{-/-}* mice indicated TH17 cell involvement.

The initial flow cytometric analysis was, therefore, aimed to investigate this specific T cell subset in livers of *Mdr2^{-/-}* and *Tnfr1^{-/-}/Mdr2^{-/-}* mice. TH17 cells were identified by their simultaneous expression of the common beta chain of the TCR (TCR β), CD4 and their signature cytokine IL-17A.

Figure 18A-B shows that *Mdr2^{-/-}* and *Tnfr1^{-/-}/Mdr2^{-/-}* mice displayed similar frequencies of conventional T cells and the CD4⁺ subtype of T cells. However, within the CD4⁺ T cell population the frequency of IL-17A expressing TH17 cells is dramatically increased in the *Tnfr1^{-/-}/Mdr2^{-/-}* mice compared to *Mdr2^{-/-}* mice (Figure 18C). Therefore, the assumed increased infiltration of TH17 cells into the injured liver of *Tnfr1^{-/-}/Mdr2^{-/-}* mice could be confirmed.

3.2.2 Correlation between IL-17A production of hepatic non-parenchymal cells and extent of tissue injury in *Tnfr1^{-/-}/Mdr2^{-/-}* mice

As each T cell subset has their own unique cytokine signature, isolated hepatic NPCs were restimulated *ex vivo* [50 g/mL PMA and 1 ng/mL ionomycin; 4 h] and cytokine concentrations were measured in the supernatant via a bead based multiplex analysis.

Figure 19A shows that TNF α secretion did not differ significantly between hepatic NPCs from *Mdr2^{-/-}* and *Tnfr1^{-/-}/Mdr2^{-/-}* mice. The same is observed for IL-2 (Figure 19B), the TH1 cytokine IFN γ (Figure 19C) and the TH2 cytokine IL-4 (Figure 19D). In line with increased frequencies of TH17 cells in livers of *Tnfr1^{-/-}/Mdr2^{-/-}* mice, elevated concentration of IL-17A could be detected in the supernatants of restimulated hepatic NPCs from *Tnfr1^{-/-}/Mdr2^{-/-}* mice compared to *Mdr2^{-/-}* mice (Figure 19D). Moreover, the IL-17A production of the isolated NPCs from *Tnfr1^{-/-}/Mdr2^{-/-}* mice were correlated to the extent of tissue injury defined by plasma levels of ALT (Figure 19E). The same correlation was not observed for *Mdr2^{-/-}* mice (Figure 19F). Which indicates that IL-17 might be involved in the pathology of *Tnfr1^{-/-}/Mdr2^{-/-}* but not *Mdr2^{-/-}* mice.

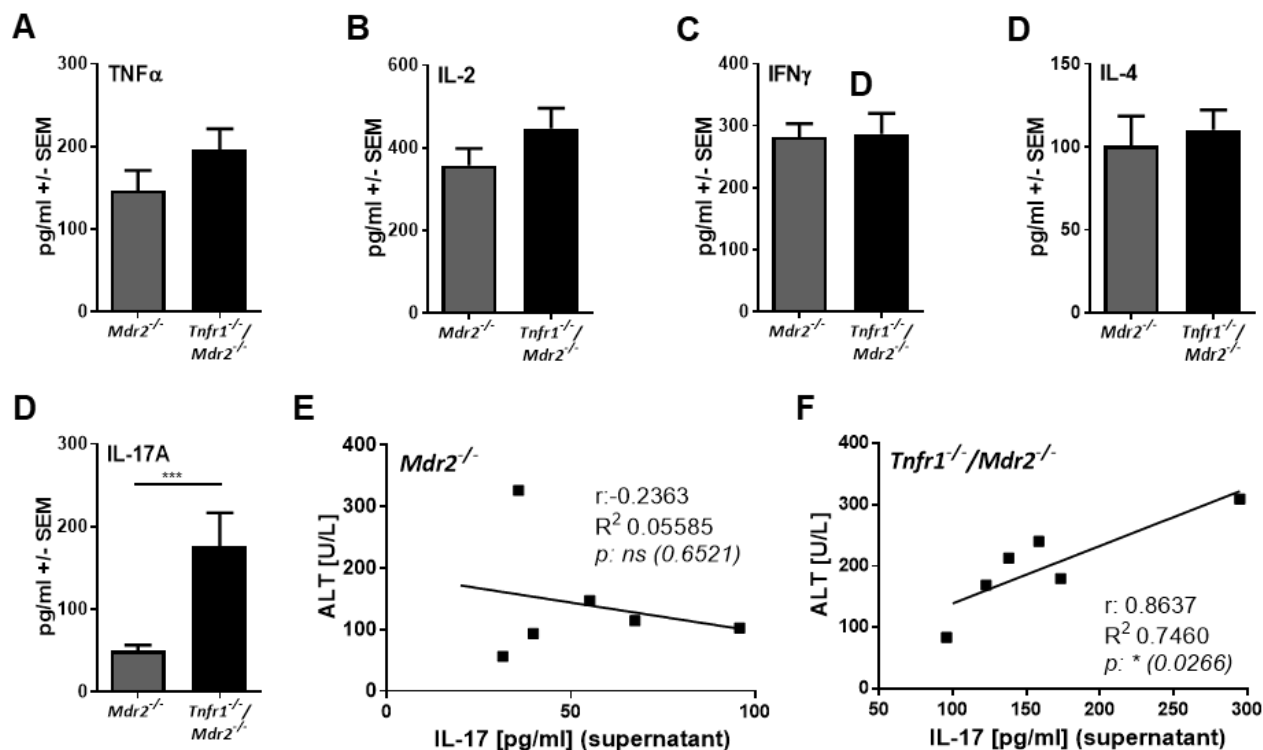


Figure 19: Cytokine concentrations in supernatants of *ex vivo* restimulated hepatic NPCs. (A) Concentration of TNF α , (B) IL-2, (C) IFN γ , (D) IL-4, and (E) IL-17 in the supernatant of *ex vivo* restimulated NPCs isolated from the livers of $Mdr2^{-/-}$ (n = 6) and $Tnfr1^{-/-}/Mdr2^{-/-}$ (n = 6) mice. (F-G) Correlation between IL-17 production of restimulated hepatic NPCs with plasma ALT levels of mice described above. *P \leq 0.05, ***P \leq 0.001.

3.2.3 Hepatic chemokine expression profile of $Tnfr1^{-/-}/Mdr2^{-/-}$ mice

Immune cell trafficking into injured tissue is a highly controlled process which is initiated by binding of chemokines to their cognate receptors. Chemokines induce subset specific migration of leukocytes by creating a specific microenvironment.¹²

Gene expression analyses displayed in Figure 20 show differentially expressed chemokines and chemokine receptors in livers of $Mdr2^{-/-}$ and $Tnfr1^{-/-}/Mdr2^{-/-}$ mice. Figure 20A shows that $Mdr2^{-/-}$ and $Tnfr1^{-/-}/Mdr2^{-/-}$ mice both show elevated expression levels of *Ccl2* expression, however only $Tnfr1^{-/-}/Mdr2^{-/-}$ mice display significantly increased expression levels compared to WT mice. Furthermore, $Tnfr1^{-/-}/Mdr2^{-/-}$ mice show significantly elevated hepatic gene expression of *Cxcl1*, *Ccr6*, and *Cxcr6* compared to all other genotypes (Figure 20B-C).

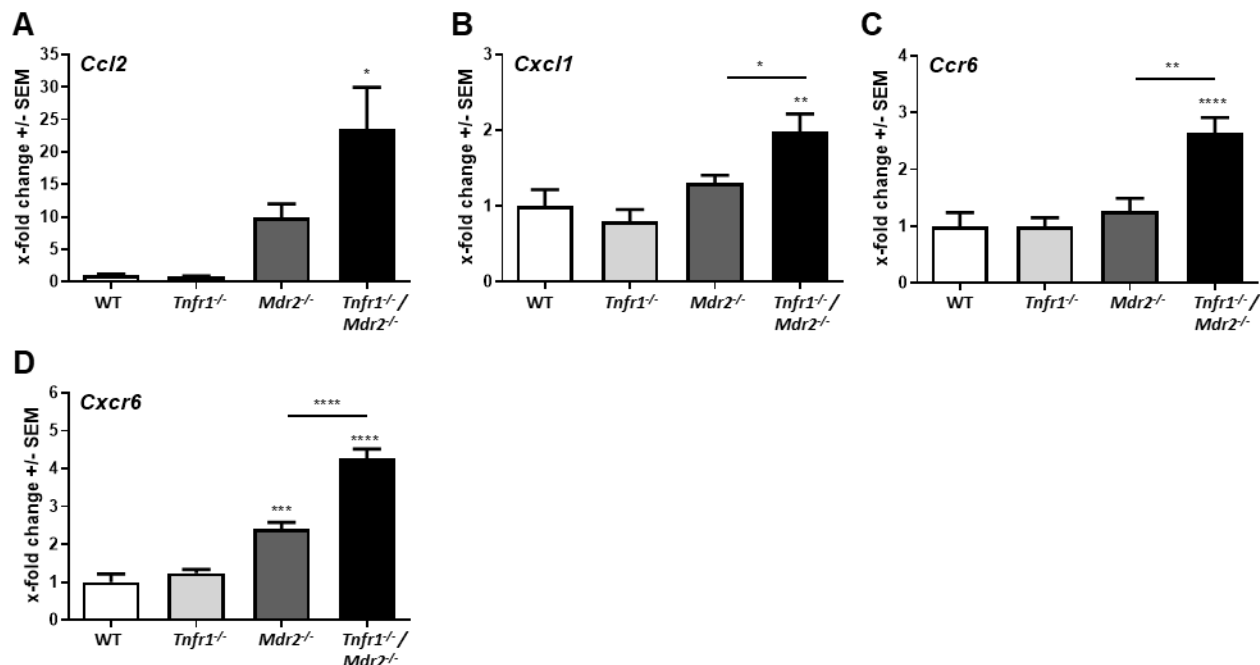


Figure 20: Hepatic gene expression of chemokines and chemokine receptors in *Mdr2*^{-/-} and *Tnfr1*^{-/-}/*Mdr2*^{-/-} mice. Relative hepatic expression levels of chemokine (A) *Ccl2* as well as (B) *Cxcl1*, and chemokine receptors (C) *Ccr6* and (D) *Cxcr6* of WT (n ≥ 4), *Tnfr1*^{-/-} (n ≥ 5), *Mdr2*^{-/-} (n ≥ 7), and *Tnfr1*^{-/-}/*Mdr2*^{-/-} (n ≥ 6) mice determined by RT-qPCR. *P ≤ 0.05, **P ≤ 0.01, ***P ≤ 0.001, ****P ≤ 0.0001.

The above mentioned signaling molecules were expressed on several immune cells, however they all have been associated with either T_H17 cell recruitment or crosstalk between T_H17 cells and other immune cells such as monocytes and neutrophils.⁶⁵

3.2.4 Myeloid cell subsets in livers of *Tnfr1*^{-/-}/*Mdr2*^{-/-} mice

Next to T cells, myeloid cells play an integral part in acute as well as chronic liver inflammation. The myeloid cell compartment is composed of three groups of terminally differentiated cell types macrophages, DCs and granulocytes, which can be further divided into numerous subgroups with a very diverse set of functions.⁶⁶

Since the absence of TNFR1 in the *Mdr2*^{-/-} mouse model led to an increased presence of T_H17 cells and a skewed hepatic cytokine and chemokine microenvironment, an effect on the myeloid cell compartment is to be expected. Major myeloid cell populations were identified using CD11b, F4/80 and Ly6G staining in *Mdr2*^{-/-} and *Tnfr1*^{-/-}/*Mdr2*^{-/-} mice. While CD11b is an integrin found on most myeloid cells types as well as NK cells, F4/80 is a member of the epidermal growth factor (EGF)-transmembrane 7 (TM7) family used to identify monocytes

and macrophages, and Ly6G is a glycosylphosphatidylinositol anchored protein found on the cell surface of neutrophils⁶⁷.

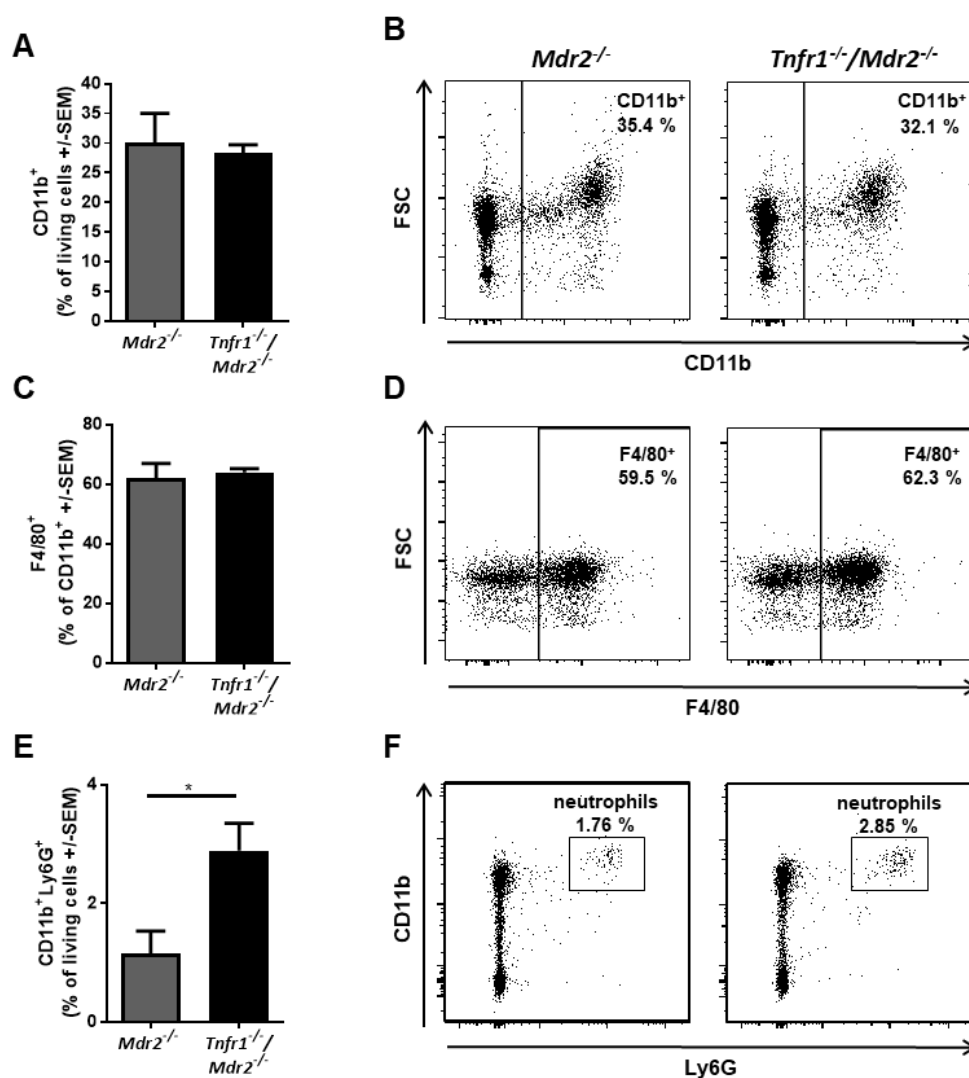


Figure 21: Frequencies of myeloid subsets in the livers of *Mdr2*^{-/-} and *Tnfr1*^{-/-}/*Mdr2*^{-/-} mice. (A) Frequencies (left) and representative dot plots (right) of CD11b⁺ myeloid cells, (B) F4/80⁺ macrophages within the CD11b⁺ cell population, and (C) CD11b⁺Ly6G⁺ neutrophils in livers of *Mdr2*^{-/-} (n ≥ 6), and *Tnfr1*^{-/-}/*Mdr2*^{-/-} (n ≥ 5) mice determined by flow cytometry. ****P ≤ 0.0001.

Figure 21A-B show no differences between frequencies of CD11b⁺ cells in livers from *Mdr2*^{-/-} or *Tnfr1*^{-/-}/*Mdr2*^{-/-} mice. Hepatic monocytes including macrophages are characterized by their high level of plasticity. Pro- as well as anti-inflammatory functions are attributed to these cells, which are known to drive progression as well as resolution of inflammation depending on the microenvironment⁶⁸. Furthermore, *Mdr2*^{-/-} and *Tnfr1*^{-/-}/*Mdr2*^{-/-} mice show

similar frequencies of F4/80⁺ macrophages (Figure 21C-D). In contrast, CD11b⁺Ly6G⁺ neutrophils are significantly enriched in livers from *Tnfr1*^{-/-}/*Mdr2*^{-/-} mice compared to *Mdr2*^{-/-} mice (Figure 21E-F). Overall, the absence of TNFR1 appears to influence specific myeloid cell types rather than perturbing general myeloid cell infiltration into the injured liver.

3.3 Role of RIPK3 in livers of *Tnfr1*^{-/-}/*Mdr2*^{-/-} mice

While an overall increase of monocytes could not be seen in livers of *Tnfr1*^{-/-}/*Mdr2*^{-/-} mice (Figure 21), increased presence of proteins associated with specific monocytic subsets could be observed. As described in section 3.2 (Figure 11), increased levels of activated RIPK3, which were not associated with necroptotic activity, were detected in livers of *Tnfr1*^{-/-}/*Mdr2*^{-/-} mice. Further qRT-PCR analysis confirmed elevated hepatic expression of *Ripk3* (Figure 22A). In addition, increased hepatic expression levels of *Cx3cr1* as well as its ligand *Cx3cl1* (Figure 22B) in *Tnfr1*^{-/-}/*Mdr2*^{-/-} compared to *Mdr2*^{-/-} mice were seen.

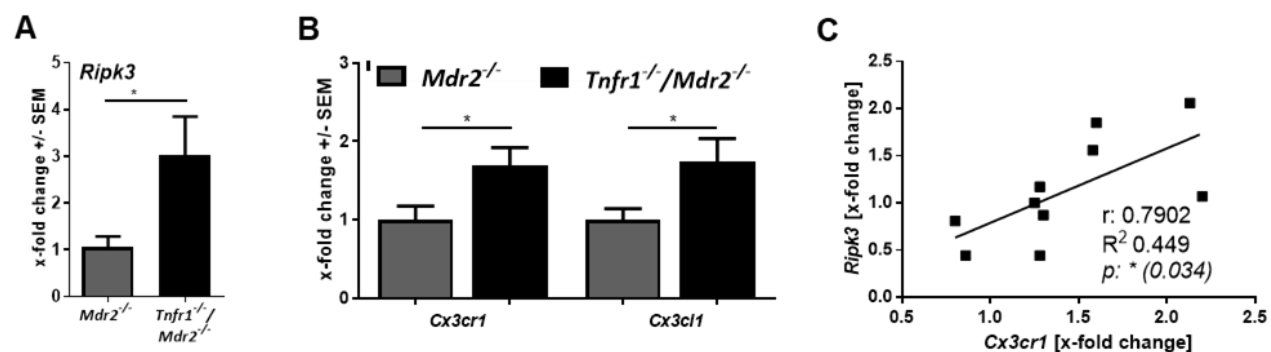


Figure 22: Correlation between hepatic *Ripk3* and *Cx3cr1* expression in livers of *Tnfr1*^{-/-}/*Mdr2*^{-/-} mice. (A) Hepatic gene expression analysis of *Ripk3*, (B) *Cx3cr1* and *Cx3cl1* in *Mdr2*^{-/-} ($n \geq 5$) and *Tnfr1*^{-/-}/*Mdr2*^{-/-} ($n \geq 6$) mice, determined by qRT-PCR. Correlation analysis of hepatic expression levels of *Ripk3* with *Cx3cr1* of *Tnfr1*^{-/-}/*Mdr2*^{-/-} mice. r : correlation coefficient, R^2 : coefficient of determination. $*P \leq 0.05$.

CX3CR1 is a chemokine receptor expressed on numerous cell types including monocytes and macrophages.⁶⁹ By binding to its receptor, CX3CL1 is involved in chemotaxis of immune cell recruitment into inflamed tissue, but also directs immune surveillance during homeostasis⁶⁹. In previous reports, a necroptosis-independent function of RIPK3 activity has been linked to cytokine production in a CX3CR1⁺ monocytic cell population.⁷⁰ Correlation analysis showed

that animals in which hepatic *Ripk3* expression was increased also expressed higher levels of the gene for chemokine receptor *Cx3cr1* (Figure 22C).

The data presented in Figure 22 implicates that the increased activity of RIPK3 in livers of *Tnfr1*^{-/-}/*Mdr2*^{-/-} mice may be associated with increased hepatic expression of *Cx3cr1*.

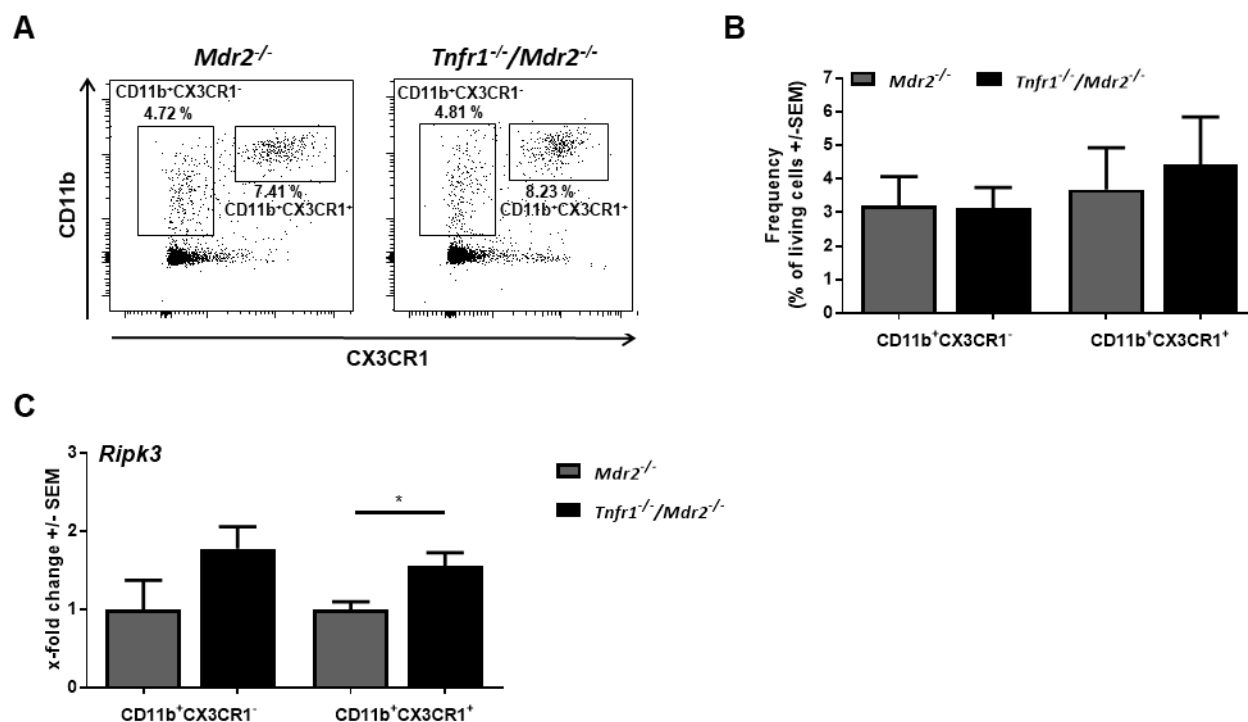


Figure 23: *Ripk3* gene expression is upregulated in CD11b⁺CX3CR1⁺ cells derived from livers of *Tnfr1*^{-/-}/*Mdr2*^{-/-} mice. (A) Representative dot plots and (B) quantification of flow cytometric analysis of CD11b⁺CX3CR1⁺ and CD11b⁺CX3CR1⁻ cell populations in the livers of *Mdr2*^{-/-} (n ≥ 4) and *Tnfr1*^{-/-}/*Mdr2*^{-/-} (n ≥ 3) mice. (C) Relative expression of *Ripk3* in FACS sorted CD11b⁺CX3CR1⁺ and CD11b⁺CX3CR1⁻ cells from livers of mice described above. *P ≤ 0.05.

In order to clarify, whether this observation may be associated with an increased recruitment of CX3CR1⁺ monocytes into the injured liver of *Tnfr1*^{-/-}/*Mdr2*^{-/-} mice, the myeloid cell compartment of *Mdr2*^{-/-} and *Tnfr1*^{-/-}/*Mdr2*^{-/-} mice were analyzed for the presence of CX3CR1⁺ myeloid cells. For that purpose, hepatic NPCs of *Mdr2*^{-/-} and *Tnfr1*^{-/-}/*Mdr2*^{-/-} mice were stained for CD11b and CX3CR1 and sorted via flow cytometry.

As Figure 23A-B shows, both *Mdr2*^{-/-} and *Tnfr1*^{-/-}/*Mdr2*^{-/-} mice display comparable hepatic frequencies of CD11⁺CX3CR1⁻ as well as CD11b⁺CX3CR1⁺ cells. RNA from the sorted cells was isolated, translated into cDNA and analyzed for *Ripk3* expression via qRT-PCR analysis.

Figure 23C shows that, CD11b⁺CX3CR1⁺ cells isolated from livers of *Tnfr1*^{-/-}/*Mdr2*^{-/-} mice express significantly increased levels of *Ripk3* compared to those from *Mdr2*^{-/-} mice, while CD11b⁺CX3CR1⁻ cells from *Tnfr1*^{-/-}/*Mdr2*^{-/-} mice only show a slight and insignificant increase of *Ripk3* expression.

These results indicate that the absence of TNFR1 mediated signaling leads to increased *Ripk3* expression in CX3CR1⁺ monocytes which coincides with an overall increase of RIPK3 activity in chronically inflamed livers of *Tnfr1*^{-/-}/*Mdr2*^{-/-} mice.

3.4 Immune cell accumulation in livers of *Tnfr1*^{-/-}/*Mdr2*^{-/-} mice over time

CLD is a progressive disease with distinct phases each defined by specific features⁹. While *Ripk3* expression was increased in hepatic CD11b⁺CX3CR1⁺ monocytes of 12-week-old *Tnfr1*^{-/-}/*Mdr2*^{-/-} mice, no increased amounts of these cells were observed at that age.

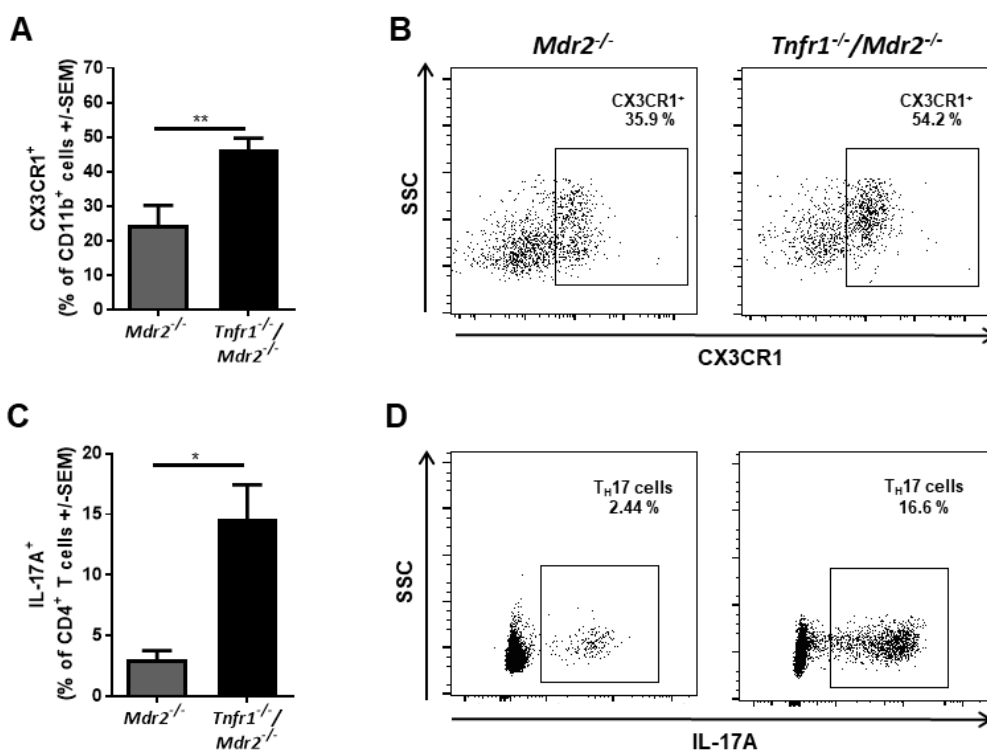


Figure 24: CX3CR1⁺ monocytes and TH17 cells accumulate in livers of *Tnfr1*^{-/-}/*Mdr2*^{-/-} mice with disease progression. (A) Frequencies of CD11b⁺CX3CR1⁺ cell populations in livers of 24-week-old *Mdr2*^{-/-} (n ≥ 3), and *Tnfr1*^{-/-}/*Mdr2*^{-/-} (n ≥ 6) mice determined by flow cytometry. (B) Representative dot plots of flow cytometric analysis described in A. (C) Frequencies of TCRβ⁺CD4⁺IL-17⁺ TH17 cell populations in livers of mice described in A determined by flow cytometry. (D) Representative dot plots of flow cytometric analysis described in C. *P ≤ 0.05 **P ≤ 0.01.

In order to rule out age- or disease stage-dependent effects, we also analyzed the hepatic immune cell composition in livers of 24-week-old *Mdr2*^{-/-} and *Tnfr1*^{-/-}*Mdr2*^{-/-} mice via flow cytometry.

Figure 24A-B shows that the frequency of CD11b⁺CX3CR1⁺ cells was significantly increased in aged *Tnfr1*^{-/-}*Mdr2*^{-/-} mice compared to age-matched *Mdr2*^{-/-} mice. This observation implicates CX3CR1⁺ monocytes are involved in the disease progression of the *Tnfr1*^{-/-}*Mdr2*^{-/-} phenotype. In the same animals T_H17 cell frequencies were also evaluated. While within the group of *Mdr2*^{-/-} mice the frequency of T_H17 cells increased from a mean of 0.45 % at 12 weeks of age (Figure 18E) to 3.73 % in 24-week-old animals (Figure 24C), it is still significantly less than the frequency of T_H17 cells observed in livers of 24-week-old *Tnfr1*^{-/-}*Mdr2*^{-/-} mice (Figure 24C-D). In summary, both CD11b⁺CX3CR1⁺ monocytes as well as T_H17 cells accumulate in the livers of *Tnfr1*^{-/-}*Mdr2*^{-/-} mice with disease progression which is less pronounced in *Mdr2*^{-/-} mice.

Collectively, the data presented above showed that *Tnfr1*^{-/-}*Mdr2*^{-/-} mice displayed increased disease severity, accompanied with distinct molecular and cellular differences in pathology compared to *Mdr2*^{-/-} mice.

4 Discussion

The term CLD encompasses a variety of liver pathologies with different types of liver injury. A unifying element of all types is that the ensuing inflammatory response is the driving force behind disease progression. In many cases, specific treatment options have proved difficult to establish because the underlying pathologies remain poorly understood. Therefore, extensive research has been aimed at developing strategies to suppress specific pathological inflammatory processes.⁷ Due to the strong pro-inflammatory properties of TNF α , neutralizing antibodies against TNF α have been successfully applied to alleviate serious inflammatory pathologies, including, rheumatoid arthritis, psoriasis, and IBD.⁷¹ However, it understandably also bears risks to functionally repress a cytokine with a broad functional spectrum that includes several protective effects.^{18,72} Anti-TNF α has been reported to be relatively safe. Nonetheless, some reports showed severe side effects with varying frequencies. Increased susceptibility or reactivation of latent infection is a rather common result of TNF α suppression, which underlines the importance of TNF α in the defense against pathogens.⁷² A small group of patients treated with anti-TNF α therapy also showed symptoms of demyelination disorders of the central nervous system and liver toxicity, which in rare cases culminated in acute liver failure. Despite the fact that interfering with TNF α mediated signaling has potentially harmful effects on the liver, anti-TNF α treatment has been shown to be beneficial in difficult-to-treat cases of autoimmune hepatitis. The hepatotoxic effect of TNF α antagonists has been monitored carefully throughout the years. Nevertheless, the underlying mechanism of hepatic injury remains elusive. One approach to target the pathological effects of TNF α more exclusively, while keeping the impact on essential immunological functions to a minimum, is to target one of its two known receptors rather than TNF α itself. Numerous studies have demonstrated that TNFR1 is critically involved in inflammatory and fibrotic processes during liver disease.⁷³⁻⁷⁵ In contrast, TNFR2 is often shown to mediate protective effects, especially through the induction and expansion of anti-inflammatory regulatory T cells.⁷⁶ Arguably, that raises the question of whether specific targeting of TNFR1 may be more suitable than neutralizing total TNF α .

This study investigated the effect of TNFR1 ablation in a mouse model of chronic liver inflammation and inflammation associated HCC. The presented data showed that the absence

of TNFR1 mediated signaling in *Mdr2*^{-/-} mice led to a more severe disease manifestation rather than serve a protective effect. This work outlines the differences between the pathologies of *Mdr2*^{-/-} mice and *Tnfr1*^{-/-}/*Mdr2*^{-/-} mice and emphasizes the complexity of inflammatory signaling networks involved in chronic liver inflammatory diseases.

4.1 Ablation of TNFR1 does not protect from tissue injury and fibrosis

TNFR1 is a well-described death receptor that is known to induce apoptotic and necroptotic cell death while simultaneously promoting cell survival via the NFκB pathway.^{60,77} In this study, *Tnfr1*^{-/-}/*Mdr2*^{-/-} mice displayed increased plasma levels of common markers for liver injury (ALT, ALP), signs of cholestasis (bilirubin, cholesterol) and more pronounced disease features in histological analysis compared to *Mdr2*^{-/-} mice. This suggests that the absence of TNFR1 caused increased susceptibility to cellular decay during chronic inflammation. TNFR1 induced types of cell death differ in their pro inflammatory potential. While apoptotic cell death leads to a minimal release of pro-inflammatory DAMPs, excessive amounts are released during necroptosis.⁷⁸

Western blot analysis showed similar levels of activated Casp3 in liver lysates of both *Mdr2*^{-/-} mice and *Tnfr1*^{-/-}/*Mdr2*^{-/-} mice. While that is in line with persistent cellular demise during chronic inflammation, it also shows that induction of apoptosis was sustained in the absence of TNFR1. It is feasible that the lack of TNFR1 induced pro-survival signaling renders cells more susceptible to alternative activation of apoptosis, such as mitochondrial stress or other death receptors such as Fas. Leist *et al.* could show that both TNFR1 and Fas are expressed on hepatocytes and that the induction of either suffices to trigger apoptotic liver failure.⁷⁹

It is well established that RIPK3 mediated necroptosis is induced by TNFR1. However, it should be noted that other inflammatory receptors, including Toll-like receptors (TLRs) are equally potent inducers of necroptosis.²³ Under physiological conditions, *Tnfr1*^{-/-} animals show virtual no active RIPK3 in liver samples, which indicates that TNFR1 is essential for baseline RIPK3 activation. *Mdr2*^{-/-} mice also showed reduced levels of RIPK3, supporting the assumption that apoptosis is the prominent form of cell death in this mouse model. In contrast, *Tnfr1*^{-/-}/*Mdr2*^{-/-} mice display dramatically increased amounts of active RIPK3 in the

liver. This implies that under inflammatory conditions, RIPK3 may either be activated by alternative mechanisms or that RIPK3 activation is not sufficiently regulated in the absence of TNFR1. Increased activity of RIPK3 would suggest increased necroptotic cell death in livers of these mice. However, activation of MLKL could not be observed. Since MLKL facilitates necroptosis through pore formation, necroptotic cell death does not appear to be a major contributor to tissue injury in livers of *Tnfr1^{-/-}/Mdr2^{-/-}* mice. It does, however, raise the question of what necroptotic independent function RIPK3 may perform during chronic liver injury in the absence of TNFR1. And furthermore, whether it is involved in the pathological phenotype observed in *Tnfr1^{-/-}/Mdr2^{-/-}* mice. This objective is discussed in more detail in section 4.5. Overall, the absence of TNFR did not have a major effect on cell death induction in the chronically inflamed liver.

Liver injury of any cause induces a compensatory fibrotic response, which leads to the accumulation of fibrous scar tissue in place of dead parenchymal cells. This process is mediated by HSCs. Previous studies have shown that the knockout of TNFR1 diminished HSC activation and subsequent pro-collagen expression *in vitro* and in mice after carbon tetrachloride (CCl₄) induced liver injury.^{16,74} However, HSCs are known to be activated in response to multiple inflammatory stimuli including DAMPS, PAMPS, as well as several growth factors such as TGFβ and platelet-derived growth factors (PDGFs). The observed increase of fibrotic markers in livers of *Tnfr1^{-/-}/Mdr2^{-/-}* mice can, therefore, be described as the direct result of the aggravated inflammatory response.

4.2 Ablation of TNFR1 does not compromise regenerative proliferation

Several studies over the last decades have investigated the role of TNFR1 in the hepatic regenerative response to injury. It has been confirmed that NFκB activation downstream of TNFR1 is essential for restorative proliferation after partial hepatectomy and CCl₄ treatment.^{17,80} In the liver, TNFR1 has been shown to induce regeneration primarily through the NFκB mediated expression of IL-6, which in turn activates proliferation through the activation of the signal transducer and activator of transcription 3 (STAT3) in target cells. It was, therefore, hypothesized that the increased pathological phenotype of *Tnfr1^{-/-}/Mdr2^{-/-}* mice may be the result of a diminished ability to restore healthy liver

parenchyma. This assumption could not be confirmed, as *Tnfr1^{-/-}/Mdr2^{-/-}* mice displayed elevated expression levels of several genes of prominent proliferation markers (*Pcna*, *CcnA2*, *Cdk1*), accompanied by robust plasma levels IL-6. It is possible that in *Tnfr1^{-/-}/Mdr2^{-/-}* mice infiltrating immune cells serve as an alternative source of IL-6. Furthermore, *Tnfr1^{-/-}/Mdr2^{-/-}* mice displayed significantly increased plasma levels of IL-22, which has been confirmed to efficiently induce liver regeneration via STAT3 activation.⁸¹ It is therefore likely, that the activation of the regenerative response in *Tnfr1^{-/-}/Mdr2^{-/-}* mice is the result of a skewed immune cell composition which includes IL-22 producing cell types.

Chronic liver inflammation and fibrosis are known to create a tumor susceptible microenvironment.^{82,83} Expression analysis showed that genes previously described to be up-regulated in malignant or pre-malignant cells (*Tnfaip*, *Spp1*, *Afp*) were up-regulated in *Tnfr1^{-/-}/Mdr2^{-/-}* mice compared to WT mice.⁵⁶⁻⁵⁸ In comparison *Mdr2^{-/-}* mice showed only a significant increase of *Spp1* expression when compared to WT mice.

However, the age of the mice analyzed was only 12 weeks and neither macro- nor microscopic analysis of the tissue revealed signs of malignant transformation. One explanation for that may be that despite their role as tumor markers, these proteins are also involved in several pro-inflammatory, pro-fibrotic, or regenerative processes. A20, which is encoded in the *Tnfaip* gene, regulates NFκB signaling in response to TNFα, IL-1, or IL-17 signaling.⁸⁴ It is therefore upregulated in direct response to NFκB activation. OPN (*Spp1*), has been shown to promote various processes during CLD, including the recruitment of neutrophils and macrophages, the activation of HSCs, and regenerative but also malignant proliferation.⁸⁵ AFP (*Afp*) is a dedifferentiation marker, as it is not expressed in adult hepatocytes. It is, however, highly expressed in oval cells. Oval cells are stem cell-like cells of the liver, which proliferate and differentiate into hepatocytes in response to strong or prolonged liver injury. The upregulation of *Afp* expression in livers of *Tnfr1^{-/-}/Mdr2^{-/-}* mice may, therefore, be indicative of oval cell proliferation. However, Knight *et al.* could show that in a mouse model of chronic liver injury, loss of TNFR1 mediated signaling greatly impaired oval cell proliferation.⁸⁶

Considering the pronounced inflammatory and fibrotic responses in combination with increased expression of tumor markers, it is unlikely that the absence of TNFR1 will protect

against inflammation-associated tumor development in this mouse model. Long-term studies will have to show, how the absence of TNFR1 signaling alters the tumor development in these mice.

4.3 Ablation of TNFR1 alters the cytokine milieu in the chronically inflamed liver

Cytokines are essential mediators of immune cell communication and cellular responses to inflammatory stimuli, including the induction of differentiation, proliferation and, cell death.¹⁴ TNF α has been termed as master regulator of pro-inflammatory cytokine production.⁸⁷ It is therefore to be expected that the absence of one of its receptors alters the prevailing cytokine milieu.

Initial analysis of the plasma cytokine profile did not indicate major differences in either overall T cell activation (IL-2), nor in specific T_H1 (IFN γ) or T_H2 (IL-4) responses between *Tnfr1*^{-/-}/*Mdr2*^{-/-} mice and *Mdr2*^{-/-} mice. However, increased levels of TNF α and IL-22 could be detected in *Tnfr1*^{-/-}/*Mdr2*^{-/-} mice but not in *Mdr2*^{-/-} mice. The increased levels of TNF α are in line with observations by Peschon *et al.*⁸⁸. They could show that lipopolysaccharide (LPS) challenge in mice deficient of either TNFR1 or TNFR2 leads to increased plasma levels of TNF α , most likely due to insufficient turnover.⁸⁸ As soluble TNF α primarily interacts with TNFR1, the increased plasma level will presumably have little effect on the immune response in *Tnfr1*^{-/-}/*Mdr2*^{-/-} mice. IL-22 is known to be produced in large quantities by T_H17 and T_H22 cells and is most prominently known for its role in the maintenance of epithelial tissue integrity in the intestine, but also for inducing regenerative responses in secondary organs as described above. During chronic liver disease IL-22 has been shown to be hepatoprotective, anti-fibrotic, and to promote recruitment of anti-inflammatory cell types. Because IL-22 production is upregulated in response to chronic liver injury, it has been shown to function as a predictive indicator of disease severity in cirrhosis.⁸⁹ Increased IL-22 levels are in line with a more severe phenotype in *Tnfr1*^{-/-}/*Mdr2*^{-/-} mice but are also indicative of an increased activation of IL-22 producing cell types in the absence of TNFR1. Interestingly, unlike WT mice, *Tnfr1*^{-/-} mice also showed detectable levels of IL-22 in plasma samples. This implies that the absence of TNFR1 in animals without an underlying pathology

has a modulatory effect on the immune cell compartment. Fang *et al.* showed that anti-TNF α therapy in patients with Crohn's disease led to an increase in IL-22 producing T cells in the intestine, which implies a regulatory effect of TNF α mediated signaling on IL-22 expression.⁹⁰

Hepatic gene expression analysis revealed that genes encoding for IL-1 β , IL-23, and TGF β were upregulated in livers of *Tnfr1*^{-/-}/*Mdr2*^{-/-} mice compared to *Mdr2*^{-/-} mice. While each of these cytokines has unique pro-inflammatory and pro-fibrotic properties; in combination they create a microenvironment that favors T_H17 differentiation and activation. Accordingly, *Tnfr1*^{-/-}/*Mdr2*^{-/-} mice showed a significantly increased gene expression of the T_H17 cell signature cytokine *Il17a* (IL-17A) and *Rorc* (ROR γ t) the master transcription factor of T_H17 cell differentiation.⁹¹

4.4 Ablation of TNFR1 leads to an increased presence of T_H17 cells and neutrophils in the chronically inflamed liver

Deregulated immune cell activity is inherent to almost all types of inflammatory diseases. Upon liver injury, immune cells are recruited into the liver and promote unique inflammatory processes that exacerbate tissue injury. Flow cytometric analysis confirmed the suspected increase of T_H17 cells in livers of *Tnfr1*^{-/-}/*Mdr2*^{-/-} mice, which was indicated by the hepatic cytokine expression profile. T_H17 cells have been positively correlated with disease severity in many types of chronic liver disease including ALD, AIH, PSC, and chronic biliary cirrhosis.⁹¹ Most of the pathological effects of T_H17 cells during chronic liver disease have been linked to IL-17 mediated signaling. The IL-17 receptor (IL-17R) is expressed on most liver resident parenchymal and non-parenchymal cells.⁹ Activation of IL-17R in the liver leads to the induction of pro-inflammatory pathways including NF κ B, MAPK, and STAT3. In addition, IL-17R induces the expression of pro-inflammatory cytokines (IL-1 β , IL-6, TNF α), chemokines (CCL2 and CXCL1), and further promotes fibrosis via direct activation of HSCs.⁸⁵⁻⁸⁷ Accumulation of pathogenic T_H17 cells, in response to abrogated TNF α mediated signaling, is in line with findings in mouse models of rheumatoid arthritis and psoriasis. Notley *et al.* could show opposing effects of anti-TNF therapy during collagen-induced arthritis.⁹⁵ Treatment with either a TNFR-Fc fusion protein or an anti-TNF α antibody successfully reduced arthritic disease severity through inhibiting T_H1 and T_H17 cell

accumulation in inflamed joints. In contrast, anti-TNF α treatment simultaneously caused an expansion of pathogenic T cells (T_H1 and T_H17) in peripheral lymphoid organs and blood. This study further showed that TNFR1 but not TNFR2 is crucially involved in regulating pathogenic T_H17 cell expansion by suppressing the gene expression of the p40 subunit of IL-12 and IL-23.⁹⁵ A similar effect was shown by Ma *et al.* in a mouse model of psoriasis. They could also show that TNF α neutralization led to increased gene expression of T_H17 cell cytokines, which positively correlated with disease severity.^{96,97}

Cytokine analysis of supernatants of re-stimulated NPCs derived from livers of *Tnfr1*^{-/-}/*Mdr2*^{-/-} mice and *Mdr2*^{-/-} mice showed that the absence of TNFR1 had no significant effect on IL-2, IFN γ , and IL-4 production, which supports the assumption that T_H1 and T_H2 cell responses in the inflamed liver are not affected by the ablation of TNFR1. Consistent with the increased frequencies of T_H17 cells detected via flow cytometry, NPCs derived from livers of *Tnfr1*^{-/-}/*Mdr2*^{-/-} mice produced significantly more IL-17 than those from *Mdr2*^{-/-} mice. Additionally, the concentration of IL-17 positively correlated with disease severity in these animals. It can be assumed that IL-17 plays a central role in disease progression in *Tnfr1*^{-/-}/*Mdr2*^{-/-} mice. The same effect could not be seen for *Mdr2*^{-/-} mice, indicating a less crucial role for IL-17 in these mice. A different observation was made by Tedesco *et al.*⁹⁸ who showed that disease progression in *Mdr2*^{-/-} mice with an FVB background was associated with an increased infiltration of IL-17 producing unconventional $\gamma\delta$ T cells into the injured liver. They furthermore showed that FVB/*Mdr2*^{-/-} mice displayed an altered microbial composition in the intestine (dysbiosis) accompanied by increased intestinal permeability leading to the translocation of intestinal bacteria into the venous circulation and subsequent colonization of the liver.⁹⁸ It is well established that abnormal bile acid composition or disruption of the bile flow during cholestatic liver disease in patients affects the intestine often leading to dysbiosis and impaired barrier function of the intestinal epithelium.⁹⁹ FVB/*Mdr2*^{-/-} mice display a more aggravated liver injury, inflammation, and fibrosis over time compared to C57/Bl6/*Mdr2*^{-/-} mice.¹⁰⁰ It is, therefore, feasible that the more severe phenotype of FVB/*Mdr2*^{-/-}, in comparison to C57/Bl6/*Mdr2*^{-/-} mice, led to a more pronounced effect on intestinal integrity, which in turn aggravated liver disease via the induction of the $\gamma\delta$ T cell response. However, the underlying mechanisms driving $\gamma\delta$ T cell responses in FVB/*Mdr2*^{-/-} but not C57/Bl6/*Mdr2*^{-/-} mice will have to be addressed in future studies.

Both T_H17 cells and $\gamma\delta$ T cells have been reported to be increased in livers of PSC patients and both cell types promote disease progression through IL-17 production.^{98,101} It can, therefore, be concluded that IL-17 plays a central role in cholestatic liver disease in mice and men, and the loss of TNFR1 mediated signaling negatively influences disease severity by causing an influx of IL-17 producing cell type in livers of *Tnfr1*^{-/-}/*Mdr2*^{-/-} mice.

Gene expression analysis of chemokines and chemokine receptors associated with T_H17 cell migration and activation showed an upregulated expression of *Ccl2*, *Cxcl1*, *Ccr6*, and *Cxcr6* in *Tnfr1*^{-/-}/*Mdr2*^{-/-} mice compared to *Mdr2*^{-/-} mice. As described above CCL2 and CXCL1 are well-known mediators of neutrophil recruitment in response to IL-17 mediated signaling.⁶⁵ In addition, *Tnfr1*^{-/-}/*Mdr2*^{-/-} mice showed an increased hepatic expression of *Ccr6* and *Cxcr6*, which have been described as important homing receptors on both T_H17 cells and neutrophils.^{65,102} In line with that, an increased frequency of neutrophils was observed in livers of *Tnfr1*^{-/-}/*Mdr2*^{-/-} mice compared to *Mdr2*^{-/-} mice.

4.5 RIPK3 performs a necroptosis independent role in livers of *Tnfr1*^{-/-}/*Mdr2*^{-/-} mice

Flow cytometric analysis of CD11b⁺ cells in the livers of *Tnfr1*^{-/-}/*Mdr2*^{-/-} mice and *Mdr2*^{-/-} mice did not indicate significant differences in the frequency of overall myeloid cells. However, the myeloid cell compartment includes a diverse subset including macrophages, dendritic cells, and monocytes. Infiltrating monocytic subsets have been shown to mediate important pro- as well as anti-inflammatory functions during CLD.⁶⁸ CCR2 and CX3CR1 are analyzed to identify specific monocytic cell subsets.²⁸ It has already been established that *Tnfr1*^{-/-}/*Mdr2*^{-/-} mice show higher gene expression of the CCR2 ligand *Ccl2* compared to *Mdr2*^{-/-} mice. Additional analysis showed increased gene expression of both the *Cx3cr1* and its ligand in the livers of *Tnfr1*^{-/-}/*Mdr2*^{-/-} mice. Interestingly, the gene expression of *Cx3cr1* positively correlated to the hepatic expression of *Ripk3* in *Tnfr1*^{-/-}/*Mdr2*^{-/-} mice. WB analysis discussed in section 4.1, showed an increased presence of active RIPK3, which was not associated with necroptotic cell death, in the livers of *Tnfr1*^{-/-}/*Mdr2*^{-/-} mice. Moriwaki *et al.*⁷⁰ have shown that in monocyte-derived CX3CR1⁺ macrophages and dendritic cells, RIPK3 mediates the production of cytokines including IL-1 β and IL-23, which subsequently induce

the production of IL-22. In that model, RIPK3 activation and subsequent IL-22 expression were shown to promote regeneration in response to tissue injury in the intestine.⁷⁰ While the frequency of CD11b⁺CX3CR⁺ cells did not differ between livers of *Tnfr1*^{-/-}/*Mdr2*^{-/-} mice and *Mdr2*^{-/-} mice, cells derived from livers of *Tnfr1*^{-/-}/*Mdr2*^{-/-} mice did express significantly higher levels of RIPK3. Furthermore, the analysis of CD11b⁺CX3CR1⁺ cells in 24-week-old mice showed a significant increase of these cells, which was accompanied by a further increased presence of TH17 cells, in livers of *Tnfr1*^{-/-}/*Mdr2*^{-/-} mice compared to *Mdr2*^{-/-} mice. This indicates a more pronounced role of CX3CR1⁺ monocytes in later stages of the disease progression. In the intestine, CX3CR1⁺ monocytes have been shown to induce commensal-specific TH17 cell responses.¹⁰³ The hepatic gene expression of *Il1b* and *Il23*, as well as plasma levels of IL-22, were increased in *Tnfr1*^{-/-}/*Mdr2*^{-/-} mice compared to *Mdr2*^{-/-} mice, which may be associated with the increased presence of *Ripk3* expressing CX3CR1⁺ monocytes. In the liver CX3CR1⁺ macrophages have been reported to promote anti-inflammatory and regenerative processes during cholestatic liver disease.²⁸ The specific role of CX3CR1⁺ monocytes in the progression of chronic liver inflammation in *Tnfr1*^{-/-}/*Mdr2*^{-/-} mice remains to be determined. It is feasible that CX3CR1⁺ monocytes promote regeneration in response to TH17 mediated tissue injury. However, if CX3CR1⁺ monocytes promote the expression IL-1 β and IL-23 in the livers of *Tnfr1*^{-/-}/*Mdr2*^{-/-} mice, they may also contribute to the activation and stabilization of the pathogenic TH17 cell response.

In summary, it can be concluded that the ablation of TNFR1 signaling exacerbated the pathological phenotype of *Mdr2*^{-/-} mice, which is seen in increased liver injury and more pronounced fibrotic features in the livers of *Tnfr1*^{-/-}/*Mdr2*^{-/-} mice. The ablation of TNFR1 had distinct effects on both cytokine and chemokine production which was accompanied by an increased presence of TH17 cells, neutrophils and an accumulation of CX3CR1⁺ monocytes in livers over time. Moreover, exacerbated disease progression in the absence of TNFR1 could be directly correlated to the increased production of IL-17 by liver immune cells. Overall, the presented data above indicates that targeting TNFR1 mediated signaling does not appear suitable to improve chronic cholestatic liver inflammation and subsequent adverse events.

4.6 Outlook

This thesis aimed to elucidate the role of TNFR1-mediated signaling during chronic cholestatic liver disease in *Mdr2*^{-/-} mice. Overall, the presented data above clearly shows that the absence of TNFR1-mediated signaling aggravates disease progression in the *Mdr2*^{-/-} mouse model. This work outlines several cellular and molecular processes that were influenced by the absence of TNFR1. The key feature driving disease progression in *Tnfr1*^{-/-}/*Mdr2*^{-/-} mice appears to be the expansion of IL-17 producing pathogenic T_H17 cells in the chronically inflamed liver.

Pathogenic T_H17 cell responses in both, patients of cholestatic liver diseases and FVB/*Mdr2*^{-/-} mice have been associated with dysbiosis, increased gut permeability, and frequent comorbid inflammatory disorders of the intestine.^{32,98,104,105} Nakamoto *et al.* could show that microbiota derived from PSC patients could induce pathogenic T_H17 cell responses both in the intestine as well as in the liver of gnotobiotic mice.¹⁰⁶ While anti-TNF α therapy successfully alleviates disease severity in multiple inflammatory disorders, recent reports have indicated that ablation of TNF α signaling may negatively influence intestinal homeostasis. Banzin *et al.* could show that anti-TNF α treatment in patients with arthritis led to dysbiosis.¹⁰⁷ Another study could show that anti-TNF α treatment, as well as TNFR deficiency, reduces the proliferation of intestinal epithelial cells and mucosal regeneration resulting in increased gut permeability.¹⁰⁸

It is therefore feasible that the pathogenic T_H17 cell response in *Tnfr1*^{-/-}/*Mdr2*^{-/-} mice may be the result of dysbiosis and degeneration of intestinal epithelium. Future research should investigate whether the TNFR1 deficiency in *Mdr2*^{-/-} mice influences the microbial composition and the barrier function of the intestine. If a protective role of TNFR1 for intestinal homeostasis can be confirmed, it should be investigated whether treatment with either antibiotics or pro-biotics can help to stabilize the microbial composition and consequently intestinal tissue integrity. An alternative approach would be treating *Tnfr1*^{-/-}/*Mdr2*^{-/-} mice with either ROR γ t inhibitors or anti-IL17 antibodies to inhibit T_H17 cell differentiation or neutralization of IL-17, respectively. Combined treatment with anti-TNF and anti-IL-17 antibodies has been discussed as a possible treatment option for rheumatoid

arthritis. An obvious caveat to this approach would be that the inhibition of an even broader spectrum of essential protective pathways severely impacts immunological functions that ultimately render patients more susceptible to infection and potential tumor development due to impaired immune surveillance. Nevertheless, treatment options for CLD remain limited and uncontrolled inflammatory responses are still the main cause of the high mortality rate.⁷ Until the underlying mechanisms of disease progression are better understood, constraining the inflammatory response remains the best treatment strategy.

5 Abstract

Tumor necrosis factor receptor 1 (TNFR1) is a ubiquitously expressed pro-inflammatory cytokine receptor. It is known to promote disease progression of chronic liver disease (CLD) through the induction of cell death as well as the release of pro-inflammatory and pro-fibrotic mediators. In contrast, it is also involved in mediating pro-survival signaling and regeneration. This work analyzed how the absence of TNFR1 affects disease progression in *Mdr2*^{-/-} mice, a mouse model of chronic liver inflammation and inflammation-induced HCC. For that purpose, *Tnfr1*^{-/-} mice were crossed with *Mdr2*^{-/-} mice, creating *Tnfr1*^{-/-}/*Mdr2*^{-/-} mice.

TNFR1 deficient *Mdr2*^{-/-} mice displayed a more severe phenotype indicated by increased plasma levels of the liver enzymes alanine aminotransferase (ALT) and alkaline phosphatase. Increased plasma levels of bilirubin with concomitant reduction cholesterol indicated impaired biliary excretion of livers of TNFR1 deficient *Mdr2*^{-/-}. TNFR1 deficiency in the chronically inflamed liver did not abrogate apoptotic cell as seen in western blot analysis of an active subunit of caspase 3 (Casp3), nor did it appear to affect the induction of regenerative proliferation indicated by increased gene expression of proliferation markers (*Pcna*, *Ccna2*, *Cdk1*). Compared to *Mdr2*^{-/-} mice, *Tnfr1*^{-/-}/*Mdr2*^{-/-} mice displayed a more pronounced fibrotic response seen in significantly higher collagen content, and gene expression of fibrotic markers including α -smooth muscle actin (α -sma), matrix metalloproteinases (MMPs), and their tissue inhibitors (TIMPs). The absence of TNFR1 influenced the gene expression of inflammatory cytokines (*Il1b*, *Il23*, *Tgfb1*, *Il17a*), chemokines (*Ccl2*, *Cxcl1*, *Cx3cl1*) and chemokine receptors (*Ccr6*, *Cxcr6*, *Cx3cr1*) in livers of *Tnfr1*^{-/-}/*Mdr2*^{-/-} mice, which in combination created a microenvironment favoring T_H17 cell activation. Flow cytometric analysis showed that the hepatic immune cell compartment of *Tnfr1*^{-/-}/*Mdr2*^{-/-} mice was enriched in IL-17 producing T_H17 cells as well as neutrophils. The aggravated tissue injury in *Tnfr1*^{-/-}/*Mdr2*^{-/-} mice positively correlated with enhanced IL-17 production in the injured liver. Additionally, western blot analysis of liver lysates revealed that *Tnfr1*^{-/-}/*Mdr2*^{-/-} mice displayed increased hepatic activation of receptor interacting protein Serine/Threonine kinase 3 (RIPK3), which was not related to necroptotic cell death. Instead, frequencies of infiltrating CX3CR1⁺ monocytes increased over time in

livers of *Tnfr1^{-/-}/Mdr2^{-/-}* mice, which expressed significantly higher levels of *Ripk3* expression than those of *Mdr2^{-/-}* mice.

Overall, it can be concluded that the ablation of TNFR1 exacerbated disease progression of chronic liver inflammation in the *Mdr2^{-/-}*. This work adds to the extensive research aimed to delineate underlying mechanisms of CLD disease progression, to improve treatment options and consequently disease outcomes. Future research should be aimed at identifying the underlying mechanism by which TNFR1 deficiency promotes pathogenic T_H17 cell responses during chronic liver disease.

5.1 Graphical abstract

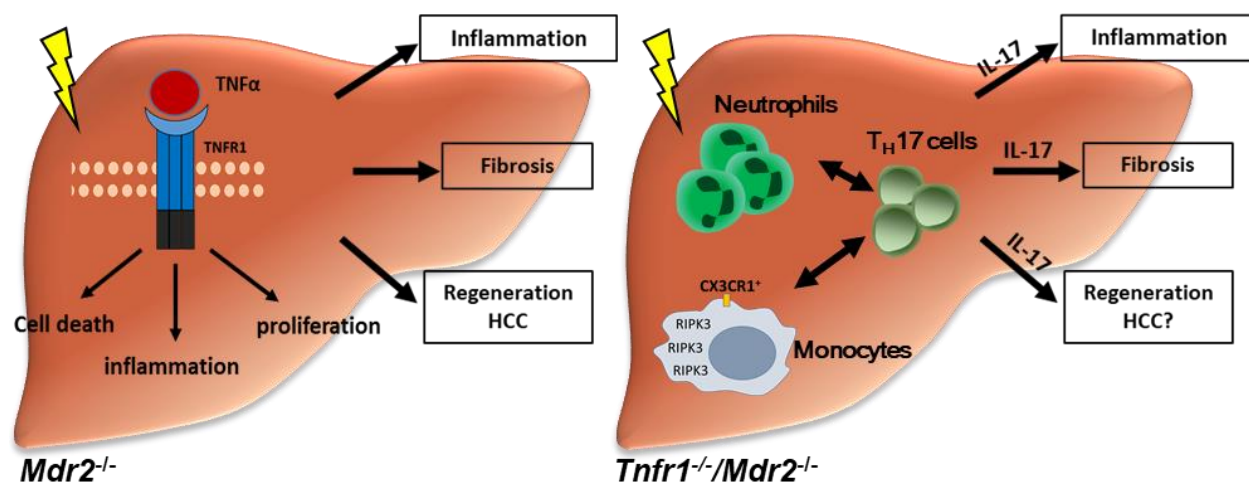


Figure 25: Graphical abstract. Tumor necrosis factor receptor 1 mediated signaling is known to induce cell death as well as pro-inflammatory and pro-fibrotic processes during chronic liver injury. In contrast, it has also been shown to be essential in the induction of proliferation in response to injury. Increased TNFR1 mediated signaling has been associated with disease progression by promoting inflammation, fibrosis as well as malignant proliferation and therefore has been identified as a possible drug target in CLD. The genetic ablation of TNFR1 in multi-drug resistance knockout mice (*Mdr2^{-/-}*), a mouse model of chronic cholestatic liver disease (right), showed that the absence of TNFR1 mediated signaling did not attenuate but rather aggravated tissue injury in *TNFR1^{-/-}/Mdr2^{-/-}* mice. The more severe pathology of *TNFR1^{-/-}/Mdr2^{-/-}* mice was associated with an increased presence of T_H17 cells, neutrophils and RIPK3 expression in CX3CR1⁺ monocytes. The significant increase of IL-17 production by hepatic NPCs is positively correlated with tissue injury in these mice and is therefore assumed to be responsible for the more severe disease features. Hepatic regeneration appears to be maintained in the absence of TNFR1, which may create a pro-tumor microenvironment in the chronically inflamed livers of *TNFR1^{-/-}/Mdr2^{-/-}* mice. T_H17 derived IL-17 has been shown to promote inflammation, fibrosis, and regeneration during chronic inflammatory diseases and may, therefore, compensate for the loss of TNFR1 in this mouse model.

6 Zusammenfassung

Der Tumornekrosefaktor-Rezeptor 1 (TNFR1) ist ein ubiquitär exprimierter Zytokinrezeptor, welcher an akuten und chronischen Entzündungsreaktionen, wie in chronischen Lebererkrankungen (*chronic liver diseases*, CLD), beteiligt ist. Die TNFR1 induzierte Signaltransduktion fördert die Induktion von Zelltod, sowie die Freisetzung von pro-inflammatorischen und pro-fibrotischen Mediatoren. Darüber hinaus ist jedoch auch bekannt, dass TNFR1 an der Vermittlung von wichtigen Überlebenssignalwegen und der Induktion von Regenerationsprozessen beteiligt ist.

In dieser Arbeit wurde der Einfluss einer gezielten Ablation von TNFR1 auf die Pathogenese von CLD in dem bekannten *multidrug-resistant p glycoprotein knockout* (*Mdr2*^{-/-}) Mausmodell für chronische Leberentzündung untersucht. Zu diesem Zweck wurden TNFR1 knockout (*Tnfr1*^{-/-}) Mäuse mit *Mdr2*^{-/-} Mäusen gekreuzt, wodurch eine neue *Tnfr1*^{-/-}/*Mdr2*^{-/-} Mauslinie erzeugt wurde. Erhöhte Plasmaspiegel der Leberenzyme Alanin-Aminotransferase (ALT) und alkalischen Phosphatase in *Tnfr1*^{-/-}/*Mdr2*^{-/-} Mäusen wiesen im Vergleich zu *Mdr2*^{-/-} Mäusen auf einen stärker ausgeprägten Leberschaden hin. Eine Beeinträchtigung des Gallenflusses wurde durch erhöhte Plasmaspiegel von Bilirubin mit einhergehender Reduktion der Cholesterinwerte angezeigt. Die Ablation des TNFR1 in der chronisch entzündeten Leber hatte keinen Einfluss auf die Induktion von Apoptose, wie die Western Blot Analyse einer aktiven Untereinheit von Caspase 3 (Casp3) gezeigt hat. Ferner legt die erhöhte Genexpression von Proliferationsmarkern (*Pcna*, *Ccna2*, *Cdk1*) in Lebern von *Tnfr1*^{-/-}/*Mdr2*^{-/-} Mäusen nahe, dass die Induktion regenerativer Proliferation ebenfalls nicht durch den Mangel an TNFR1 beeinflusst wurde. Im Vergleich zu *Mdr2*^{-/-} Mäusen zeigten *Tnfr1*^{-/-}/*Mdr2*^{-/-} Mäuse eine stärker ausgeprägte Fibrose. Dies wurde durch einen signifikant erhöhten Kollagengehalt und die gesteigerte Genexpression von Fibrose-Markern, einschließlich des glatten Muskelaktins (*α-smooth muscle actin*, *α-sma*), der Matrix-Metalloproteinasen (MMPs) und deren Gewebsinhibitoren (*tissue inhibitor of MMP*, TIMPs), verdeutlicht. Darüber hinaus wurde die Genexpression von pro-inflammatorischen Zytokinen (*Il1b*, *Il23*, *Tgfb1*, *Il17a*), Chemokinen (*Ccl2*, *Cxcl1*, *Cx3cl1*) und Chemokinrezeptoren (*Ccr6*, *Cxcr6*, *Cx3cr1*) durch das Fehlen von TNFR1 in den Lebern von *Tnfr1*^{-/-}/*Mdr2*^{-/-} Mäusen erhöht, welche zusammengenommen die Differenzierung und

Aktivierung von T_H17-Zellen begünstigen. Durchflusszytometrische Analysen zeigten eine erhöhte Präsenz von T_H17 Zellen und Neutrophilen in Lebern von *Tnfr1*^{-/-}/*Mdr2*^{-/-} Mäusen. Der verstärkte Leberschaden in *Tnfr1*^{-/-}/*Mdr2*^{-/-} Mäusen korrelierte ebenfalls positiv mit der IL-17-Produktion hepatischer non-parenchymaler Zellen in der geschädigten Leber, was auf eine zentrale Rolle von IL-17 in der Pathogenese in *Tnfr1*^{-/-}/*Mdr2*^{-/-} schließen lässt. Zusätzlich konnte gezeigt werden, dass *Tnfr1*^{-/-}/*Mdr2*^{-/-} Mäuse eine gesteigerte Aktivierung des Rezeptor-interagierenden Proteins Serin/Threonine kinase 3 (RIPK3) aufweisen, was nicht auf nekroptotischen Zelltod zurückgeführt werden konnte. Stattdessen zeigte sich eine, mit dem Alter ansteigende, Infiltration von CX3CR1⁺ Monozyten in Lebern von *Tnfr1*^{-/-}/*Mdr2*^{-/-}, die im Vergleich zu CX3CR1⁺ Monozyten aus Lebern von *Mdr2*^{-/-} Mäusen signifikant erhöhte *Ripk3* Genexpressionswerte aufwiesen. Zusammenfassend kann geschlussfolgert werden, dass die Ablation von TNFR1 die Pathogenese der chronischen Leberentzündung im *Mdr2*^{-/-} Mausmodell verstärkt.

Diese Arbeit trägt dazu bei, krankheitsfördernde Mechanismen der chronischen Leberentzündung besser zu verstehen und kann dazu beitragen Behandlungsstrategien zu verbessern, um einen positiven Einfluss auf den Krankheitsverlauf zu nehmen. Die Aufklärung der regulatorischen Funktion von TNFR1 auf chronisch entzündliche Prozesse, insbesondere auf die Induktion pathogener T_H17 Zellantworten, ist Gegenstand aktueller Forschung.

7 References

1. Barikbin, R. *et al.* Early heme oxygenase 1 induction delays tumour initiation and enhances DNA damage repair in liver macrophages of Mdr2^{-/-} mice. *Sci. Rep.* **8**, 16238 (2018).
2. Berkhout, L. *et al.* Deletion of tumour necrosis factor α receptor 1 elicits an increased TH17 immune response in the chronically inflamed liver. *Sci. Rep.* **9**, 4232 (2019).
3. Ravichandran, G. *et al.* Interferon- γ -dependent immune responses contribute to the pathogenesis of sclerosing cholangitis in mice. *J. Hepatol.* (2019). doi:10.1016/j.jhep.2019.05.023
4. Sanyal, A. J., Boyer, T., Terault, N. & Lindor, K. *Zakim and Boyer's hepatology: a textbook of liver disease.* (Elsevier, 2018). doi:https://doi.org/10.1016/C2013-0-19055-1
5. Freitas-Lopes, M. A., Mafra, K., David, B. A., Carvalho-Gontijo, R. & Menezes, G. B. Differential Location and Distribution of Hepatic Immune Cells. *Cells* **6**, 48 (2017).
6. Krenkel, O. & Tacke, F. Liver macrophages in tissue homeostasis and disease. *Nat. Rev. Immunol.* **17**, 306 (2017).
7. Marcellin, P. & Kutala, B. K. Liver diseases: A major, neglected global public health problem requiring urgent actions and large-scale screening. *Liver Int.* **38 Suppl 1**, 2–6 (2018).
8. Dancygier, H. Clinical hepatology: Principles and practice of hepatobiliary diseases. *Clin. Hepatol. Princ. Pract. Hepatobiliary Dis.* 1–538 (2010). doi:10.1007/978-3-540-93842-2
9. Pellicoro, A., Ramachandran, P., Iredale, J. P. & Fallowfield, J. A. Liver fibrosis and repair: Immune regulation of wound healing in a solid organ. *Nat. Rev. Immunol.* **14**, 181–194 (2014).
10. Ghouri, Y. A., Mian, I. & Rowe, J. H. Review of hepatocellular carcinoma: Epidemiology, etiology, and carcinogenesis. *J. Carcinog.* **16**, 1 (2017).
11. Bray, F. *et al.* Global cancer statistics 2018: GLOBOCAN estimates of incidence and mortality worldwide for 36 cancers in 185 countries. *CA. Cancer J. Clin.* **68**, 394–424 (2018).
12. Stein, J. V & Nombela-Arrieta, C. Chemokine control of lymphocyte trafficking: a general overview. *Immunology* **116**, 1–12 (2005).
13. Marra, F. & Tacke, F. Roles for Chemokines in Liver Disease. *Gastroenterology* **147**, 577–594.e1 (2014).
14. Turner, M. D., Nedjai, B., Hurst, T. & Pennington, D. J. Cytokines and chemokines: At the crossroads of cell signalling and inflammatory disease. *Biochim. Biophys. Acta - Mol. Cell Res.* **1843**, 2563–2582 (2014).
15. MacEwan, D. J. TNF receptor subtype signalling: Differences and cellular consequences.

- Cell. Signal.* **14**, 477–492 (2002).
16. Sudo, K., Yamada, Y., Moriwaki, H., Saito, K. & Seishima, M. Lack of tumor necrosis factor receptor type 1 inhibits liver fibrosis induced by carbon tetrachloride in mice. *Cytokine* **29**, 236–244 (2005).
 17. Yamada, Y., Kirillova, I., Peschon, J. J. & Fausto, N. Initiation of liver growth by tumor necrosis factor: deficient liver regeneration in mice lacking type I tumor necrosis factor receptor. *Proc. Natl. Acad. Sci. U. S. A.* **94**, 1441–1446 (1997).
 18. SASS, G., SHEMBADE, N. D. & TIEGS, G. Tumour necrosis factor α (TNF)–TNF receptor 1-inducible cytoprotective proteins in the mouse liver: relevance of suppressors of cytokine signalling. *Biochem. J.* **385**, 537–544 (2005).
 19. Kalliolias, G. D. & Ivashkiv, L. B. TNF biology, pathogenic mechanisms and emerging therapeutic strategies. *Nat. Rev. Rheumatol.* **12**, 49 (2015).
 20. Ting, A. T. & Bertrand, M. J. M. More to Life than NF-kappaB in TNFR1 Signaling. *Trends Immunol.* **37**, 535–545 (2016).
 21. Sabio, G. & Davis, R. J. TNF and MAP kinase signalling pathways. *Semin. Immunol.* **26**, 237–245 (2014).
 22. Wajant, H. & Siegmund, D. TNFR1 and TNFR2 in the Control of the Life and Death Balance of Macrophages. *Front. Cell Dev. Biol.* **7**, 91 (2019).
 23. Galluzzi, L. & Vitale, I. Molecular mechanisms of cell death : recommendations of the Nomenclature Committee on Cell Death 2018. 486–541 (2018). doi:10.1038/s41418-017-0012-4
 24. Kubes, P. & Jenne, C. Immune Responses in the Liver. *Annu. Rev. Immunol.* **36**, (2018).
 25. Gaffen, S. L., Jain, R., Garg, A. V & Cua, D. J. The IL-23-IL-17 immune axis: from mechanisms to therapeutic testing. *Nat. Rev. Immunol.* **14**, 585–600 (2014).
 26. Wang, C., Collins, M. & Kuchroo, V. K. Effector T cell differentiation: are master regulators of effector T cells still the masters? *Curr. Opin. Immunol.* **37**, 6–10 (2015).
 27. Xu, R., Huang, H., Zhang, Z. & Wang, F.-S. The role of neutrophils in the development of liver diseases. *Cell. Mol. Immunol.* **11**, 224–231 (2014).
 28. Tacke, F. Functional role of intrahepatic monocyte subsets for the progression of liver inflammation and liver fibrosis in vivo. *Fibrogenesis Tissue Repair* **5**, S27 (2012).
 29. Vannella, K. M. & Wynn, T. A. Mechanisms of Organ Injury and Repair by Macrophages. *Annu. Rev. Physiol.* **79**, 593–617 (2017).
 30. Boyer, J. L. Bile formation and secretion. *Compr. Physiol.* **3**, 1035–1078 (2013).
 31. Vallim, T. Q. D. A., Tarling, E. J. & Edwards, P. A. Review Pleiotropic Roles of Bile Acids in Metabolism. *Cell Metab.* **17**, 657–669 (2013).
 32. Palmela, C., Peerani, F., Castaneda, D., Torres, J. & Itzkowitz, S. H. Inflammatory Bowel Disease and Primary Sclerosing Cholangitis: A Review of the Phenotype and Associated

- Specific Features. *Gut Liver* **12**, 17–29 (2017).
33. Karlsen, T. H., Folseraas, T., Thorburn, D. & Vesterhus, M. Primary sclerosing cholangitis – a comprehensive review. *J. Hepatol.* **67**, 1298–1323 (2017).
 34. Fickert, P. *et al.* Regurgitation of bile acids from leaky bile ducts causes sclerosing cholangitis in Mdr2 (Abcb4) knockout mice. *Gastroenterology* **127**, 261–274 (2004).
 35. Oude Elferink, R. P. J. & Paulusma, C. C. Function and pathophysiological importance of ABCB4 (MDR3 P-glycoprotein). *Pflugers Arch. Eur. J. Physiol.* **453**, 601–610 (2007).
 36. Oude Elferink, R. P. J. & Paulusma, C. C. Function and pathophysiological importance of ABCB4 (MDR3 P-glycoprotein). *Pflugers Arch.* **453**, 601–610 (2007).
 37. Smit, J. J. M. *et al.* Homozygous disruption of the murine MDR2 P-glycoprotein gene leads to a complete absence of phospholipid from bile and to liver disease. *Cell* **75**, 451–462 (1993).
 38. Katzenellenbogen, M. *et al.* Molecular Mechanisms of Liver Carcinogenesis in the Mdr2-Knockout Mice. *Mol. Cancer Res.* **5**, 1159–1170 (2007).
 39. Van Nieuwerk, C. M. J. *et al.* The role of bile salt composition in liver pathology of mdr2 (-/-) mice: Differences between males and females. *J. Hepatol.* **26**, 138–145 (1997).
 40. Barikbin, R. *et al.* Induction of heme oxygenase 1 prevents progression of liver fibrosis in Mdr2 knockout mice. *Hepatology* **55**, 553–562 (2012).
 41. Uchinami, H., Seki, E., Brenner, D. A. & D’Armiento, J. Loss of MMP 13 attenuates murine hepatic injury and fibrosis during cholestasis. *Hepatology* **44**, 420–429 (2006).
 42. McGill, M. R. The past and present of serum aminotransferases and the future of liver injury biomarkers. *EXCLI J.* **15**, 817–828 (2016).
 43. Liebert, M. A., Schnell, M. A., Hardy, C., Hawley, M. & Propert, K. J. O. Y. Effect of Blood Collection Technique in Mice on Clinical Pathology Parameters. **162**, (2002).
 44. Voshol, P. J. *et al.* Dietary cholesterol does not normalize low plasma cholesterol levels but induces hyperbilirubinemia and hypercholanemia in Mdr2 P-glycoprotein-deficient mice. *J. Hepatol.* **34**, 202–209 (2001).
 45. Declercq, W., Vanden Berghe, T. & Vandenabeele, P. RIP Kinases at the Crossroads of Cell Death and Survival. *Cell* **138**, 229–232 (2009).
 46. Han, Z., Hendrickson, E. A., Bremner, T. A. & Wyche, J. H. A sequential two-step mechanism for the production of the mature p17:p12 form of caspase-3 in vitro. *J. Biol. Chem.* **272**, 13432–13436 (1997).
 47. Weber, K., Roelandt, R., Bruggeman, I., Estornes, Y. & Vandenabeele, P. Nuclear RIPK3 and MLKL contribute to cytosolic necrosome formation and necroptosis. *Commun. Biol.* **1**, 6 (2018).
 48. Weber, K., Roelandt, R., Bruggeman, I., Estornes, Y. & Vandenabeele, P. Nuclear RIPK3 and MLKL contribute to cytosolic necrosome formation and necroptosis. *Commun. Biol.*

- 1, 6 (2018).
49. Pellicoro, A. *et al.* Elastin accumulation is regulated at the level of degradation by macrophage metalloelastase (MMP-12) during experimental liver fibrosis. *Hepatology* **55**, 1965–1975 (2012).
 50. Bataller, R. & Brenner, D. Liver fibrosis. *J. Clin. Invest.* **115**, 209–218 (2005).
 51. Schmitt-Graff, A., Chakroun, G. & Gabbiani, G. Modulation of perisinusoidal cell cytoskeletal features during experimental hepatic fibrosis. *Virchows Arch. A. Pathol. Anat. Histopathol.* **422**, 99–107 (1993).
 52. Knittel, T. *et al.* Expression of matrix metalloproteinases and their inhibitors during hepatic tissue repair in the rat. *Histochem Cell Biol* **113**, 443–453 (2000).
 53. White, E. S. & Mantovani, A. R. Inflammation, wound repair, and fibrosis: reassessing the spectrum of tissue injury and resolution. *J Pathol* **229**, 141–144 (2013).
 54. Yamada, Y. & Fausto, N. Deficient liver regeneration after carbon tetrachloride injury in mice lacking type 1 but not type 2 tumor necrosis factor receptor. *Am J Pathol* **152**, 1577–1589 (1998).
 55. Yu, L.-X., Ling, Y. & Wang, H.-Y. Role of nonresolving inflammation in hepatocellular carcinoma development and progression. *NPJ Precis. Oncol.* **2**, 6 (2018).
 56. Dong, B., Lv, G., Wang, Q. & Wang, G. Targeting A20 enhances TRAIL-induced apoptosis in hepatocellular carcinoma cells. *Biochem. Biophys. Res. Commun.* **418**, 433–438 (2012).
 57. Cao, L. *et al.* Osteopontin promotes a cancer stem cell-like phenotype in hepatocellular carcinoma cells via an integrin–NF- κ B–HIF-1 α pathway. *Oncotarget* **6**, 6627–6640 (2015).
 58. Wang, X. & Wang, Q. Alpha-Fetoprotein and Hepatocellular Carcinoma Immunity. *Can. J. Gastroenterol. Hepatol.* **2018**, 9049252 (2018).
 59. Stenger, S. & Röllinghoff, M. Role of cytokines in the innate immune response to intracellular pathogens. *Ann. Rheum. Dis.* **60**, iii43 LP-iii46 (2001).
 60. Sedger, L. M. & McDermott, M. F. TNF and TNF-receptors: From mediators of cell death and inflammation to therapeutic giants - past, present and future. *Cytokine Growth Factor Rev.* **25**, 453–472 (2014).
 61. McKarns, S. C. & Schwartz, R. H. Biphasic regulation of Il2 transcription in CD4+ T cells: roles for TNF-alpha receptor signaling and chromatin structure. *J. Immunol.* **181**, 1272–1281 (2008).
 62. Gabay, C. Interleukin-6 and chronic inflammation. *Arthritis Res. Ther.* **8 Suppl 2**, S3–S3 (2006).
 63. Rutz, S., Eidenschenk, C. & Ouyang, W. IL-22, not simply a Th17 cytokine. *Immunol. Rev.* **252**, 116–132 (2013).

64. Robinson, M. W., Harmon, C. & O'Farrelly, C. Liver immunology and its role in inflammation and homeostasis. *Cell. Mol. Immunol.* **13**, 267–276 (2016).
65. Pelletier, M. *et al.* Evidence for a cross-talk between human neutrophils and Th17 cells. *Blood* **115**, 335–343 (2010).
66. Gabrilovich, D. I., Ostrand-Rosenberg, S. & Bronte, V. Coordinated regulation of myeloid cells by tumours. *Nat. Rev. Immunol.* **12**, 253 (2012).
67. Yu, Y.-R. A. *et al.* A Protocol for the Comprehensive Flow Cytometric Analysis of Immune Cells in Normal and Inflamed Murine Non-Lymphoid Tissues. *PLoS One* **11**, e0150606 (2016).
68. Brempelis, K. J. & Crispe, I. N. Infiltrating monocytes in liver injury and repair. *Clin. Transl. Immunol.* **5**, e113–e113 (2016).
69. Lee, M., Lee, Y., Song, J., Lee, J. & Chang, S.-Y. Tissue-specific Role of CX3CR1 Expressing Immune Cells and Their Relationships with Human Disease. *Immune Netw.* **18**, e5 (2018).
70. Moriwaki, K., Balaji, S., Bertin, J., Gough, P. J. & Chan, F. K.-M. Distinct Kinase-Independent Role of RIPK3 in CD11c(+) Mononuclear Phagocytes in Cytokine-Induced Tissue Repair. *Cell reports* **18**, 2441–2451 (2017).
71. Van Hauwermeiren, F., Vandenbroucke, R. E. & Libert, C. Treatment of TNF mediated diseases by selective inhibition of soluble TNF or TNFR1. *Cytokine Growth Factor Rev* **22**, 311–319 (2011).
72. Ali, T. *et al.* Clinical use of anti-TNF therapy and increased risk of infections. *Drug Heal. Patient Saf* **5**, 79–99 (2013).
73. Cubero, F. J. *et al.* TNFR1 determines progression of chronic liver injury in the IKKgamma/Nemo genetic model. *Cell Death Differ* **20**, 1580–1592 (2013).
74. Tarrats, N. *et al.* Critical role of tumor necrosis factor receptor 1, but not 2, in hepatic stellate cell proliferation, extracellular matrix remodeling, and liver fibrogenesis. *Hepatology* **54**, 319–327 (2011).
75. Shibata, H. *et al.* The therapeutic effect of TNFR1-selective antagonistic mutant TNF-alpha in murine hepatitis models. *Cytokine* **44**, 229–233 (2008).
76. Yang, S., Wang, J., Brand, D. D. & Zheng, S. G. Role of TNF-TNF Receptor 2 Signal in Regulatory T Cells and Its Therapeutic Implications. *Front. Immunol.* **9**, 784 (2018).
77. Simeonova, P. P. *et al.* The Role of Tumor Necrosis Factor- α in Liver Toxicity, Inflammation, and Fibrosis Induced by Carbon Tetrachloride. *Toxicol. Appl. Pharmacol.* **177**, 112–120 (2001).
78. Kaczmarek, A., Vandenabeele, P. & Krysko, D. V. Necroptosis: the release of damage-associated molecular patterns and its physiological relevance. *Immunity* **38**, 209–223 (2013).
79. Leist, M. *et al.* The 55-kD tumor necrosis factor receptor and CD95 independently

- signal murine hepatocyte apoptosis and subsequent liver failure. *Mol. Med.* **2**, 109–124 (1996).
80. Kirillova, I., Chaisson, M. & Fausto, N. Tumor necrosis factor induces DNA replication in hepatic cells through nuclear factor kappaB activation. *Cell Growth Differ.* **10**, 819–828 (1999).
 81. Nguyen, P. M., Putoczki, T. L. & Ernst, M. STAT3-Activating Cytokines: A Therapeutic Opportunity for Inflammatory Bowel Disease? *J Interf. Cytokine Res* **35**, 340–350 (2015).
 82. Wallace, M. C. & Friedman, S. L. Hepatic fibrosis and the microenvironment: fertile soil for hepatocellular carcinoma development. *Gene Expr* **16**, 77–84 (2014).
 83. Hernandez-Gea, V., Toffanin, S., Friedman, S. L. & Llovet, J. M. Role of the microenvironment in the pathogenesis and treatment of hepatocellular carcinoma. *Gastroenterology* **144**, 512–527 (2013).
 84. Catrysse, L., Vereecke, L., Beyaert, R. & van Loo, G. A20 in inflammation and autoimmunity. *Trends Immunol.* **35**, 22–31 (2014).
 85. Wen, Y., Jeong, S., Xia, Q. & Kong, X. Role of Osteopontin in Liver Diseases. *Int. J. Biol. Sci.* **12**, 1121–1128 (2016).
 86. Li, G.-C. Tumor markers for hepatocellular carcinoma (Review). *Mol. Clin. Oncol.* 593–598 (2013). doi:10.3892/mco.2013.119
 87. Parameswaran, N. & Patial, S. Tumor necrosis factor- α signaling in macrophages. *Crit. Rev. Eukaryot. Gene Expr.* **20**, 87–103 (2010).
 88. Peschon, J. J. *et al.* TNF Receptor-Deficient Mice Reveal Divergent Roles for p55 and p75 in Several Models of Inflammation. *J. Immunol.* **160**, 943–952 (1998).
 89. Caparrós, E. & Francés, R. The Interleukin-20 Cytokine Family in Liver Disease. *Front. Immunol.* **9**, 1155 (2018).
 90. Fang, L. *et al.* Anti-TNF Therapy Induces CD4+ T-Cell Production of IL-22 and Promotes Epithelial Repairs in Patients With Crohn’s Disease. *Inflamm. Bowel Dis.* **24**, 1733–1744 (2018).
 91. Hammerich, L., Heymann, F. & Tacke, F. Role of IL-17 and Th17 cells in liver diseases. *Clin Dev Immunol* **2011**, 345803 (2011).
 92. Meng, F. *et al.* IL-17 signaling in inflammatory cells, Kupffer cells and Hepatic Stellate cells exacerbates liver fibrosis Fanli. *Gastroenterology* **143**, 1–18 (2012).
 93. Jovanovic, D. V. *et al.* IL-17 stimulates the production and expression of proinflammatory cytokines, IL-beta and TNF-alpha, by human macrophages. *J Immunol* **160**, 3513–3521 (1998).
 94. Tan, Z. *et al.* IL-17A plays a critical role in the pathogenesis of liver fibrosis through hepatic stellate cell activation. *J Immunol* **191**, 1835–1844 (2013).

95. Notley, C. A. *et al.* Blockade of tumor necrosis factor in collagen-induced arthritis reveals a novel immunoregulatory pathway for Th1 and Th17 cells. *J. Exp. Med.* **205**, 2491–2497 (2008).
96. Ma, H.-L. *et al.* Tumor necrosis factor alpha blockade exacerbates murine psoriasis-like disease by enhancing Th17 function and decreasing expansion of Treg cells. *Arthritis Rheum.* **62**, 430–440 (2010).
97. Van Hauwermeiren, F., Vandenbroucke, R. E. & Libert, C. Treatment of TNF mediated diseases by selective inhibition of soluble TNF or TNFR1. *Cytokine Growth Factor Rev.* **22**, 311–319 (2011).
98. Tedesco, D. *et al.* Alterations in Intestinal Microbiota Lead to Production of Interleukin 17 by Intrahepatic $\gamma\delta$ T-cell Receptor-positive Cells and Pathogenesis of Cholestatic Liver Disease. *Gastroenterology* **154**, 2178–2193 (2018).
99. Chiang, J. Y. L. & Ferrell, J. M. Bile Acid Metabolism in Liver Pathobiology. *Gene Expr.* **18**, 71–87 (2018).
100. Potikha, T. *et al.* Interstrain differences in chronic hepatitis and tumor development in a murine model of inflammation-mediated hepatocarcinogenesis. *Hepatology* **58**, 192–204 (2013).
101. Katt, J. *et al.* Increased T helper type 17 response to pathogen stimulation in patients with primary sclerosing cholangitis. *Hepatology* **58**, 1084–1093 (2013).
102. Wojkowska, D. W., Szpakowski, P., Ksiazek-Winiarek, D., Leszczynski, M. & Glabinski, A. Interactions between neutrophils, Th17 cells, and chemokines during the initiation of experimental model of multiple sclerosis. *Mediators Inflamm.* **2014**, 590409 (2014).
103. Panea, C. *et al.* Intestinal Monocyte-Derived Macrophages Control Commensal-Specific Th17 Responses. *Cell Rep.* **12**, 1314–1324 (2015).
104. Patman, G. CX3CR1 - A direct line to gut-liver crosstalk? *Nat. Rev. Gastroenterol. Hepatol.* **12**, 490 (2015).
105. Eksteen, B. The Gut-Liver Axis in Primary Sclerosing Cholangitis. *Clin. Liver Dis.* **20**, 1–14 (2016).
106. Nakamoto, N. *et al.* Gut pathobionts underlie intestinal barrier dysfunction and liver T helper 17 cell immune response in primary sclerosing cholangitis. *Nat. Microbiol.* **4**, 492–503 (2019).
107. Bazin, T. *et al.* Microbiota Composition May Predict Anti-Tnf Alpha Response in Spondyloarthritis Patients: an Exploratory Study. *Sci. Rep.* **8**, 5446 (2018).
108. Bradford, E. M. *et al.* Epithelial TNF Receptor Signaling Promotes Mucosal Repair in Inflammatory Bowel Disease. *J. Immunol.* **199**, 1886–1897 (2017).

8 Danksagung

Zu guter Letzt möchte ich mich für die umfangreiche Unterstützung bedanken, ohne die es mir nicht möglich gewesen wäre diese Arbeit zu erstellen.

Zunächst möchte ich mich herzlich bei Prof. Dr. Gisa Tiegs für das Überlassen dieses spannenden Forschungsprojektes bedanken. Insbesondere für die Motivation zum selbständigen Arbeiten und das anhaltende Vertrauen auch nach Misserfolgen bin ich ihr sehr dankbar.

Ebenfalls zu Dank verpflichtet bin ich Dr. Roja Barikbin, die mich durch meinen Master und die ersten Jahre meiner Doktorarbeit begleitet und unterstützt hat.

Für die Übernahme des Zweitgutachtens bedanke ich mich Herrn PD Dr. Hartwig Lüthen.

Des Weiteren möchte ich mich bei den Mitgliedern meiner Betreuungskommission, PD Dr. Thomas Jacobs und Dr. Johannes Kluwe bedanken, welche meine Arbeit im Rahmen des Graduiertenkollegs „Entzündung und Regeneration“ im SFB 841 mit Diskussionen und Anregungen unterstützt haben.

Den Co-Autoren meiner veröffentlichten Arbeiten danke ich für ihren substanziellen Beitrag und ihre fortwährende Unterstützung.

Elena Tasika und Carsten Rothkegel danke ich für die exzellente technische und emotionale Unterstützung zu früher und später Stunde. Ferner danke ich euch für euren unermüdlichen Einsatz zur Aufrechterhaltung von stabilen Strukturen, die uns allen das erfolgreiche Arbeiten erst ermöglichen.

Auch den Kollegen der FACS Core Facility des Uniklinikums Eppendorf möchte ich meinen aufrichtigen Dank für ihre tatkräftige Unterstützung aussprechen.

Ich möchte mich bei der gesamten Arbeitsgruppe und ehemaligen Kollegen für die freundschaftliche Atmosphäre inner- und außerhalb des Labors, die stete Hilfsbereitschaft, „comic relief“ und das magische Auftauchen von Schokolade, wenn man sie ganz dringend braucht, bedanken.

Ein ganz besonderer Dank geht an Dr. Birgit Schiller und Gevitha Ravichandran, für die vielen Stunden, Tage und „gelegentliche“ Nächte in Experimenten oder der Gestaltung von Postern, Manuskripten und Präsentationen, die es ohne euch nicht gegeben hätte.

Zum Schluss möchte ich mich bei meiner Familie und Freunden bedanken, die den Glauben nie verloren haben, dass diese Arbeit einmal existieren wird. Der Beitrag, den eure Unterstützung zu dieser Arbeit geleistet hat, lässt sich nicht in Worte fassen.

Insbesondere meiner Mutter danke ich für einfach alles.

Christopher Tod Woods

Studienbüro Biologie
MIN Fakultät
Universität Hamburg
Biozentrum Klein Flottbeck
Ohnhorststraße 8
22609 Hamburg

28.10.2019

Sehr geehrte Damen und Herren,

hiermit bestätige ich, dass die von Frau Laura Katharina Berkhout mit dem Titel " Role of Tumour necrosis factor α receptor 1 in a mouse model of chronic liver inflammation" vorgelegte Doktorarbeit in korrektem Englisch geschrieben ist.

Mit freundlichen Grüßen,

A handwritten signature in black ink that reads "Christopher Tod Woods". The signature is written in a cursive, flowing style.

Christopher Tod Woods
(Amerikaner)